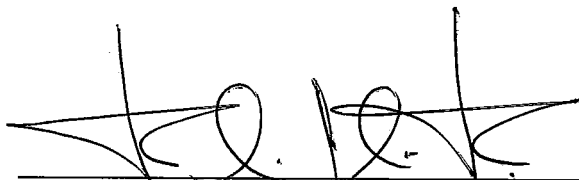# PRODUZINDO PADRÕES RÍTMICOS ARBITRÁRIOS: CARACTERÍSTICAS BIOLÓGICAS EM SISTEMAS NEUROLOCOMOTORES ARTIFICIAIS

Zhijun Yang

TESE SUBMETIDA AO CORPO DOCENTE DA COORDENAÇÃO DOS PROGRAMAS DE PÓS-GRADUAÇÃO DE ENGENHARIA DA UNIVERSIDADE FEDERAL DO RIO DE JANEIRO COMO PARTE DOS REQUISITOS NECESSÁRIOS PARA A OBTENÇÃO DO GRAU DE DOUTOR EM CIÊNCIAS EM ENGENHARIA DE SISTEMAS E COMPUTAÇÃO.
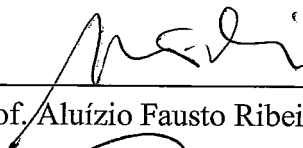
Aprovada por:
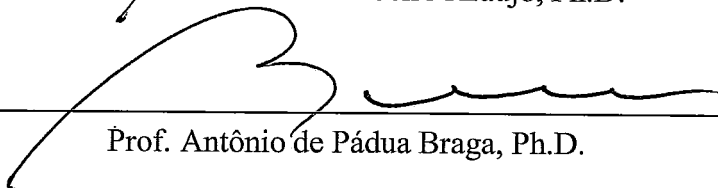
_____
Prof. Felipe Maia Galvão França, Ph.D.

_____
Prof. Max Suell Dutra, Dr.-Ing.

_____
Prof. Sérgio Exel Gonçalves, D.Sc.

_____
Prof. Aluízio Fausto Ribeiro Araújo, Ph.D.

_____
Prof. Antônio de Pádua Braga, Ph.D.

_____
Prof. Carlos Henrique Costa Ribeiro, Ph.D.

RIO DE JANEIRO, RJ - BRASIL

DEZEMBRO DE 1999

À minha esposa e meu filho
Wenfeng e Jianpeng,
por seu apoio e paciência

Agradecimentos

Primeiro, gostaria de agradecer meu orientador, Professor Felipe M.G. França, por me permitir desenvolver este projeto e me orientar e apoiar ao longo do curso de minha pesquisa. Sou extremamente afortunado por ter alguém que sabe como encorajar criatividade e inspirar excelência em pesquisa.

Também gostaria de agradecer aos outros membros da minha banca de exame de qualificação, Professores Valmir C. Barbosa e Aluízio F.R. Araújo, e aos membros da minha banca de defesa, Professores Max S. Dutra, Sérgio E. Gonçalves, Antônio P. Braga e Carlos H.C. Ribeiro. Professor Barbosa era meu professor de curso e um dos fomentadores principais do algoritmos distribuídos empregados nesta tese. Professor Araújo me ajudou a melhorar minha monografia de qualificação e ofereceu várias sugestões importantes para a preparação desta tese.

Muito obrigado também ao Professor Vladimir C. Alves e ao seu curso de VLSI que inspirou algumas idéias inovadoras em circuitos reconfiguraveis para implementação futura. Também agradeço à Professora Inês C. Dutra pelas suas sugestões valiosas para a preparação da documentação, e ao Dr. Jiang Zhu pela descrição útil de alguns conceitos matemáticos.

Obrigado especial vão para meus colegas da UFRJ pela ajuda que eles me deram no idioma e muitos outros assuntos: Amarildo T. Costa, Gabriel Silva, João Marcelo, Moisés A. Silva, Ana P. Leitão, Nivea de Carvalho Ferreira, Alexandre R. Henrique, Rodrigo Basilio, Ricardo, e à todos nos laboratórios LPC, LAM e LIA.

Agradeço também à Universidade Federal do Rio de Janeiro e, em especial ao Programa de Sistemas e Computação da Coordenação dos Programas de Pós-graduação em Engenharia, por ter contribuído para a minha formação. Não posso deixar de agradecer também ao Conselho Nacional de Pesquisa e Desenvolvimento pelo apoio financeiro

recebido durante todos os meus anos de estudo.

Finalmente, gostaria de agradecer à minha família pelo apoio e encorajamento. Especialmente, não posso achar uma palavra satisfatória para expressar meus sentimentos pela contribuição que minha esposa teve em minha pesquisa, é impossível descrever apenas com "obrigado". Não é um exagero dizer que, sem a compreensão, apoio e resistência significativa da minha esposa a realização desta tese seria completamente inimaginável.

Resumo da Tese apresentada à COPPE/UFRJ como parte dos requisitos necessários para a obtenção do grau de Doutor em Ciências (D.Sc)

PRODUZINDO PADRÕES RÍTMICOS ARBITRÁRIOS: CARACTERÍSTICAS BIOLÓGICAS EM SISTEMAS NEUROLOCOMOTORES ARTIFICIAIS

Zhijun Yang

Dezembro/1999

Orientador: Felipe Maia Galvão França

Programa: Engenharia de Sistemas e Computação

Como uma máquina comum à quase todos os fenômenos de vida, *Oscillatory Neural Networks* (ONN) têm um papel crucial nas atividades de todos os animais. Depois de revisar alguns resultados de pesquisa novos em *Central Pattern Generators* (CPGs), que é um ramo concreto de estudos em ONN, esta tese apresenta uma abordagem nova, *macroscópica* e generalizante na reprodução de oscilações neurais acopladas observadas em CPGs biológicos durante o controle do andar. Baseado em *Scheduling by Multiple Edge Reversal* (SMER), um sincronizador distribuído simples e poderoso, vários *Oscillatory Building Blocks* (OBBs) podem ser configurados para a produção de padrões rítmicos complicados observados no andar dos mais diversos animais dotados de um número de pernas pareados. Finalmente, uma metodologia original é provida para construção de uma arquitetura alvo de CPG artificial como uma rede neural de Hopfield assimétrica que se comporta como SMER.

Abstract of Thesis presented to COPPE/UFRJ as a partial fulfillment of the requirements for the degree of Doctor of Science (D.Sc.)

ON PRODUCING ARBITRARY RHYTHMIC PATTERNS: BIOLOGICAL CHARACTERISTICS IN ARTIFICIAL NEUROLOCOMOTOR SYSTEMS

Zhijun Yang

December/1999

Advisor: Felipe Maia Galvão França

Department: Computing and Systems Engineering

As an engine of almost all life phenomena, *Oscillatory Neural Networks* play a crucial role in the activities of all animals. After reviewing on some new research results on locomotor *Central Pattern Generators* (CPGs), which is a concrete branch of studies on *Oscillatory Neural Networks*, this thesis presents a novel, macroscopic and model-independent approach for the retrieval of coupled neural oscillations observed in biological CPGs during the control of walking. Based on *Scheduling by Multiple Edge Reversal* (SMER), a simple and powerful distributed synchronizer, various *Oscillatory Building Blocks* (OBBs) can be configured for the production of complicated rhythmic patterns and a methodology is provided for the construction of a target artificial CPGs architecture behaving as a *SMER-like asymmetric Hopfield neural networks*.

Conteúdo

Lista de Figuras

Lista de Tabelas

Capítulo 1

Introdução

Análise de andadura é uma ciência antiga. Já à dois mil anos atrás, Aristóteles [4] descreveu o passeio de um cavalo em seu tratado *De Incessu Animalium*: *"As pernas de parte de trás movem-se diagonalmente em relação às pernas dianteiras; depois do movimento de perna dianteira direita os animais movem a perna esquerda traseira, então a perna dianteira esquerda, e depois disto a perna traseira direita.* Porém, ele acreditou erroneamente que o salto era impossível: Se os cavalos movessem as pernas dianteiras ao mesmo tempo e primeiro, a progressão seria interrompida ou eles tropeçariam até mesmo adiante... Por isto, então, animais não moveriam separadamente suas pernas traseiras e dianteiras.

De acordo com uma estória, a análise de andadura moderna originou também com um cavalo: isto é, uma aposta relativa à andadura do animal [73]. Nos anos 1870s, Leland Stanford, ex-governador do estado da Califórnia, foi envolvido num argumento com Frederick MacCrellish sobre o posicionamento dos pés de um cavalo trotando. Stanford pôs 25,000 dólares em sua convicção de que às vezes durante o trote um cavalo coloca todos os seus pés fora o solo. Para realizar a aposta, um fotógrafo local, Eadweard Muybridge, foi requisitado a fotografar as diferentes fases da andadura de um cavalo. De fato, Stanford estava correto na afirmação corajosa dele [21].

As percepções do Aristótele e Stanford em andaduras do cavalo podem ser entendidas como representações clássicas das idéias embrionárias que guiam os estudos modernos da formação dos padrões. Depois do caso de Stanford, seguiram-se aproximadamente oitenta anos de tempo silencioso até os anos cinqüenta, quando Turing [75] analisou anéis de celas como modelos de morphogenesis e propôs que aqueles anéis isolados poderiam responder pelos tentáculos de hidrante e enrolamento de folhas de certas plantas. En-

quanto isso Hodgkin e Huxley publicaram um interessante artigo [50] sobre um circuito e modelo matemático do potencial de membrana de superfície e corrente de uma fibra de nervo gigante. A história nunca tinha visto uma era tão próspera no desenvolvimento de ciência e tecnologia durante os recentes quarenta anos. Com a explosão de métodos e técnicas computacionais, nasceram muitas grande interdisciplinas científicas como *redes neurais* e estas cresceram incrivelmente. Obviamente não é nenhum exagero dizer que os trabalhos pioneiros de Turing et al. em formação de padrões são o berço de conexionismo moderno. Também é interessante notar que as aproximações micro e macroscópicas coexistiram desde a fase inicial da pesquisa moderna sobre padrões rítmicos biológicos, da mesma maneira que os dois exemplos acima estabelecem.

1.1   Motivações nas Pesquisas sobre Padrões Biológicos

Assuntos biológicos relacionados, incluindo inteligência biológica e fenômenos de comportamento, foram mantidos indubitavelmente como um dos assuntos mais ativamente investigados, como resultado do aparecimento de modernas metodologias de pesquisa científica. Por exemplo, *Inteligência Artifical* e *Redes Neurais Artificiais* são inspiradas pelos fenômenos biológicos. Diferentemente do mecanismo implícito das atividades inteligentes, a existência do comportamento biológico é explícita e visível, porém, de modo algum, significa que a pesquisa de comportamento é um trabalho trivial.

Para realizar um análogo artificial para exploração adaptável da natureza, comportamentos rítmicos tais como locomoção, respiração, pulso de coração e mastigação foram estudadas intensivamente como exemplos de sistemas biológicos de motor complexo [37][63][13].

Apesar da diversidade de ritmos e movimentos exibidos, não só em um único organismo mas também por espécies, a geração de movimentos rítmicos compartilha um base neuronal comum [38], isto é, o animal poderia produzir comportamentos bastante diferentes por modulação contínua de uma única rede [47]. Esta declaração heurística é fundamental para pesquisas futuras sobre neurolocomoção e sua implementação possível em VLSI.

2

1.1.1 Padrões rítmicos em ANNs Biológicas

Acredita-se amplamente que a locomoção de animais é gerada e controlada, em parte por *Central Pattern Generators* (CPGs), os quais seriam redes de neurônios no Sistema Nervoso Central - CNS (*Central Nervous System*)capazes de produzirem saída rítmica. Técnicas atuais de neurofisiologia são incapazes de isolar tais circuitos de conexões neurais complicadas em animais complexos, mas a evidência experimental indireta para a existência de GPCs é forte [44][45][64][70].

Padrões rítmicos biológicos são as saídas de sistemas neuro-osciladores governadas por CPGs. O estudo de CPGs é um ramo interdisciplinar da computação neural que envolve matemática, biologia, neurofisiologia e ciência da computação. Embora o mecanismo de CNS explicando os CPGs não seja bastante claro até agora [23], *Redes Neurais Atificiais* - ANN -(*Artificial Neural Networks*) tem sido amplamente aplicadas para mapear a possível organização funcional de redes CPGs em sistemas de motor muscular orientado à locomoção.

Os componentes do sistema locomotivo motor são osciladores não lineares acoplados e representam *flexor* e *extensor* como dois neurônios simplificados neurofisiologicamente. Tipos diferentes de neuro-osciladores podem ser escolhidos e organizados em um modo acoplado projetado e normalmente com a topologia satisfatóriamente amoldada para simular a locomoção de animais parecidos [56][74][10]. Todos os parâmetros internos e pesos de conexão acopladas da rede osciladora são controlados pela entradas externas, instruções do CNS e pela própria rede. *Processamento Paralelo e Distribuído* - PDP - (*Parallel and Distributed Processing*) é a característica mais eminente deste circuito oscilatório que pode ser canonicamente descrita por um grupo de *Equações Diferenciais Ordinárias* - ODE -(*Ordinary Differential Equation*) como um sistema autônomo. Em outras palavras, um sistema gerador de ritmos biológicos, i.e., CPGs e redes oscilatórias, pode ter uma implementação artificial concreta como uma ANN.

1.1.2 Implementação de CPGs Artificiais como Sistemas Restritos por Vizinhança

Do ponto de vista filosófico, o mundo está repleto de sistemas restritos-por-vizinhança, talvez o maior sistema restrito-por-vizinhança seja o próprio universo [35]. Para nosso

caso de CPGs compostos de conexões de neurônios puramente inibitórios [1] que é essencialmente um sistema restrito-por-vizinhança, o método de pesquisa tradicional é investigar ODE ou PDE estabelecido para todos os neurônios. A solução numérica precisa para um grupo de ODE não tem um significado físico explícito, no sentido de que um estado fixo definido de locomoção normalmente corresponde a um padrão periódico estável. Além disso, é difícil construir um grupo de ODE que represente uma arquitetura de CPGs complicada com várias soluções periódicas para várias andaduras. Assim, análise qualitativa dinâmica poderia ser uma estratégia muito mais popular que aproximação numérica quantitativa.

Porém, por causa da complexidade do sistema neuronal locomotor, descrições matemáticas precisas são normalmente impossíveis, de modo que simplificações devem ser feitas. Como uma alternativa, uma série de fundamentos e algoritmos modernos utilizando PDP, que seriam *Scheduling by Edge Reversal* (SER) e *Scheduling by Multiple Edge Reversal* (SMER) [7] [35], mostram-se eficientes especialmente tratando CPGs cuja topologia seria representável. Adotando um esquema auto-temporizado, que é uma técnica chave na aproximação de SER/SMER, sistemas de CPGs em alta-escala podem ser construídos naturalmente, com imunidade de *fome* (*starvation*) e *bloqueio perpétuo* (*deadlock*), ou melhor dizendo, estes CPGs construídos artificialmente podem operar sem problemas indesejados.

Como sabemos, qualquer atividade no mundo físico poderia ser expressa e investigada em um eixo espaço-temporal. As perguntas tempo-relacionadas são tópicos eternos comum a todos os problemas científicos. É comum em trabalhos de pesquisa perguntar algo como " Quando será/foi isto..."?, como nas vidas ordinárias. Em nosso campo acadêmico, onde estudamos sistemas distribuídos compartilhando recursos atômicos e sua implementação em forma de circuitos eletrônicos, o esquema de temporização possui uma função crucial no sentido de que sistemas e circuitos normalmente são classificados em modos de operação como síncronos e assíncronos de acordo com os padrões pelos quais as informações dos sistemas ou circuitos poderiam ser processadas e trocadas. Não importa que tipo de esquema de temporização um sistema compartilhando recurso poderia adotar,

---

[1]Os neurônios dentro CPGs pode ser acoplado com tipos de conexão diferentes, por exemplo, excitatório, inhibitório ou conexões híbridas. Sem perda de generalidade, nós poremos muito mais ênfase nas conexões inibitórias.

(i) concorrência, (ii) bloqueio perpétuo, e (iii) fome são as principais preocupações nas estratégias de escalonamento para tais sistemas. Naturalmente, concorrências deveriam ser maximizadas enquanto bloqueio perpétuo e fome devem ser eliminadas [35].

Baseado nestes fundamentos, SER, estudado por Barbosa e Gafni [6], fornece uma solução potencialmente ótima para o *problema dos filósofos jantando* de Dijkstra que é um problema de compartilhamento de recursos canônico. SER foi inventado na suposição de que os sistemas designados estavam debaixo da alta carga e em ambientes restritos-por-vizinhança, isto é, processos estão constantemente exigindo acesso a *todos* os recursos compartilhados, e processos vizinhos no sistema têm que se alternar em suas vezes para operar. Este mecanismo de escalonamento foi demonstrado como tendo o potencial para prover a maior concorrência entre os esquemas de escalonamento com característica de restrição-por-vizinhança, enquanto também é capaz de evitar problemas tradicionais como bloqueio perpétuo e fome.

Como um primeiro estudo, SMER, uma generalização de SER, foi proposto por França para modelar prioridades de operação diferentes entre processos coexistindo em um sistema restrito-por-vizinhança concorrente [35]. Diferente da definição de alta carga que SER possui implícito, a *justiça* [2] é um das considerações básicas de estratégias de escalonamento para sistemas compartilhando recursos, SMER permite a modelagem de políticas de escalonamento *injustas*. A suposição de alta carga na definição original de SER é relaxada para modelar processos com prioridades de acesso diferentes aos recursos compartilhados. Com SMER é possível aos processos operar com freqüências diferentes sem comprometer as propriedades de *fome-livres* e *paralisações-livres*. Em descrição adicional, veremos a fundo como SER/SMER e as metodologias de otimização e implementação relacionadas a eles podem ser utilizadas como uma ferramenta de reconstrução para nossas pesquisas de formação de padrões [36].

Postinhibitory Rebound (PIR) é adotado para explicar o mecanismo de fuga de muitos sistemas motores biológicos que oscilam alternativamente [38] [3]. Este mecanismo simples pode ser descrito como um par de neurônios acoplado e oscilando alternadamente: um deles é ativo enquanto o outro é refratário. Para uma cela inativa, seu potencial

---

[2]Uma operação é uma ação do nó na transição do estado *ativo* para *inativo*. Sob SER, a justiça pode ser entendida como que, qualquer nó da uma rede não pode operar menos que todos os outros nós observando-se o sistema durante um tempo relativamente longo.

é fortemente inativado de forma que uma hiperpolarização de duração e amplitude sufi-
ciente é requerida para desativar o potencial e assim produzir um potencial despolarizado
transitório e *excitação de rebote* depois da remoção da hiperpolarização [77]. Este meca-
nismo tem uma equivalência quase direta com sistemas SER/SMER-dirigidos no sentido
de que cada nodo inibe a operação simultânea de todos seus nodos vizinhos que, ao seu
redor, o estimularam a operar ao final da operação do nodo inibido durante esse intervalo
[35]. A Figura 1.1 é a demonstração gráfica desta idéia.
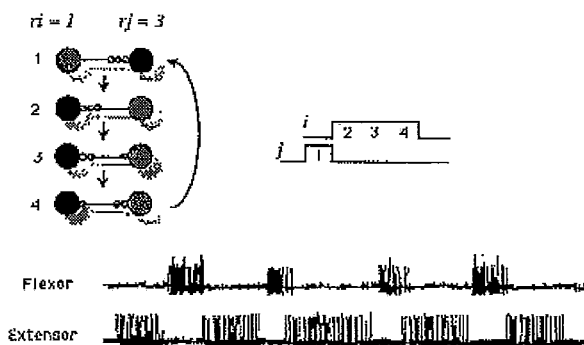
Figura 1.1: Imitando CPGs com redes SER/SMER-dirigidas - atividade de neurônios motores
de músculo flexor e extensor durante a caminhada de uma barata e sua simulação utilizando
SER/SMER análoga (reproduzido da tese de França [35]).

Outra vantagem da abordagem SER/SMER é que, ao contrário de muitas soluções por
redes neurais tradicionais como a rede de Hopfield [52] que é baseada na conexão global
entre todos os componentes, um neurônio em rede SER/SMER pode ser conectado local-
mente, somente com seus vizinhos acoplados. Esta característica facilitará grandemente
implementações VLSI no futuro.

1.2 Objetivos

Entre os numerosos estudos em comportamento animal, oscilações acopladas e mecanis-
mos de CPGs foram pesquisados (veja Apêndice *B* para referência). No entanto, embora
as tentativas de empregar propriedades emergentes de ANNs nestes estudos pareçam ter
êxito, contribuições aplicáveis na implementação de sistemas neurolocomotores artificiais
são escassas.

Este trabalho propõe uma nova abordagem quanto a previsão ou simulação da
dinâmica de comportamentos oscilatórios complexos baseado em *building blocks*. Como

veremos, podem ser concebidos vários sub-blocos funcionais, isto é *Oscillatory Building Blocks* (OBBs), de acordo com a relação de fase coordenada entre as pernas do animal alvo. Cada building block consiste em dois neurônios, um visando o músculo flexor e o outro o músculo extensor, e são construídos usando estratégia de SER/SMER. Então, via seleção e organização satisfatória de diversos building blocks, diferentes modelos de padrão de andadura podem ser alcançados por recobrar protótipos realistas e facilitar sua síntese em VLSI.
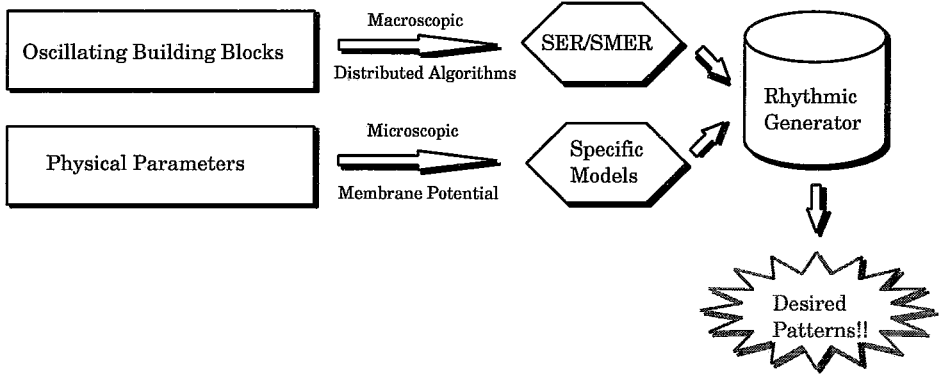
Figura 1.2: Dois fluxos de projeto de aproximação macro e microscópica para reconstrução de modelo de CPGs.

Neste trabalho, nós recorremos à *Teoria da Representação de Grupos* [42] como uma solução matemática formal para os problemas de geração dos padrões de andaduras dos animais, onde o esquema de SER/SMER está no papel da máquina de dinâmica de grafos, ou o núcleo da implementação. Nós mostraremos que estes dois métodos podem ser combinados perfeitamente devido que todos eles dependam da expressão da topologia dos objetos. Este método híbrido é considerado como *macroscópico*, no sentido de que em ambos, computação distribuída e teoria de grupo (que não se envolvem nos detalhes da dinâmica), o objetivo comum é o comportamento global de uma rede de neurônios. A expressão da topologia dos objetos deveria conter as relações de fase ou temporização rotuladas explicitamente, com os parâmetros de resultado da análise de teoria de grupo e os parâmetros de entrada do estágio de implementação.

Outra possível abordagem que é considerada como estratégia *microscópica* pode ser induzida de *Cellular Neural Networks* (CNN), um circuito não linear proposto inicialmente em 1988 [16][17] com a capacidade de produzir muitos fenômenos dinâmicos. O sistema completo geralmente é descrito por um grupo de ODE autônomo, embora o tem-

7

po não seja expresso explicitamente, representa um papel importante no comportamento dinâmico. Fazendo proveito da característica de conexão local possuída por CNN, que é um pouco análogo com a máquina dinâmica dos algoritmos SER/SMER, algumas formas das ondas bidimensionais e tridimensionais como o *autowave* e *ondas espirais* [19][5] podem ser gerados devido a reação-difusão no meio. A breve introdução de CNN neste capítulo visa dar um exemplo concreto do método microscópico, entretanto esta tese é dedicada às metodologias macroscópicas.

1.3 Trabalhos relacionados

Aqui alguns tópicos teóricos, ou sejam, neurodinâmica e teoria de grupo para bifurcação com simetria e suas aplicações na formação de padrões, são escolhidos para discussão. Além disso, o emergente campo das chamadas CNN será introduzido brevemente em seu grande potencial na dinâmica de padrões, como uma contrapartida à abordagem macroscópica desta tese. É mostrado mais adiante como esses padrões rítmicos gerados pelas bifurcações de Hopf com característica de quebra-de-simetria podem ser sintetizados com redes SMER.

1.3.1 Teoria de Grupo para Bifurcação com Simetria

Entre vários tipos de bifurcações, a bifurcação de Hopf pode ser aplicada com sucesso à análise de diferentes sistemas físicos [58]. A bifurcação de Hopf é uma das fontes mais comuns de estados periódicos em sistemas nonlineares. Porém, bifurcação de Hopf ordinária não pode ser aplicada aos sistemas dinâmicos com simetria devido ao fato que a mesma não pode ser possível para autovalores imaginários simples de acontecer. De fato, quando um sistema tem simetria, os autovalores podem geralmente ser forçados a ser múltiplos [42].

Uma teoria geral de simetrias espaço-temporais em bifurcação de Hopf foi desenvolvida por Golubitsky e Stewart [42]. Tal trabalho provê técnicas abstratas baseadas em teoria de grupo para predizer a ocorrência de combinações particulares de simetrias espaciais e temporais quando uma rede simétrica de osciladores nonlineares sofre bifurcação de Hopf. É concluído que sua análise pode ser aplicada a qualquer sistema dinâmico com

simetria.

Em resumo, o teorema de Golubitsky afirma que para um análogo simétrico de uma bifurcação de Hopf, um ou mais ramos de soluções periódicas, normalmente vários, se bifurque. Estas oscilações podem ser distinguidas por seus grupos de simetria espaço-temporais Σ, os quais são subgrupos do $\Gamma \times S^1$. Os subgrupos isotrópicos medem a quantidade de simetria presente nas soluções de ramo. O problema da existência de simetria-quebrando oscilações é reduzida assim para cálculo da teoria de grupo puramente e só depende da simetria assumida no sistema. O ponto principal aqui é que os padrões de oscilação típicos do sistema podem ser preditos em termos de suas simetrias, sem investigar os detalhes de suas equações dinâmicas .

Uma aproximação geral para estudar osciladores biológicos acoplados foi proposta por Collins e Stewart, que utilizou teoria de grupo na natureza, baseado no achado de que cadeias de aneis simétricos de osciladores nonlineares acoplados possuem padrões genéricos de oscilações de fase-fechadas [22][23]. A análise associada é independente dos detalhes matemáticos da dinâmica intrínseca dos osciladores e a natureza do acoplamento entre eles, desde que eles adotaram a metodologia de bifurcação de Hopf com simetria de Golubitsky. Esta abordagem provê um trabalho para distinguir o comportamento da dinâmica universal dado que depende de estrutura simetria adicional. Como discutido, transições entre padrões diferentes de atividade, por exemplo, a transição de andadura de um animal, pode ser modelada como bifurcação de Hopf com quebra-de-simetria.

1.3.2 *Cellular Neural Networks*

Desde sua invenção em 1988, *Cellular Neural Networks* tem sido utilizada em vários campos, tais como processamento de imagem, formação e reconhecimento de padrões [16] [17], e muitas outras pesquisas relacionadas com sistemas dinâmicos. A unidade de circuito básico das CNN é chamada de *célula*, que contém elementos de circuitos lineares e não lineares que tipicamente são capacitores e resistores lineares, fontes lineares e não lineares controladas, e fontes independentes não lineares.

Como um modelo geral, CNN possui a característica chave das redes neurais artificiais, isto é, processamento paralelo assíncrono, com dinâmica de tempo continuo; embora substituindo a interação global dos elementos das redes neurais, CNN mantêm uma

arquitetura de conexão local dentro dos vizinhos mais próximos. Projetando e ajustando os *modelos clones* dos operadores das células interativas da CNN, vários tipos de saídas, incluindo ordenadas e caóticas, podem ser geradas refletindo a relação entre a entrada, estados internos e a saída dos parâmetros de espaço. Por exemplo, em uma aplicação em processamento de imagem, definindo alguma função de restrição, se tivermos um estado inicial $|V_{xij}(0)| \leq 1$, depois da dinâmica, adquirimos um estado de equilíbrio $\left|V_{xij}^{\star}\right| > 1$, e a saída será $(-1,1)^{M \times N}$. Isto significa que foi obtida uma matriz $M \times N$ com todos os dados que são ± 1 nisto, onde cada elemento da matriz representa um pixel em uma imagem preta e branca.

Como redes neurais, CNN é um circuito analógico não linear em largo escalo que processa sinais em tempo real. Como automata celular, CNN é feito de um agregado volumoso de clones de circuito regularmente espaçados, chamadas células, que comunicam-se com outros diretamente apenas através de seus vizinhos mais próximos [16] [18]. Assim, CNN compartilha as melhores características de ambos os mundos e sua característica de continuidade no tempo permite o processamento de sinais em tempo real procurado no domínio digital e sua característica de interconexão local torna-a implementável em VLSI.

1.4   Esboço da Tese

Antes de entrar em uma visão mais detalhada dos conteúdos de cada capítulo e apêndice seguinte, uma explicação sobre a estrutura básica do trabalho inteiro será oferecida aqui. São distribuídas as contribuições práticas e teóricas entre apêndices diferentes de modo a tornar ao máximo cada apêndice auto-contido em seu tópico específico baseado na linha principal da computação paralela de geração de andadura animal. Por exemplo, o Apêndice C provê um método de geração de andadura na visão macroscópica através da aplicação de algoritmos SMER, uma pessoa também pode obter só algumas percepções úteis do seu conteúdo de um ponto de vista de passatempo. Como um tratamento formal para os fenômenos biológicos, esta tese é organizada em um estilo rígido com todos os fenômenos descritos formalmente.

O Capítulo 2 apresenta a conclusão desta tese. Uma avaliação global é feita e é seguida

por alguma discussão na relação entre os temas principais deste trabalho e certas atividades em estudos neurobiológicos encontradas na literatura, como a análise de andadura. Também são apresentadas sugestões para trabalhos futuros.

O Apêndice A introduz dois modelos teóricos importantes: Teorema da Bifurcação de Hopf Equivariante e o mecanismo de SER/SMER. Na Seção $A.2$ existe uma descrição detalhada do teorema da bifurcação de Hopf equivariante, incluindo o conhecimento necessário de teoria de grupo. Seção $A.3$ contém os princípios das estratégias de SER/SMER. Um resumo é determinado na Seção $A.4$. Embora ambos sejam necessários para entender as declarações dos apêndices subsequentes, a aplicação do algoritmo de SMER em geração de andadura é uma ênfase da tese.

O Apêndice B é uma introdução do estado-da-arte de pesquisas recentes em neurolocomoção, do ponto de vista dos aspectos macroscópicos e microscópicos. Ele inclui alguns modelos dinâmicos da formação de padrões que é utilizada amplamente, e o estado recente das pesquisas em andadura. Seção $B.2$ enumera os modelos mais populares de neuro-oscilador. Seção $B.3$ esboça brevemente alguns resultados atuais em pesquisa de andadura, especialmente com o método macroscópico. Seção $B.4$ exemplifica um modelo moderno que é desenvolvido em teoria de grupo e teoria da bifurcação como uma plataforma física de computação paralela.

O Apêndice C apresenta a primeira aplicação do algoritmo de SMER em pesquisa de andadura, empregando vários casos de estudo de animais hexapodais para os quais é mostrado, do ponto de vista macroscópico, que a dinâmica SMER é um mecanismo satisfatório em imitar a computação neuronal assíncrona com características discretas em larga escala. Seção $C.4$ contém uma estratégia baseada na SMER para robôs com pernas.

O Apêndice D apresenta um modelo de rede neural artificial com características de tempo contínuo e estado contínuo que se comporta como o mecanismo distribído de SMER a qual, como uma rede de Hopfield assimétrica, conserva todas as características das redes neurais artificiais tais como o processamento paralelo e auto-organização. Este novo modelo de rede estende a dinâmica de SMER do domínio de análise discreto para o domínio de sistema autônomo contínuo onde uma rede neuronal oscilatória que se comporta como SMER pode ser formulada para muitos padrões organizados complexamente. Uma descrição rígida e detalhada da conversão SMER-ANN está disponível ao

longo deste apêndice.

São apresentadas muitas andaduras diferentes no Apêndice *E* através de um método unificado induzido a partir das redes neuronais propostas anteriormente. A partir deste apêndice pode-se verificar que os padrões rítmicos biológicos arbitrários podem ser controladas por um mecanismo unificado que é conhecido amplamente como CPG. Neste apêndice o novo modelo, chamado *SMER*-like asymmetric Hopfield neural networks, provê uma simulação perfeita da funcionalidade dos CPGs biológicos.

Capítulo 2

Conclusão e Estudos Adicionais

Esta tese apresenta uma aproximação distinta de ponto-de-visão macroscópico, baseado em computação paralela ampla exercitada em espécimes biológicas com pernas. O significado deste método macroscópico e modelo relacionado é duplo. Primeiro, é possível aplicar o método macroscópico e modelo relacionado diretamente em recobrar cada andadura de um animal independentemente, como mostrado no Apêndice 5; segundo, este método enfatiza em prover uma simulação geral e de espectro inteiro de qualquer tipo de andadura sem os limites de modelos matemáticos. A presunção exclusiva em relação ao objeto é saber sua existência espaço-temporal.

2.1   Avaliação

Em consistência com a contribuição de trabalhos originais de Barbosa e França [6][35], a motivação central desta tese é o conceito de sistemas vizinhança-constrangidos que apóiam implementação maciçamente paralela e distribuída de ANN modelos. Um modelo geral que pode produzir numerosos padrões rítmicos biológicos foi desenvolvido como redes neurais de Hopfield modificadas combinando método de computação de SMER. No Apêndice 5 foi mostrado que este modelo é capaz de recuperar todos os padrões de andadura propostos pela teoria de geração de padrão geral do Golubitsky através do cálculo de matrizes amplas em ambiente de equações discretas. Uma descrição matemática precisa é determinada no Apêndice 4 para construir tais redes neurais oscilatórias bem como projetar equações de sistema e matrizes de parâmetros críticos.

A característica mais significante de redes neurais de Hopfield modificadas, ou redes neurais assimétricas de Hopfield combinando SMER em sentido mais geral, fica em que

cada entrada booleana de cada macroneurônio pode influenciar sua saída significativamente por causa da relação de multiplicação entre entradas e saída de macroneurônios. Porém, a influência de uma entrada sozinha da célula da rede de Hopfield tradicional pode não ser determinante para a sua saída, a influência pode ser só gradiente a menos que a acumulação de valores de entradas de uma célula tenha ultrapassado o limiar dela que conduz a uma mudança de saída abruptamente.

As contribuições principais deste trabalho podem ser resumidas da seguinte forma:

1. Um modelo geral de ANN embutindo algoritmo de SEM/SMER foi proposto. Foram demonstradas definições preliminares que incluem exigências de topologias básicas e as características de novas redes.

2. As equivalências entre o modelo de ANN novo e as funcionalidades plausíveis de CPGs foram produzidas. Mostraram-se OBBs básicos e compostos para padrões rítmicos diferentes especialmente eficientes em construir o sistema discreto interno-analógico, externo-booleana com características de ego-cronometrado e implementação extremista-ampla de redes neurais oscilatórias.

3. A estimação e conexão nova entre ANN e teoria computacional paralela e distribuída foram feitas com exatidão matemática. Uma estratégia generalizada e distribuída para atualizar o controle na implementação de sistemas neurais paralelos foi definido ainda consistentemente com as contribuições de [35]. Domínios temporais e de espaço de padrões rítmicos biológicos eram integrados em uma esquema generalizado atualizado. Também foram abordados aspectos de consistência de sistemas SMER-dirigidos com topologias dinâmicas.

4. As simulações numéricas ilustraram a eficiência deste modelo de ANN na recuperação de padrões rítmicos biológicos, i.e., o comportamento de locomoção comum. Um procedimento completo, de aspectos teóricos e aplicáveis, é ilustrado com ajuda de conceitos matemáticos como a teoria de grupo.

2.2 Efetividade do Modelo

Embora a prova fisiológica direta da existência de CPG seja difícil, muitos cientistas demonstraram as possibilidades de sua existência. A análise de andadura clínica é, por exemplo, um dos tópicos favoritos em centros médicos no mundo inteiro. Como um resultado de pesquisa, é bem conhecido que o *centro de pressão* (CoP) oscila aproximadamente com o *centro de massa* (CoM) enquanto uma pessoa está ficando de pé estaticamente. Devido às demoras de condução de CNS para a estrutura muscular (principalmente tornozelo) da perna, uma demora de fase entre CoM e CoP deveria ser perceptível se um processo de controle central estivesse ativo [80]. Num experimento administrado recentemente por um grupo de pesquisa, um voluntário ficou de pé em um par de plataformas de força e voluntariamente balançou para trás e para frente, lentamente, sincronizado por um metrônomo. O CoM era medido usando um sistema com 6 câmeras de Vicon e modelo de corpo inteiro de BodyBuilder [29]. Pela lógica acima, poderia ser esperado ver um atraso de fase (tempo), provavelmente ao redor 150-250 ms, entre CoM e CoP dado que o movimento foi gerado conscientemente pelo voluntário. Porém, como podemos ver na Figura 2.1, não há nenhum atraso de tempo (atraso de fase) entre os dois sinais.
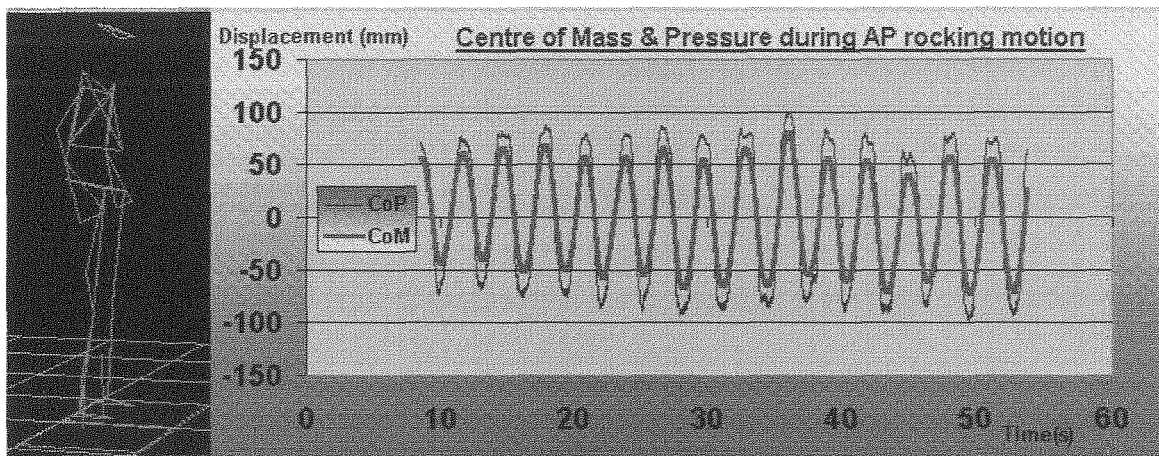
Figura 2.1: A relação de fase entre CoP e CoM da posição estática de uma pessoa.

Uma explicação razoável pode ser que, o significado biológico de atraso de fase pode ser dupla na sensação que, se o voluntário é consciente do movimento dele durante posição estática, parece que deveria existir algum atraso por causa da demora de condução do CNS; caso contrário o comportamento dele poderia ser controlado por CPG, um orgão

15

biologicamente plausível de padrão pré-programado ou estrutura equivalente provavelmente localizada na corda espinhal. Neste caso o atraso poderia ser desprezível. Baseado nesta suposição, o modelo de CPG introduzido nesta tese seria especialmente valioso para recuperar padrões biológicos, como nós esperamos.

Esta tese provê uma arquitetura e metodologia geral em modelagem de andadura em um estilo coincidente, sendo que algumas modificações adicionais podem ser esperadas enquanto a pessoa emprega este método em assuntos relacionados com desenvolvimento individual de andadura. Por exemplo, no projeto de um robô com cada perna (ou dizendo juntas) tendo múltiplos graus de liberdade, a pessoa pode considerar organizar uma rede de OBB para cada junta e fazer conexões entre todas as redes de OBB. Deste modo uma arquitetura de CPG diferente é concebível, mas ainda baseado nas *SMER*-like asymmetric Hopfield neural networks, que é o modelo geral.

2.3 Trabalhos Futuros

Como uma aproximação recentemente proposta em estrutura de CPG e computação biológica, haverá alguns trabalhos adicionais para explorar. Um dos trabalhos previsíveis é determinar características dinâmicas de modelos de OBB em uma armação matemática mais detalhada, por exemplo, a investigação de estabilidade de sistema analisando as características de simetria de matrizes de parâmetros de sistema.

Há outra direção interessante na qual a metodologia geral de *SMER*-like asymmetric Hopfield neural networks pode ser aplicado e pode ser melhorado. Como um dos objetos desejados desta tese é prover uma estrutura de redes reconfiguráveis em OBBs simples e composto, uma arquitetura de CPGs acoplada específica deveria ser construída de acordo com o espécime diferente sob pesquisa. Falando de modo geral, quanto mais informações detalhadas na arquitetura de CPGs, tal como o número de neurônios ou situação acoplada, são determinadas, mais percepções podem ser obtidas para melhorar as características do modelo como tolerância de erro. No apêndice 5. as andaduras de bípede são recuperadas com um modelo composto asperamente de só quatro macroneurônios para a oscilação de relaxamento das duas pernas, porém, é possível trabalhar um modelo muito mais detalhado que consiste em mais macroneurônios acoplados com uma força de acoplação

diferente. Deste modo uma arquitetura CPGs de bípede pode ter 11 macroneurônios flexores acoplados significando dedões do pé, calcanhares, tornozelos, joelhos, tronco e até mesmo dois braços respectivamente, com a força de acoplação maior entre um par de dedões do pé e calcanhares enquanto o menor entre um par de braços e joelhos. É esperado que o modelo mais detalhado seja mais razoável fisiologicamente na sensação que, lá existe algumas relações de acoplação fracas entre um par de braços e joelhos durante o caminhar, e nenhum grande impacto em locomoção pode ser alcançado depois que dois braços são amputados a menos que algum tipo de instabilidade seja introduzido.

Apêndice A

Background and preliminary studies

A.1 Introduction

Two distinct concepts, i.e., equivariant Hopf bifurcation theorem and scheduling by multiple edge reversal (SMER) are introduced in this appendix as a theoretical background for our pattern generation strategy. SER and SMER mechanisms have been shown to offer a potentially powerful method for simulating physical systems with asynchronous, signal-driven circuits, with special efficiency. For instance, in synthesizing time-evolving, distributed dynamical models [36]. However, since SER/SMER strategies depends heavily on the graph theoretic description, for our realization purpose of various animal gait patterns' generation and transition, it is necessary to build up the general topological models from the corresponding biological prototypes as the first step. In this general, unbifurcated model, we assume that the whole symmetries are retained, i.e., the model can undergo various bifurcations, which are equivalent to various gait pattern transitions, to break some symmetries while keep the others, hence the new gait patterns are generated in the meantime. This transition procedure is called the symmetry-breaking Hopf bifurcation in the sense that, when it proceeds, more and more symmetries are broken and simultaneously more and more complicated periodic movements can be achieved. Theoretically this procedure could continue until the chaotic phenomena are observed.

Equivariant Hopf bifurcation theory, developed by Golubitsky et al., is a formal mathematical method to treat the Hopf bifurcation phenomenon in presence of symmetry [39] [40] [41] [42]. This theory will be exploited as a theoretic background for our pattern formation research. After we've gotten a reasonable explanation of the locomotive mechanism, the following step is, naturally, to take advantage of the dynamical engine
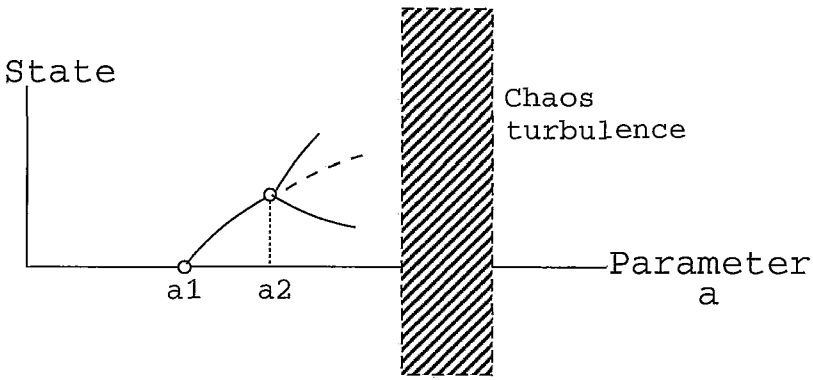
Figura A.1: A demonstration of bifurcation diagram, which shows bifurcation may lead to symmetry-breaking branch and finally chaos.

underlying SER/SMER for implementation purposes. In future works we'll see that this engine is capable of retrieving the whole range of gait patterns, or say, arbitrary gait patterns, without compromising the major feature of the real world such as the distributed and real-time dynamics, provided that the suitable biological building blocks are correctly constructed and configured.

With these ideas in mind, the concepts of the two methodologies are indispensable. This appendix is so organized as following: Section $A.2$ is a brief description of equivariant Hopf bifurcation theory, with Subsection $A.2.1 - A.2.2$ designed as background and basic concepts. The SER/SMER strategies can be found in Section $A.3$, and followed by Section $A.4$, the summary.

A.2 Rationale of the Equivariant Hopf Bifurcation Theorem

A.2.1 Standard Hopf Bifurcation Theorem

The terminology, namely Hopf bifurcation, refers to a phenomenon in which a steady state of a dynamical system evolves into a periodic orbit as a bifurcation parameter is varied. It is the most common source of periodic behavior in nature, and the Hopf bifurcation theorem provides sufficient conditions for determining when this behavior occurs[41].

Linear and Nonlinear examples of Hopf bifurcation

Example 1: Linear system case.

Consider a two order linear dynamical system of ODE

$$dx/dt = f(x,\lambda), f(x,\lambda) = \begin{pmatrix} \lambda & -1 \\ 1 & \lambda \end{pmatrix} x \tag{A.1}$$

With initial condition $x(0) = (a,0)$, it's easy to get the solution as

$$x(t) = (x_1(t), x_2(t)) = ae^{\lambda t}(cost, sint) \tag{A.2}$$

When λ changes, we can get the corresponding phase portrait as Fig.A.2.

(a)   (b)   (c)
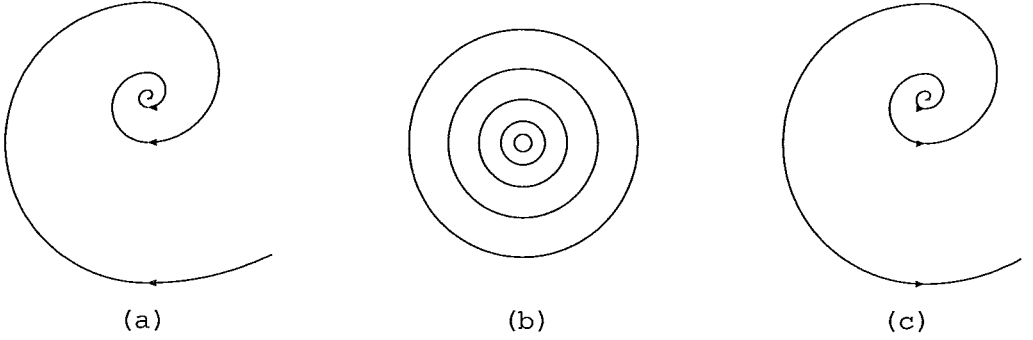
Figura A.2: Phase portraits for a linear ODE. (a) $\lambda < 0$, the steady state $x = 0$ is stable. (b) $\lambda = 0$, the steady state $x = 0$ is center. (c) $\lambda > 0$, the steady state $x = 0$ is unstable.

Example 2: Nonlinear system case.

Consider a two order nonlinear dynamical system of ODE

$$dx/dt = f(x,\lambda), f(x,\lambda) = \begin{pmatrix} \lambda & -1 \\ 1 & \lambda \end{pmatrix} x - |x|^2 x \tag{A.3}$$

or it may be written in another form as

$$\begin{cases} \dot{x}_1 = x_2 - x_1\left(x_1^2 + x_2^2 - \lambda\right) \\ \dot{x}_2 = -x_1 - x_2\left(x_1^2 + x_2^2 - \lambda\right) \end{cases} \tag{A.4}$$

The phase portrait for this system are given in Figure A.3, when $\lambda < 0$, its steady state $x = 0$ is stable; The new phenomenon is that for each $\lambda > 0$ there is exactly one periodic solution of $(A.3)$. Moreover, this periodic solution is stable in the sense that all nearby orbits approach this periodic solution, which is known as a stable limit cycle [1], a more concrete example of this kind can be found in appendix B, the Fitzhugh-Nagumo oscillation model.

---

[1]Roughly speaking, in real life stable oscillation must be produced by nonlinear system. There are nonlinear systems which can go into an oscillation of fixed amplitude and frequency, irrespective of the initial state, this type of oscillation is known as a limit cycle.
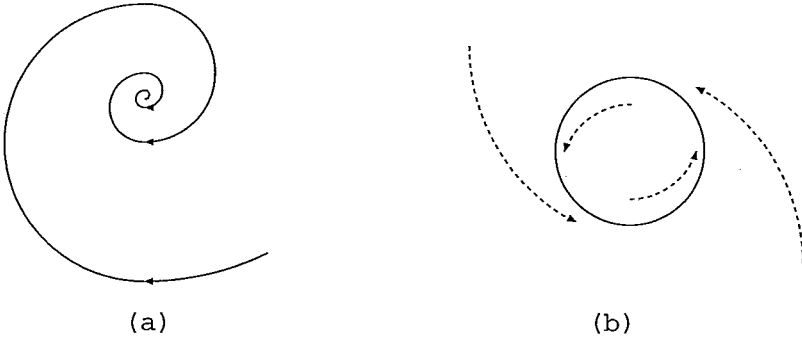
Figura A.3: Phase portrait for a nonlinear ODE. (a) $\lambda < 0$, the steady state $x = 0$ is stable. (b) $\lambda > 0$, the steady state $x = 0$ is unstable, there is a limit cycle formed.

Standard Hopf Bifurcation Theorem

Consider an autonomous system of ODEs

$$dx/dt = f(x, \lambda), f(0, \lambda) = 0 \tag{A.5}$$

where $x \in \Re^n$, $\lambda \in \Re$ is the bifurcation parameter, and $f : \Re^n \times \Re \to \Re^n$ is a smooth (C^∞) mapping defined near $(0, \lambda_0)$. In general f is nonlinear and we suppose $x = 0$ is always a steady state solution for all λ. Let $J(\lambda) = (df)_{0,\lambda}$ be the $n * n$ Jacobian matrix of f along the steady state. There are two main Hopf assumption as following.

The first Hopf assumption is:

- $J(0)$ [2] has simple eigenvalues $\pm i\omega$, and

- $J(0)$ has no other eigenvalues lying on the imaginary axis. (H1)

Normally $J(\lambda)$ has simple eigenvalues of the form $\sigma(\lambda) \pm i\omega(\lambda)$, where $\sigma(0) = 0$, $\omega(0) = 1$, σ and ω are smooth. It implies that the ordinary eigenvalues of $J(\lambda)$ have both real and imaginary parts. The second Hopf assumption is:

- $\sigma\prime(0) \neq 0$ (H2)

It means at the bifurcation point($\lambda = 0$), the imaginary eigenvalues of $J(\lambda)$ cross the imaginary axis with nonzero speed. There are also other two Hopf assumptions, concerning bifurcation directions and stability conditions respectively, but they don't influence the generation of Hopf bifurcation, thus we don't consider them so far.

---

[2] Here, without loss of generality, $\lambda = 0$ is regarded as the bifurcation parameter.

With the assumed system shown above, and specially the two main Hopf assumptions, we've got a sufficient condition for standard Hopf bifurcation to occur, i.e., a branch of small amplitude periodic solutions to $(A.5)$ bifurcates from the steady state $x = 0$ at $\lambda = 0$, the period approaches 2π (or $2\pi/\omega$ if the simple purely imaginary eigenvalues are $\pm i\omega$) as λ approaches 0 [41].

A.2.2   Some Basic Terminologies of Group Theory

There must exist, more or less, some kinds of symmetries in the animal locomotion behavior, e.g., quadrupedal bound gait is symmetric in the sense that two pairs of fore and hind limbs move in phase respectively while half period of phase lag existed between the two pairs. As we'll see, animal's gait transition can be regarded, theoretically, as symmetry-breaking Hopf bifurcation. When more such bifurcations occur, more gait transitions will be achieved, i.e., from the trivial gait to primary gaits, to secondary gaits, ..., and the amount of symmetry in the locomotion structure will also be less and less, at last the chaotic phenomenon can be imagined in theory, which is out of our concerned scope. The amount of symmetry in every bifurcation level can be measured by its relative isotropic subgroups [23], which is a concept in the group representation theory. In order to make precise statements about symmetries, the language and viewpoint of group theory are indispensable as a preliminary study. However, since group theory is a comprehensive mathematical branch, here we'll only investigate our research related topics.

Group

A collection of elements, $\aleph$, will be called a group if its elements A, B, C, ..., can be combined together [3] in a way which satisfies the four axioms:

- Closure. The result of combining operation of any two elements of the group is a unique element which aslo belongs to the group.

- Association. When three or more elements are multiplied, the order of the multiplications make no difference, i.e., A(BC) = (AB)C = ABC.

---

[3]The form of combination is one in which two elements combine together to give a unique third element. Here, this abstract combining operation is called multiplication and denoted as one of any possible combining operation, not a specific or unique combining operation.

- Identity. Among the elements there is an identity element, denoted by I, with the property of leaving the elements unchanged on multiplication, i.e., AI = IA = A.

- Inverse. Each element, A, in the group has an inverse (or reciprocal) A^{-1} such that, $AA^{-1} = A^{-1}A = I$.

A group doesn't need to have an infinite number of elements, e.g., the four elements $1, i, -1, -i$ may form a finite group with multiplication as the law of combination. Part of the fascination that group theory exercises on many people lies in the fact that the whole structure is erected in the logical foundation of these four simple axioms [46]. Thus, group theory can be utilized as a suitable mathematical simplification tool for our symmetry expression of gait pattern research.

Subgroup

When a number of elements selected from a group do themselves form a group, it is known as a subgroup. It is important that subgroup itself must be a group, it should obey the four basic axioms. We can see that the associative law and identity law are inheritable from the parent group, the closure and existence of inverses are, therefore, the only laws that need to be verified individually. Every group has at least one subgroup, namely the trivial one marked as I, consisting of the identity element alone [46].

To find out the subgroup of a spatio-temporal symmetry group is a crucial work for our gait models construction, since theoretically the various subgroups are classified as corresponding gait patterns while their parent spatio-temporal symmetry group is treated as the CPGs collection of the whole locomotion patterns owned by different animals.

There are different manners to determine the subgroups, and different subgroups can be found from a same group, depending on different rules. As an example, one easy way is by forming the powers of an element. The square of an element of a group A is conveniently written in a power notation, i.e.,

$$AA = A^2$$

and, by the associative law,

$$A^2 A = AA^2 = A^3$$

	I	A	A^2	A^3
I	I	A	A^2	A^3
A	A	A^2	A^3	I
A^2	A^2	A^3	I	A
A^3	A^3	I	A	A^2

	1	i	-1	$-i$
1	1	i	-1	$-i$
i	i	-1	$-i$	1
-1	-1	$-i$	1	i
$-i$	$-i$	1	i	-1

Figura A.4: Tabelas de multiplicação de dois grupos isomórficos

Using induction, we can similarly get uniquely defined A^n for interger n. Now assume the group is finite, all these powers of A must belong to the group and, to prevent their number becoming infinite, they must begin to repeat after some point. Suppose there is some integer m such that

$$A^m = I$$

for the first time, so that there is no smaller integer satisfying the same equation. The elements

$$A, A^2, A^3, ..., A^m = I \tag{A.6}$$

then form a subgroup known as the cyclic subgroup generated by A, A is called its generator.

Isomorphism

If A is the generator of a cyclic group of order four[4], marked as

$$\aleph_4 = \{I, A, A^2, A^3\}$$

and i is the generator of a numerical, cyclic group, marked as

$$\aleph_{numeric} = \{i^0, i^1, i^2, i^3\} = \{1, i, -1, -i\}$$

these two groups lead to two multiplication tables of different forms:

It is clear that $\aleph_{numeric}$ is a particular instance of the abstract group $\aleph_4$, or more generally, these two groups are isomorphic in the sense that there is some way of relabelling the elements so that the multiplication tables become identical despite the fact that the elements themselves may be of different natures and also their laws of combination. In

---

[4]The order of a finite group is the number of elements that it contains.

more precise terms, two groups Φ_1 and Φ_2 will be called isomorphic if there is some one to one correspondence between their elements such that, if $f(A)$ is the element of Φ_1 corresponding to A in Φ_2, then

$$f(A)f(B) = f(C) \text{ iff AB=C.}$$

Compact Lie Group

Let GL(n) denotes the group of all invertible linear transformations of the vector space $\Re^n$ into itself, or equivalently the group of nonsingular $n * n$ matrices over $\Re^n$. A linear Lie group can be defined to be a closed [5] subgroup Γ of GL(n). It is a theorem that every compact Lie group is topologically isomorphic to a linear Lie group [41], and Γ is compact if and only if the entries in the matrices defining Γ are bounded. For examples:

Example– The cyclic group Z_n has order n, Z_n may be identified with the group

of $2 * 2$ matrices generated by $\Re_{2\pi/n}$, obviously Z_n is a Lie group.

Example– The dihedral group D_n of order $2n$ is generated by Z_n, together with an

element of order 2 that doesn't commute with Z_n. In other words, D_n may

be identified with the group of $2 * 2$ matrices generated by $\Re_{2\pi/n}$ and the flip:

$$\kappa = \begin{pmatrix} 1 & 0 \\ 0 & -1 \end{pmatrix}$$

obviously D_n is a Lie group and also geometrically D_n is the symmetry group

of the regular n-gon.

Representations and Actions

It is not our purpose to only have some mathematical concepts of group theory, the mathematical method, here the group theory, is used as a formal tool for simplifying our research. In fact, each element in a group denotes an action, or in another point-of-view, a representation. It acts on one definite space to make some transformation, after that a bifurcation occurs and some symmetries are preserved while others are broken.

Let Γ be a compact Lie group and let V be a finite-dimensional real vector space. We say that Γ acts on V if there is a continuous mapping (or action) $\Gamma \times V \to V$, such that:

---

[5]Here "closed" means that the binary operation of any two elements from subgroup Γ will generate the unique element which still belongs to the subgroup itself.
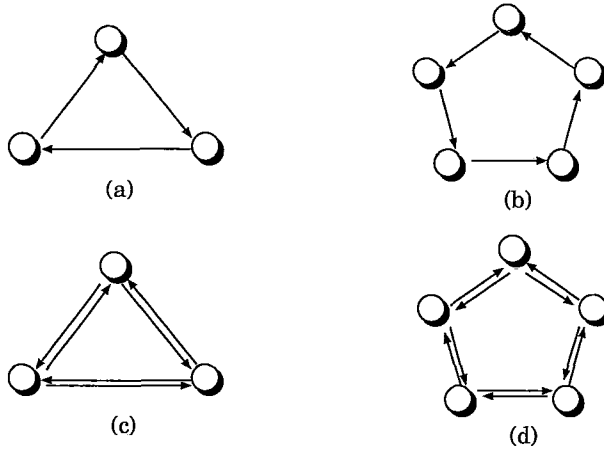
Figura A.5: Graphical representation of symmetric rings of coupled identical nonlinear oscillators. (a) three-membered ring with single coupling (Z_3 symmetry). (b) five-membered ring with single coupling (Z_5 symmetry). (c) three-membered ring with reciprocal coupling (D_3 symmetry). (d) five-membered ring with reciprocal coupling (D_5 symmetry). (reproduced from [23].)

- For each $\gamma \in \Gamma$ the mapping $\rho_\gamma : V \to V$ defined by $\rho_\gamma(v) = \gamma v$ is linear.

- If $\gamma_1, \gamma_2 \in \Gamma$, then $\gamma_1(\gamma_2 v) = (\gamma_1\gamma_2)v$.

The mapping ρ that sends γ to $\rho_\gamma \in GL(V)$ is then callled a representation of Γ on V, GL(V) is the group of invertible linear transformations $V \to V$. It is deserved to notice that linear actions and representations are essentially identical concepts, differing only in point-of-view, in the sense that an action tells us how a group element γ transforms a given element $v \in V$, while a representation tells us how γ transforms the entire space V. For examples:

Example– Every linear Lie group Γ is a group of matrices in GL(n) for some n,

i.e., Γ has a natural action on $V = \Re^n$ given by matrix multiplication.

Example– Every group Γ has a trivial action on $V = \Re^n$ defined by $\gamma x = x$ for all $x \in \Re^n, \gamma \in \Gamma$.

Example– For every integer k the circle group $S^1 = SO(2)$ has an action on $V = C \equiv \Re^2$ defined by $\theta z = e^{ik\theta}z$. Notice that $k = 0$ corresponds to the trivial action of last example.

Irreducibility

The study of a representation of a compact Lie group is often made easier by observing that it decomposes into a direct sum [6] of simpler representations, which are said to be irreducible. It can be proved that the decomposition always exists and, in general it is not unique [42].

Irreducibility

Let Γ be a compact Lie group acting linearly on the vector space V. A subspace $W \subset V$ is called Γ-invariant if $\gamma w \in W$ for all $w \in W$, $\gamma \in \Gamma$. A representation or action of Γ on V is irreducible if the only Γ-invariant subspaces of V are 0 and V. A subspace $W \subset V$ is said to be Γ-irreducible if W is Γ-invariant and the action of Γ on W is irreducible. As an instance, in the last example of subsection "Representations and actions", the actions of $SO(2)$ on $\Re^2$ are irreducible when $k \neq 0$. (if $k = 0$, obviously it is a trivial action and, there exists at least another Γ-invariant subspace such as $\Re$, except 0 and $\Re^2$.)

Absolutely Irreducibility

Let Γ be a compact Lie group acting linearly on V. A mapping $f : V \to V$ commutes with Γ or is Γ-invariant if

$$f(\gamma v) = \gamma f(v), \text{ for all } \gamma \in \Gamma, v \in V. \tag{A.7}$$

According to the definition of Golubitsky [42], a representation of a group Γ on a vector space V is absolutely irreducible if the only linear mappings on V that commute with Γ are scalar multiples of the identity.

Conditions for Imaginary Eigenvalues

It's time to recall the statement for standard Hopf theorem in subsection "Standard Hopf Bifurcation Theorem", but with the presence of symmetry as the modification. Suppose a system of ODEs:

$$dx/dt = f(x, \lambda)$$

---

[6]We say a vector space V is a direct sum of its subspaces U and W, and marked as $V = U \oplus W$ if and only if (i) $V = U + W$, (ii) $U \cap W = 0$.

where $x \in \Re^2$, $\lambda \in \Re$ is a bifurcation parameter, and $f : \Re^n \times \Re \to \Re^n$ is a smooth (C^∞) mapping commuting with the action of a compact Lie group Γ on $\Re^n$. That is,

$$f(\gamma x, \lambda) = \gamma f(x, \lambda), \text{ for all } \gamma \in \Gamma. \tag{A.8}$$

further assume that $f(0, \lambda) \equiv 0$, so there is a trivial Γ-invariant equilibrium solution $x = 0$ for all λ.

Let $(df)_{x_i, \lambda}$ be the $n * n$ Jacobian matrix of derivatives of f with respect to the variable $x_i, i = 1, 2, ..., n$, evaluated at (x_i, λ). The most important hypothesis of the standard Hopf bifurcation theorem is that $(df)_{0,0}$ should have a pair of simple purely imaginary eigenvalues [39][42]. In the presence of a symmetry group Γ, it is not always possible to arrange for eigenvalues of df to be purely imaginary. For example, if Γ acts absolutely irreducible on $\Re^n$, that is, the only linear mapping on $\Re^n$ that commutes with Γ is scalar multiples of the identity, after the derivative of f with respect to the variable X we can get the eigenvalue equation of matrix $(df)_{0,\lambda}$ as,

$$det\left((df)_{0,\lambda} - aI_n\right) = 0$$

where $(df)_{0,\lambda} = kI_n$, for all $\lambda \in \Re$, is a $n * n$ real matrix,

$$det\left(kI_n - aI_n\right) = 0$$

hence the Jacobian matrix $(df)_{0,\lambda}$ has all eigenvalues real. In this case, no stable periodic oscillation can be achieved.

In certain circumstances, however, df can have purely imaginary eigenvalues, the symmetry group Γ often forces these eigenvalues to be multiple, thus the standard Hopf bifurcation theorem cannot be applied directly. Although the symmetries complicate the analysis by forcing multiple eigenvalues, they also potentially simplifying it by placing restrictions on the form of the mapping f. We have seen this in the static bifurcation above, it can also be effectively exploited for Hopf-type bifurcation to periodic solutions. To avoid complicated induction, the necessary conditions for allowing $(df)_{0,0}$ to have purely imaginary eigenvalues are given directly, for the detailed mathematical statements and proofs, see [42] chapter XVI.

For $(df)_{0,0}$ to have purely imaginary eigenvalues, where f is a smooth mapping commuting with the action of a compact Lie group Γ on $\Re^n$, there must be a Γ-invariant subspace of $\Re^n$ which is Γ-simple, i.e., this subspace must take one of the following forms:

a. $V \oplus V$ where V are two isomorphic absolutely irreducible subspaces;

b. W where W is irreducible but not absolutely irreducible.

So far, the occurence of imaginary eigenvalues in equations with symmetry group Γ is investigated, and it is shown that there are nontrivial restrictions on the corresponding imaginary eigenvalue, specifically, it must contain a Γ-simple invariant subspace. Moreover, generically the imaginary eigenspace itself is Γ-simple. Thus for purely imaginary eigenvalues, "Γ-simple" is the equivariant analogue of "simple eigenvalue".

As a conclusion, it is interesting to see the two statements:

1 $(df)_{0,0}$ has purely imaginary eigenvalues $\pm i\omega$

2 the corresponding eigenspace of $(df)_{0,0}$ is Γ-simple.

We can get $(1) \to (2)$, but not $(2) \to (1)$, that is, the so-called condition (2) is truely not a sufficient condition for (1) to occur, we only can regard it as a necessary condition for (1). From the two examples of Chapter XVI, section 1 of [42], we can see that in the presence of symmetry, it is always possible for (1) to occur, but it seems impossible to find the sufficient conditions for (1) to occur since (1) depends strongly on specific models (such as the type of symmetry, ODEs, etc.). In other words, we can also regard the two statements take place in meta-eigenspace, where the eigenspace of statement (1) contains the eigenspace of statement (2), e.g., the multiple purely imaginary eigenvalues case.

Equivariant Hopf Bifurcation Theorem

For system of ordinary differential equations with symmetry, it may no longer be possible for simple imaginary eigenvalues to occur. Despite the limitation, it is possible for such dynamical system to undergo a symmetric analogue of Hopf bifurcation, whereby several

29

branches of symmetry-breaking periodic states (each having prescribed symmetries) bifurcate from a symmetric steady-state. A general theory of equivariant Hopf bifurcation was developed by Golubitsky and Stewart and is summarized as the following.

Let's rewrite the object ODE,

$$dx/dt = f(x, \lambda)$$

Suppose that f commutes with the action of a compact Lie group Γ on $\Re^n$, or say that f is Γ-equivariant, for Hopf bifurcation to occur, the Jacobian matrix $(df)_{x,\lambda}$ must have purely imaginary eigenvalues $\pm i\omega$ at some value λ_0 of λ. Assume that the eigenvalues cross the imaginary axis with non-zero speed. Generically the corresponding eigenspace of the derivative $J = (df)_{x,\lambda_0}$ is a Γ-simple representation; that is, it takes one of the two forms:

- $V \oplus V$ where V is absolutely irreducible, or

- W where W is non-absolutely irreducible.

Assume this generic hypothesis, and assume without loss of generality that $\Re^n$ is the real eigenspace of J for eigenvalues $\pm i\omega$. Define an action of the circle group $S^1 = \Re/Z \equiv [0, T)$ on $\Re^n$ by:

$$\theta x = e^{-2\pi\theta L} \tag{A.9}$$

If $x \in \Re^n$ then its isotropy subgroup $\sum_x \subset \Gamma \times S^1$ is defined to be:

$$\sum_x = \left\{ \gamma \in \Gamma \times S^1 \, | \gamma x = x \right\} \tag{A.10}$$

If $\sum \subset \Gamma \times S^1$ then its fixed-point space is defined to be:

$$Fix\left(\sum\right) = \{ x \in \Re^n \, | \sigma x = x, \text{ for all } \sigma \in \sum \} \tag{A.11}$$

With these assumptions, the equivariant Hopf bifurcation theorem can be stated as:

Let $\sum$ be an isotropy subgroup of $\Gamma \times S^1$ such that $dim Fix(\sum) = 2$. Then there exists a unique branch of small amplitude periodic solutions to formula (2.5) with period

near $2\pi/\omega$, having Σ as their group of spatio-temporal symmetries, where S^1 acts on a periodic solution by phase shift.

The bifurcation branches of periodic solutions are thus distinguished by their symmetry Σ, which are subgroups of $\Gamma \times S^1$. Successive bifurcations tend to break more and more symmetry.

A.3 SER/SMER in Resource-sharing System

A.3.1 Scheduling by Edge Reversal (SER)

Scheduling by Edge Reversal – Fundamental

Based on the graph theory, a potentially optimal scheduling algorithm, namely scheduling by edge reversal (SER) was formulated by Barbosa [6]. Many works have been conducted to show that this scheduling mechanism is very effective for most resource-sharing systems with neighborhood-constrained feature, mainly in the computer science scope. In this work we'll try to demonstrate its capability in the biological-related pattern formation applications, or say, the animal gait pattern generation, which is obviously with the characteristics of parallel and distributed computation.

Consider a system defined by a connected unidirected graph $G = (N, E)$, where N is the finite set of nodes (representing processes) and E the finite set of unidirected edges representing shared resource and their priorities between any two nodes. In the domain of SER/SMER algorithm, it's important to know we'll always assume the acyclic orientation of G [7], then those nodes which have all of their incident edges directed toward them are called *sinks* and marked as $sinks(\omega)$, similarly those which have all of their incident edges leaving from them are called *sources* and marked as $source(\omega)$, where $\omega \in \Omega$. G is said to be connected if for all of its n nodes there is a path to every other node.

The typical environment in which SER works is heavily loaded and neighborhood-constrained, that is, each process is constantly demanding access to an entire fixed subset of resource associated with it in order to operate. The resources of this subset may be associated with many processes but each resource can be used by only one process at a time in a typical mutual exclusion style, so, when a node operates, its neighboring nodes

---

[7]It shouldn't be confused with the symbol Z_n of group theory, which denotes the cyclic symmetry.

must be idle. Systems such as the one described above are representative of distributed resource-sharing environments. Concurrency, deadlock and starvation are the main preocupations of scheduling strategies for such system. Naturally, concurrency should be maximised while deadlock and starvation must be eliminated.

In a synchronous model of distributed computation, SER performs in the following way: starting from any acyclic orientation ω on G there is at least one sink node, that has all its edges directed to itself. All sink nodes are allowed to operate while other nodes remain idle. After operating and before the clock pulse ends, sinks reverse the orientation of their edges by sending messages (or say, releasing the access of resources) to all their neighbors, each one becoming a source. After the next synchronous pulse, new acyclic orientation is defined and the whole process is then repeated for the new set of sinks. Let $\omega_{k+1} = g(\omega_k)$ denote this greedy operation, i.e., for all $k \geq 1$, ω_{k+1} is obtained from ω_k by reversing all sinks. SER can be regarded as the endless repetition of the application of $g(\omega_k)$ upon G. Assuming that G is finite, it is intuitive that eventually a set of acyclic orientations will be repeated defining a period of length p. This simple dynamics ensures that no deadlock or starvation will ever occur since at every acyclic orientation there is at least one sink, i.e., one node allowed to operate. Also it is proved that inside any period every node operates exactly m times, $m \geq 1$ (guaranteed by corollary A.1) [6][7].
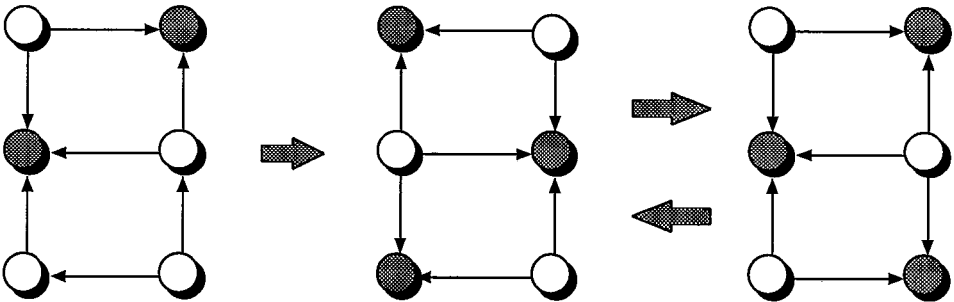
Figura A.6: A graph G under SER, with $m = 1$, operation cycle $p = 2$.

Some fundamental properties of SER lie in Barbosa's original contribution [6]. For descriptive purpose, here we just list them to deepen our understanding on this distributed mechanism.

Lemma A.1 *[6]Let ω and $\omega\prime$ be acyclic orientations of G such that $\omega\prime = g(\omega)$. A sink in $\omega\prime$ has at least one neighbor that is a sink in ω.* ∎

The proof of this lemma comes from the fact that a node cannot be a sink in two consecutive acyclic orientations and on that a source in $\omega\prime$ was a sink in ω. Let $m_i(s,q)$ be the number of times that node $i \in N$ operated in the first q orientations ($q \geq 1$) under schedule s, $s \in S$, where S denotes the set of all schedules. Considering the act of edge reversal as the definition of a node operation, i.e. a sink in an orientation just before ω becoming a source in ω, it is clear that $m_i(s,1) = 0$. The definition of this limit-case is necessary in the following theorems where other fundamental properties of SER are established.

Theorem A.1 *[6](Starvation-freedom theorem). Let the shortest path connecting nodes $i,j \in N$ have r edges, then $|m_i(s,q) - m_j(s,q)| \leq r$ for all $s \in S$ and all $q \geq 1$.* ◗

Theorem A.2 *[6](Greedy theorem). Let s be any schedule starting at ω and s_g the greedy schedule starting at ω, then $m_i(s,q) \leq m_i(s_g,q)$ for all $i \in N$ and all $q \geq 1$.* ◼

These two theorems demonstrate some essential features for any scheduling mechanisms to have. Theorem $A.1$ strongly guarantees starvation-freedom in the sense that every node under any schedule s eventually becomes a sink. Theorem $A.2$ describes the concurrency optimization of the greedy schedules over the other schedules, that is, greedy schedules are the ones in which nodes operate more frequently from any initial acyclic orientation ω.

The application of the stavation-freedom theorem to greedy schedules lead to a further fundamental property described in the following corollary:

Corollary A.1 *[6](Fairness corollary). All nodes become a sink the same number of times in a period.* ◼

Scheduling by Edge Reversal – Concurrency measure

Concurrency measure is the criterion with which we can estimate the degree of exploitation of resources, we normally expect high concurrency in the computer network application. It is obvious that different network (denoted by the graph here) topologies have the different concurrency, even in the same topology but with the different initial

orientations, concurrency is also much different. As an example, we can compare Figure A.6 and Figure A.7.
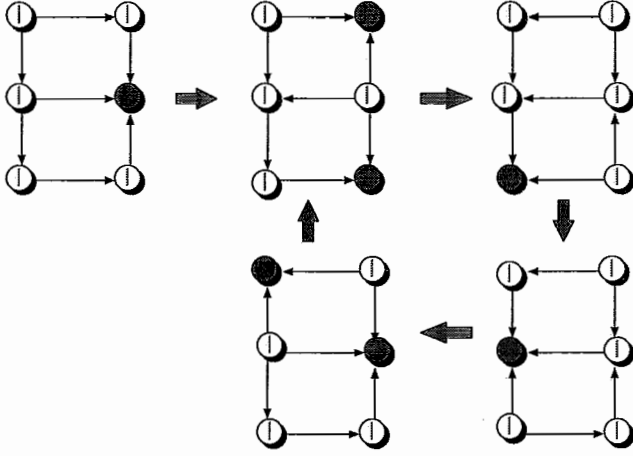
Figura A.7: A graph G under SER, with initial orientation different from Fig.A.6, leads to $m = 1$, operating cycle $p = 4$.

A natural way to define an amount of concurrent operation among processes in a distributed system is to consider the average number of times a node becomes a sink in each of the first q orientations of a generic schedule s. Let γ be a function of the form $\gamma : S \times 1, 2, \ldots \to \Re$ such that $\gamma(s, q)$, which denotes the concurrency available within the first q orientations of schedule s, $q \geq 1$, is given by

$$\gamma(s, q) = \frac{1}{qn} \sum_{i \in N} m_i(s, q)$$

The concurrency of a generic schedule s in the long run is given by $g(s) = \overline{\lim_{q \to \infty}} \gamma(s, q)$. Another concurrency measure is the concurrency obtained from an initial orientation ω defined by the function $\gamma_0 : \Omega \to \Re$ so that $\gamma_0(\omega) = max_{s \in S(\omega)} g(s)$, i.e., the maximal potential amount of concurrency found in any schedule $s \in S$ starting from ω. From theorem 3 it is clear that this maximal potential amount of concurrency is the amount of concurrency of the greedy schedule starting from ω.

Theorem A.3 [6](*Amount of Concurrency theorem*). *Let* $a_0, \ldots, a_{p-1}$ *be a period in which each node operates* m *times, then* $\gamma_0(\omega) = \frac{m}{p}$ *for all* $\omega \in \Omega(a_0, \ldots, a_{p-1})$. ∎

Notice that m, p, and therefore, $\gamma_0(\omega)$, are highly dependent upon an initial ω. Another concurrency-related factor is G's connection as it is intuitive that sparse graphs will tend

to provide greater concurrency than dense ones. For instance, in a completely connected system only one node can be a sink at each orientation, i.e., there is no concurrent orientation among nodes and each node takes n orientations to become a sink. Another extreme example is the case of bipartite graphs where nodes can operate every other orientation, that is, as frequently as possible. From these observations it's easy to induce that for all $\omega \in \Omega, \frac{1}{n} \leq \gamma_0(\omega) \leq \frac{1}{2}$.

A.3.2 Scheduling by Multiple Edge Reversal (SMER)

Zen philosophers problem is initially proposed by França as a variation of Dijkstra's paradigmatic dining philosophers problem [27], and hence scheduling by multiple edge reversal(SMER) is formulated as the generalization of SER algorithm with some conditions modified [35]. In this generalized version, the fairness feature underlying each node's operation in SER is broken and stop to be one of the basic requisites of scheduling strategies for resource-sharing systems, meanwhile the concept of unfairness is introduced, as the major characteristic of a substitute scheduling policy for distributed systems represented as multigraphs. The heavily load assumption in the original definition of SER is relaxed to model processes with different access priorities to shared resources. With SMER it is possible for processes to operate with different frequencies without compromising the starvation-free and deadlock-free properties.

Zen Philosophers Problem

The first original example of França is followed in order to have some idea on SMER. Let's imagine one definite situation and relative rules in the scenery of Zen philosophers problem, that is, two normal philosophers of Dijkstra's original problem are remained side by side along with three Zen philosophers, and instead of a fork, a pair of chopstick will be put on the same place between any two philosophers with an exception that there is only one chopstick between the two normal philosophers. During a meal, both types of philosophers are either *eating* or *thinking* as in the dining philosophers problem. A Zen philosopher cannot eat without a pair of chopsticks in each hand while a normal philosopher has to have at least one chopstick in each hand in order to eat.

With the configuration and rules in Figure A.8, two possible solutions are represented in Figure A.9 and Figure A.10. The example can be described in SER/SMER language as:
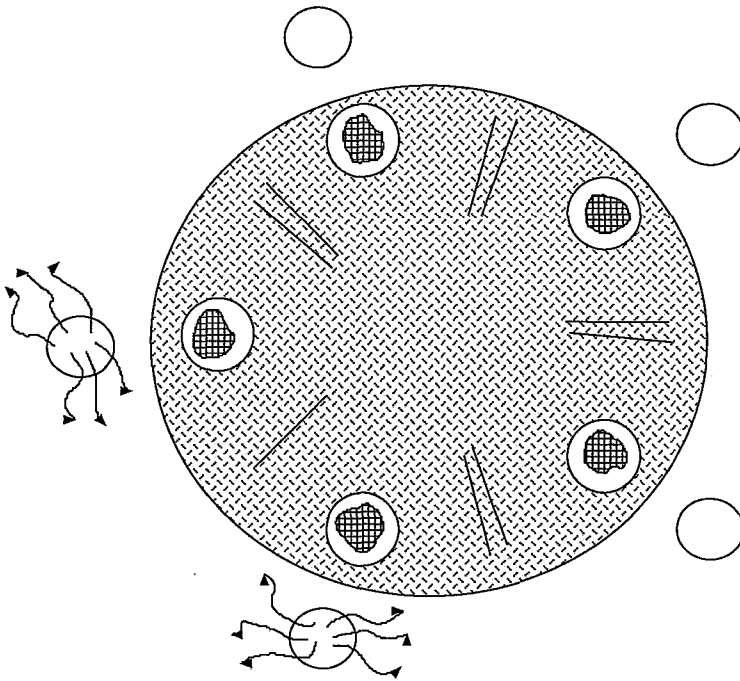
Figura A.8: The Zen philosophers problem (three Zen philosophers and two normal philosophers, reproduced from the PhD thesis of França [35]).

supposing a system under synchronous control or asychronous equivalent to synchronous control, at the end of each time period during which a Zen philosopher has had some food, both pairs of chopsticks are given back to his neighbors. After a normal philosopher has had some food, just one chopstick is given back to his neighbors. Another set of philosophers is enabled to eat after chopsticks have reverted. Similarly to SER, an initial orientation defines a particular periodic scheduling of length p.

The heuristic of Zen philosophers problem is that each node in a resource-sharing system can have different priorities, or say, threshold. When its individual priority is just satisfied (or its threshold has been just reached), this node will operate, after operation it will only release the minimum number of resources, which just allowed it operating, to its neighbors no matter how many resources it may have. In the whole orientations which constitute a period, different node may operate with different frequency, depending on its individual priority. There may also exist some nodes which operate consecutively, a case absolutely prohibited in SER algorithm. However, the access to shared resources in mutual exclusion style remains a fundamental issue and neither deadlock nor starvation can occur in the generalized version. SMER can be simplified to SER by forcing each node to have the same priority, or more exactly, SER is a special case of SMER in the
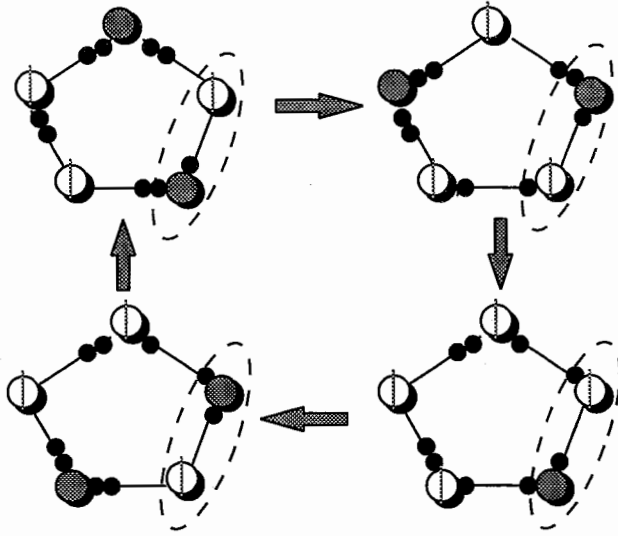
Figura A.9: One solution for Zen philosophers problem depicted in Figure A.8, (Zen philosophers, who are out of the dashed circle: $m = 1$, normal philosophers: $m = 2$) with the shortest $p = 4$.
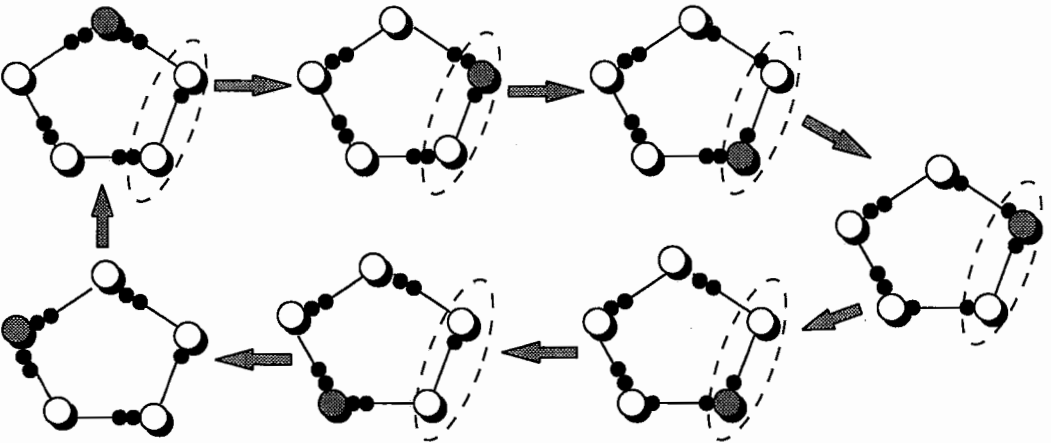
Figura A.10: Another solution for Zen philosophers problem depicted in Figure A.8, (Zen philosophers: $m = 1$, normal philosophers: $m = 2$) with the longest $p = 7$.

sense that for any two nodes $i, j \in N, 0 \leq e_{ij} \leq 1, r_i = r_j = 1$, here r_i, r_j is the reversability[8] of node i and j respectively, e_{ij} is the edge between node i and j [35].

SMER – fundamentals

We've known that SMER is a generalization of SER where a distributed resource-sharing system is represented by a multigraph $M(N, E)$ and instead of representing a shared-resource by a single oriented edge, a number of oriented edges(or little circles as the compact version) can exist between any two nodes. Some qualitative characteristics such as the different operating frequencies have been introduced before, here, we can see quantitatively that the crucial step to avoid starvation and deadlock is to define e_{ij}, the number if edges between any two nodes i and j. The following lemma shows that, to preserve the essential requirements of any useful scheduling strategy for neighborhood-constrained systems, it is necessary to define more precisely some features related to the topology of the multigraph representing that system. In the description of this lemma, gcd is the greatest common divisor and f_{ij} is the sum of the greatest multiple of $\gcd(r_i, r_j)$ that doesn't exceed the number of shared resources oriented from n_i to n_j, and from n_j to n_i, respectively in the initial orientation.

Lemma A.2 *[8] [35]Let nodes i and j be two neighbors in M. If no deadlock arises for any initial orientation of the shared resources between i and j, then* $max\{r_i, r_j\} \leq e_{ij} \leq r_i + r_j - 1$ *and* $f_{ij} = r_i + r_j - \gcd(r_i, r_j)$. ∎

In next appendix we'll have the chance to see that this lemma is a crucial theoretic basis for constructing various biological building blocks, e.g., many biological phenomena such as *postinhibitory rebound* (PIR) and *2:1 frequency-locking* can be successfully simulated using this simple and flexible graph dynamics engine, which leads to reciprocal inhibitory oscillations with different frequencies.

A.4   Summary

The major characteristics of two formal methods are summarised here. Subsection $A.4.1$ is designed in two ways: the theorem itself and its application potential on animal gait

---

[8]The reversability r_i of node i is the number of edges that shall be reversed by i towards each of its neighboring nodes indiscriminately, at the end of an operation.

pattern formation. Subsection *A.4.2* is a brief recall of key points of SER/SMER.

A.4.1 Equivariant Hopf Bifurcation Theorem

As we've seen, the equivariant Hopf theorem is a transformation of the standard Hopf bifurcation theorem in the presence of symmetry, that means, the standard Hopf theorem still serves as the basis of this transformation, where only some conditions and judgements are added/modified for adapting the new situation of symmetry. Let's follow the modification in the next compressed statements.

- The two most important hypothesis for standard Hopf bifurcation theorem to occur is, the Jacobian matrix of an ODE at $(0, 0)$, i.e., $(df)_{(0,0)}$ should have a pair of purely imaginary eigenvalues, and these eigenvalues should pass the imaginary axis with nonzero speed.

- However, in the presence of symmetry, standard Hopf bifurcation theorem cannot be used directly since the symmetry may force the Jacobian matrix of this system to have multiple eigenvalues, or in some cases, even have all eigenvalues real. The latter case corresponds to steady-state bifurcation which doesn't lead to stable periodic oscillations. For the first case, the symmetry will also potentially simplify the analysis by placing restrictions on the form of the mapping f. Roughly speaking, we can always find a Γ-invariant subspace of $\Re^n$ which is Γ-simple, this subspace commutes with the isotropy subgroup (or say, symmetry subgroup) which is a subgroup of symmetry group Γ, and the subspace on which the isotropic subgroup acts is thus called the fixed-point subspace.

- On this local fixed-point subspace, the Hopf bifurcation theorem can be used and a unique periodic solution can be obtained.

In the sense of the gait pattern research, we have the following conclusion.

- Equivariant Hopf bifurcation theorem is a formal mathematical method which can generate almost all kinds of gait patterns with some kind of symmetry, observed or unobserved [43].

39

- Through symmetry-breaking Hopf bifurcation, gait transition can be naturally modelled and various isotropy subgroups may be obtained representing the primary and secondary, etc., gaits.

A.4.2   SER/SMER Strategies

The main features of SER can be summarised as:

- SER is a fully distributed anonymous algorithms, each of the nodes in the system only has knowledge of itself and its neighbors, just a single output message is sent from each node to all of its neighbors.

- The internal operation mechanisms guarantee that SER is a deadlock- and starvation-free scheduling.

- The amount of concurrency of a definite period is defined as $\gamma_0(\omega) = m/p$.

- SER is signal-driven and timing-independent, each node doesn't depend on any global clock in order to execute SER.

SMER is a generalization version of SER where each node of the system can have a different operating frequency.

- Each node in the system has a particular reversibility r_i associated with it, in order to operate this node must have at least r_i edges directed to itself from each of its neighbors and r_i edges are reversed by this node upon operation.

- The number of edges between any two neighboring nodes i and j is given by $e_{ij} = r_i + r_j - gcd(r_i, r_j)$. It garantees that neither two neighboring nodes can operate simultaneously nor can they both refuse to operate [35].

Apêndice B

Review on Neurolocomotion

B.1 Introduction

There are many levels in which one can model neural activity from detailed models of single ionic channel and synapse up to "black box" models used to understand psychological phenomena. An "intermediate" approach to modeling is to use neural networks where each neuron is represented by a low-dimensional dynamical system. Most of the familiar works on neural nets treat their behavior using methods from statistical mechanics. In those models the connectivity between elements has no topological or spatial structure [31]. Another topic on the generation, transition and control of neural rhythmic patterns, which is also developed from the biological point of view and involved in the correlation of *central nervous system* (CNS), *central pattern generators* (CPGs) and muscle motor systems, has gradually gained more and more research interest. The main difference between *Oscillatory Neural Networks* and ordinary *Neural Networks* (NN) is that, the interactions between elements of oscillatory neural networks have some topological structure while NN, as mentioned, are not required to have. So, it determines that the research approaches for neural oscillatory networks will be somewhat different from that of NN's in the sense that, neural oscillatory networks are analyzed using more techniques of dynamical systems, e.g., dynamical pattern formation for the behavior of spatially and temporally organized neuronal structures. Many other techniques, for instance, bifurcation methods, analytic solutions and perturbation methods are widely applied to these models.

Since the biological rhythmic oscillation is a key point in neural oscillatory networks, in this appendix the most famous biological oscillator models are presented and discus-

sed in their formal sense, together with some numerical simulations in the following section. In Section $B.3$ some former, different research approaches on animal locomotion are discussed and commented. In Section $B.4$, a general gait pattern model based on spatio-temporal symmetry group theory is introduced and the relation between this general model and our realization-oriented model is implied. At last, the conclusion of this appendix is given in Section $B.5$.

B.2   Some Canonical Oscillation Models

The biological CPGs, which are usually conceived and designed as a mechanism of coupled oscillatory systems despite that current neurophysiological techniques are still unable to isolate them from the intricate neural connections of complex animals, are widely believed as the pattern source and movement engine for human beings and animals [50][78][60], just like an oscillator is the fundamental component for an electronic circuit to operate. In order to make further neurolocomotion research, it's indispensable to have some background knowledge on modern oscillation theory, which is an important branch of dynamical system theory. In this section, several important oscillation models are outlined in the chronological basis, with the numerical package *XPPAUT* developed by Ermentrout [32]. All the numerical simulations are conducted with fourth-order Runge-Kutta numerical integration method. From these models, we can also perceive that only Wilson-Cowan model emphasize on the interactions between neuronal populations which thus induce oscillations, the other neuronal oscillator models all consider oscillations as an endogenous property of a pacemaker neuron.

B.2.1   Van der Pol's Oscillation Model

In 1926, Van der Pol was involved in the study of oscillations in vacuum tube circuits, he thus proposed a differential equation to describe nonlinear "relaxation oscillators" phenomena as he observed, according to the Kirchhoff's voltage and current laws. This equation, which is called after his name, was intended rather to represent the *qualitative* properties of a wide class of physical oscillators than to give the accurate solutions fit to curves obtained from such oscillators [34]. Van der Pol model is usually used as

a general-purpose oscillator model which may show stable relaxation oscillations. This kind of oscillator may take various mathematical formats, the following is an unforced format of Van der Pol's ordinary differential equations.

$$\begin{cases} \dot{x} = -\epsilon\left(y - x + \frac{1}{3}x^3\right) \\ \dot{y} = \frac{1}{\epsilon}x \end{cases} \tag{B.1}$$

where ϵ controls the degree of "relaxation".

It is convenient to study the characteristcs of Van der Pol oscillator through the phase portrait, the model's chatacteristics are shown in Figure B.1(a) (d) to Figure B.2(a) (d). In the cases of two different values of the parameter ϵ: a small value of 0.2 and a large value of 6.0, the phase portraits show that there is a unique closed orbit called limit cycle which attracts all trajectories starting off the orbit. For $\epsilon = 0.2$ the limit cycle is a smooth orbit similar to a circle. For the large value of $\epsilon = 6$, the limit cycle is distorted, as shown in Figure B.2(a), in this case, the system performs just like a switch, i.e., it switches from one state suddenly to another state as one threshold is reached, hence oscillations with this feature are usually referred as relaxation oscillations.

From the phase portrait of these two cases, we can already imagine the situation shown in Figure B.1(c) (d) and Figure B.2(c) (d), i.e., the sinusoidal-like oscillation can be transferred to relaxation ocsillation as the parameter ϵ becomes large enough. Also from this example, we can see that the limit cycle of the Van der Pol oscillator is stable, in the sense that all trajectories in the vicinity of the limit cycle ultimately tend toward the limit cycle as $t \to \infty$ [55]. Besides the stable limit cycle, there exists one unstable equilibrium point for each case of this VDP oscillator, since the eigenvalues for small and large ϵ case are $0.100000 \pm i0.994987$ and $0.171573, 5.828427$, respectively.
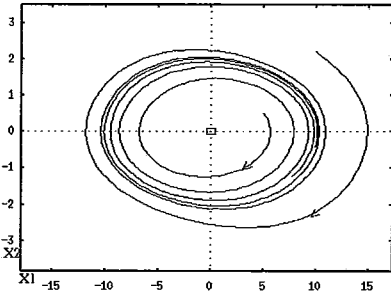
Figura B.1: (*a*). Phase portrait - the limit cycle, inner and outer trajectories with $\epsilon = 0.2$, the little dot is an equilibrium point.
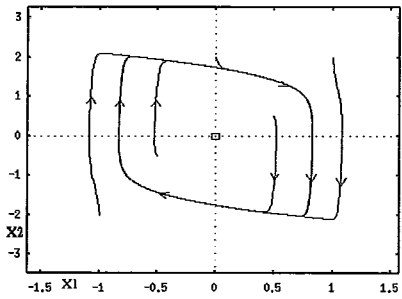
Figura B.2: (*a*). Phase portrait - the limit cycle, inner and outer trajectories with $\epsilon = 6$, the little dot is an equilibrium point.
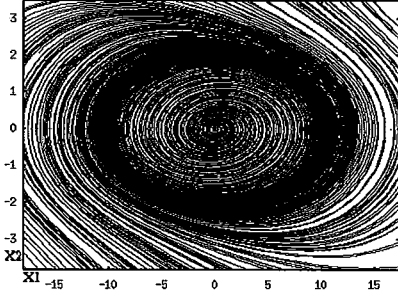
Figura B.1: (*b*). Phase portrait - the flow of trajectories denote the system dynamics.
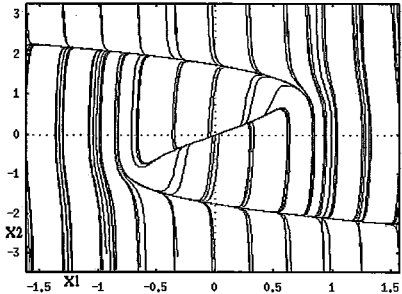
Figura B.2: (*b*). Phase portrait - the flow of trajectories denote the system dynamics.
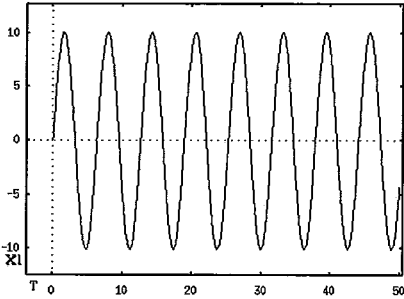
Figura B.1: (*c*). Time domain diagram - X1 vs time.
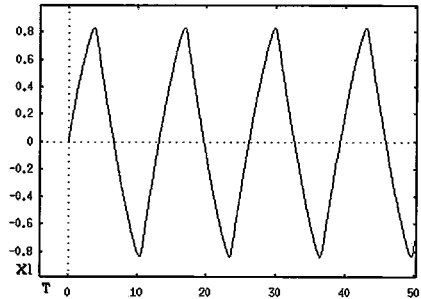
Figura B.2: (*c*). Time domain diagram - X1 vs time.
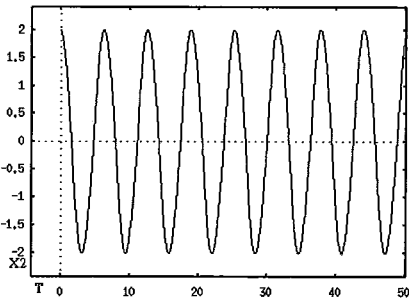
Figura B.1: (*d*). Time domain diagram - X2 vs time.
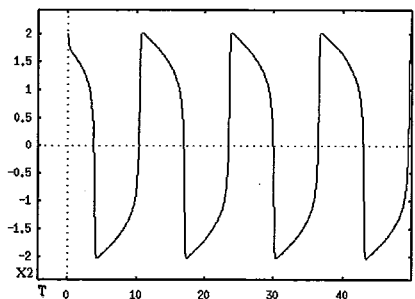
Figura B.2: (*d*). Time domain diagram - X2 vs time.

44

B.2.2 Hodgkin and Huxley's Oscillation Model

Different from the pure circuit origin of Van der Pol's oscillator model, in 1952 Hodgkin and Huxley summarized their results and proposed another oscillation model based on the research of membrane potential of a giant nerve fibre[50], which is a four-variable ODE model compared with the two-variable Van der Pol's model. Figure B.3 is the original membrane circuit on which their model builds on.
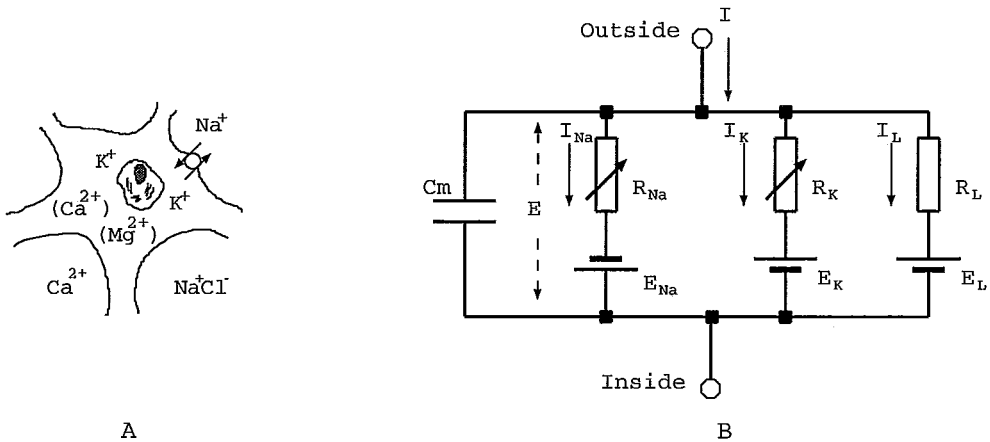
Figura B.3: (a). A physiological prototype of a cell and its environment, (b). Its corresponding circuit explanation (Fig. (b) is reproduced from [50]).

To keep alive, cells must have membrane potentials; cells that have lost their ability maintain an electrical potential across their membranes are dead cells [68]. Modern medical science has revealed the mechanism of membrane potential, as shown in Figure B.3, the main intracellular cation is potassium (K^+) while the main extracellular cation is sodium (Na^+) also with some main anion of chloride (Cl^-), these two types of cations are the major constituents which decide membrane potential. The membrane depolarization procedure, which can be treated as an inhibitory process representing a cell's transition from excitory state to inhibitory state (or the resting potential in neurobiology terminology), is formed by a transient overwhelming sodium ionic flowing into the cell, since the change of conductance for sodium ionic channel is transient and abrupt while the change of conductance for potassium ionic channel is gradual. When the resting potential is reached, the membranes become impermeable to sodium, i.e., the equilibrium potential of sodium is achieved, which initiate the repolarization procedure with the potassium conductance reaching the least, accompanying that great amount of potassium ions flowing

45

into the environment. The two procedures, namely, the action potential and refractory period, may repeat as the excitory and inhibitory states of membranes switch again and again.

In HH model, the four-dimensional (V, m, h, n), i.e., three conductances and one membrane potential, represent three ionic channels and another channel denoted by the membrane capacitor, respectively. Hodgkin and Huxley paid much more emphasis on the deduction of sodium, potassium and leakage conductances, whose analysis and calculation constitute a crucial part of their original contribution. In order to explain the experimental data of conductance variation with theoretical formula more accurately, e.g., how to simulate the beginning rise delay of potassium conductance associated with depolarization. Three variables m, h, n were assumed to form an ODE group, as following.

$$I = C_M \frac{dV}{dt} + \bar{g}_K n^4 (V - V_K) + \bar{g}_{Na} m^3 h (V - V_{Na}) + \bar{g}_l (V - V_l)$$

(B.2)

where
$\frac{dn}{dt} = \alpha_n(1 - n) - \beta_n n,$
$\frac{dm}{dt} = \alpha_m(1 - m) - \beta_m m,$
$\frac{dh}{dt} = \alpha_h(1 - h) - \beta_h h,$
$\alpha_n = 0.01(V + 10)/(exp\frac{V+10}{10} - 1),$
$\beta_n = 0.125exp(\frac{V}{80}),$
$\alpha_m = 0.1(V + 25 + /(exp\frac{V+25}{10} - 1),$
$\beta_m = 4exp(\frac{V}{18}),$
$\alpha_h = 0.07exp(\frac{V}{20}),$
$\beta_h = 1/(exp\frac{V+30}{10} + 1).$
Here I is the total membrane current density, V is the displacement of the membrane potential from its resting value, C_M is the membrane capacitance per unit area which is assumed constant, m, n, h are the assumed variables in order to achieve required nonlinearity matched with the experiments.

B.2.3   Fitzhugh-Nagumo Oscillation Model

The above Van der Pol and Hodgkin-Huxley models were studied by Fitzhugh and Nagumo et al. in 1961 and 1962, respectively. Initially called by Fitzhugh as the Bonhoeffer-van der Pol (BVP) model in his original contribution, now this popular neural dynamics

model is named after him. Just like Van der Pol's model which is a *qualitative* repre-
sentation of a wide class of oscillators, the more general FN model, in the same spirit,
represent *qualitatively* a wider class of nonlinear systems in the sense that it can show
a stable state and threshold phenomena besides stable oscillations. On the other hand,
analyses of Fitzhugh and Nagumo et al. on the HH equations have shown that the four
variables account for two essential factors: excitability, representing all-or-none response
to stimulation, and refractoriness, which is, loss and progressive recovery of excitabili-
ty following each action potential. Thus they reproduced, *qualitatively*, the dynamics of
the HH equations by two-variable systems representing the interaction of the two main
factors. As Fitzhugh argued, if the HH model is projected from the four dimensions to a
plane on some conditions, it has the same characteristics and physiological explanation
as FN model[34][61][57].

By adding terms to the Van der Pol equations, Fitzhugh obtained the original FN
equations as following:

$$\begin{cases} \dot{x} = c\left(y + x - \frac{x^3}{3} + z\right) \\ \dot{y} = -\frac{1}{c}\left(x - a + by\right) \end{cases} \tag{B.3}$$

where

$$1 - \frac{2b}{3} < a < 1, \ 0 < b < 1, \ b < c^2$$

Here a, b, c are constants, z is stimulus strength, a variable corresponding to applied
membrane current I in the HH equations. If $a = b = z = 0$, then we can retrieve Van
der Pol's equation from FN model. If we fix the constants as required and set different
stimulus values, the different membrane potential phenomena, i.e., the stable state and
stable limit cycle with threshold phenomena, can be achieved as in Figure B.4 and B.5.
If we set the parameters as $a = 0.7, b = 0.8, c = 3$, and stimulus impulse $z = -0.2$
as the initial conditions, we can get Figure B.4. Since the stimulus shock is positive or
not large enough in negative value, it couldn't pass a hidden threshold-like value which
can drive the system to oscillate stably, so this system now has a stable equilibrium point
which attracts all trajectories to it. The eigenvalues of this system are $-0.350448 \pm$
$i0.996484$. If we change the stimulus impulse to $z = -0.4$ and keep the other parameters
unchanged, then Figure B.5 is obtained. Now the equilibrium point is no longer stable

47

but instead, we can get a stable limit cycle, which means there exists a stable oscillation. In this case the eigenvalues of this system are $0.132638 \pm i0.916818$, which also proves the unstability of the equilibrium point. As Fitzhugh argued, in the stable limit cycle condition, there exists a separatrix line in the phase portrait, where all trajectories near this line will diverge from it dramatically to the left or right, producing an apparent all-or-none response, and lead to two different physiological regions named *active* and *refractory*, which entrains the threshold phenomena. The intermediate values in this separatrix line means the indetermined states. From the phase portrait of Figure B.5 we can observe the separatrix and threshold phenomena clearly.
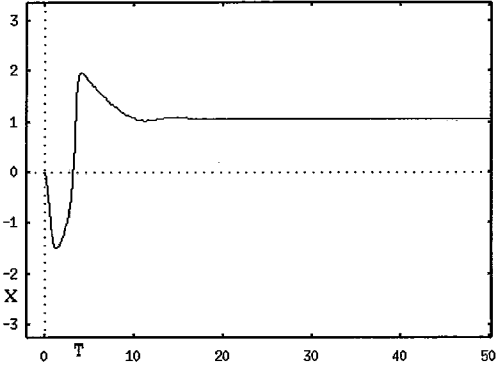
Figura B.4: (a). Time domain diagram for equilibrium point condition of FN model.
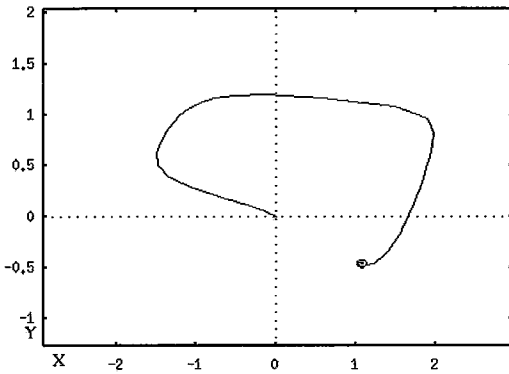
Figura B.4: (b). State space diagram for equilibrium point condition of FN model, where the circle denotes the equilibrium point.
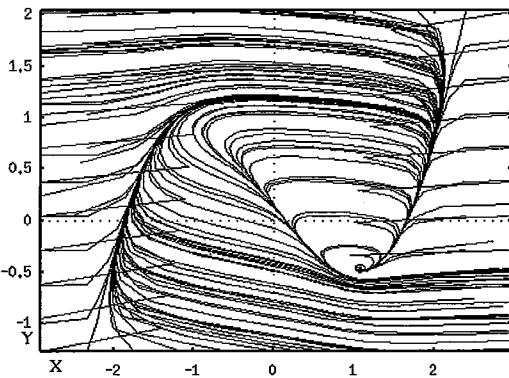
Figura B.4: (c). The portrait of flow of trajectories which approach asymptotically to the equilibrium point.
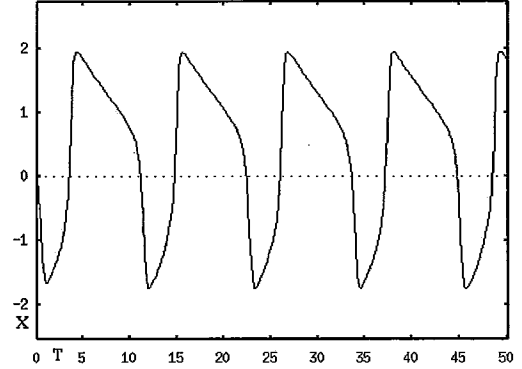
Figura B.5: (a). Time domain diagram for limit cycle condition of FN model.
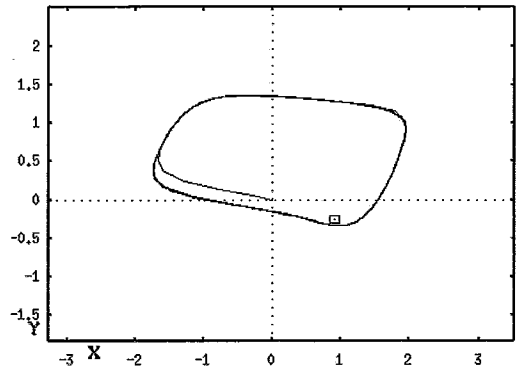
Figura B.5: (b). State space diagram for limit cycle condition of FN model.
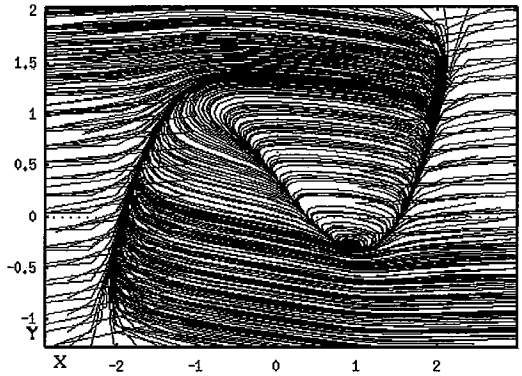
Figura B.5: (c). The portrait of flow of trajectories which approach asymptotically to the limit cycle, with double density of portrait for clearity.

B.2.4 Morris-Lecar Oscillation Model

Twenty years later C. Morris and H. Lecar studied the voltage oscillations in the barnacle muscle fiber and they proposed a seminal model which has only two voltage-dependent and non-inactivating conductances corresponding an inward Ca^{2+} current and an outward K^+ current. They argued that this simple conductance system is mathematically sufficient to predict much of the barnacle fiber behavior and further more, it allows correlations with the biophysical properties of real neurons [60]. The Morris-Lecar oscillation model, from some viewpoint, can be treated as a Fitzhugh-Nagumo/Hodgkin-Huxley hybrid, many researches on neuronal dynamics have been conducted by means of adopting this model, which is with both reasonable neurophysiological background and handy numerical solutions [66][69] [76]. The ML oscillator can be described by the following equations.

$$rC\frac{dv}{dt} = -g_{Ca}m_\infty(v)(v - v_{Ca}) - g_k w(v - v_k) - g_L(v - v_L) + I$$

(B.4)

$$r\frac{dw}{dt} = \frac{\varepsilon[w_\infty(v) - w]}{\tau_w(v)}$$

(B.5)

where
$$m_\infty(v) = 0.5[1 + tanh\frac{(v-v_1)}{v_2}]$$
$$w_\infty(v) = 0.5[1 + tanh\frac{(v-v_3)}{v_4}]$$
$$\tau_w(v) = \frac{1}{cosh\frac{(v-v_3)}{2v_4}}$$

In Morris and Lecar's analysis, if any conductance of the two-conductance system is blocked, no oscillations will be observed, only the transient, simple RC-like response or bistability with the threshold phenomena, responding to different magnitude of the stimuli, can be seen. When both conductances are recruited simultaneously, then small stimuli produce small, essentially passive depolarizations, but once a threshold voltage is reached, oscillations appear [60]. Roughly speaking, there are two types of oscillations underlying the ML oscillation system, namely, beating and burst, the alternative between

them depends on the choice of parameter ε. If $\varepsilon \ll 1$, the second equation $(B.5)$ is much slower than the first one $(B.4)$, and the oscillator will approach the relaxation limit, which entrains beating; otherwise, burst will appear.

B.2.5 Wilson-Cowan Oscillation Model

Wilson and Cowan (1972) derived the system of equations for the time coarse-grained excitatory and inhibitory activities in a homogeneous one-dimensional neuron population. In their model, it is assumed that the neurons become activated if their post-synaptic potentials exceed thresholds and if they are also sensitive (or nonrefractory). In their original, small network model, there were two populations of neurons, excitatory and inhibitory. The following are differential equations defining the average dynamics of this model.

$$\begin{cases} \tau_e \frac{dE}{dt} = -E + (1 - r_e E) F_e(w_{11}E + w_{12}I + s_1) \\ \tau_i \frac{dI}{dt} = -I + (1 - r_i I) F_i(w_{21}E + w_{22}I + s_2) \end{cases} \tag{B.6}$$

where F_e and F_i are the sigmoidal *firing rate functions* defined by F as following.

$$F = \frac{1}{1 + exp[-a(x - \theta)]}$$

Here, $E(t)$ is the proportion of excitatory cells firing per unit time at the instant t and $I(t)$ is the proportion of inhibitory cells firing per unit time at the instant t, w is the strength of each synapse, τ_e, τ_i, r_e and r_i are the constant parameters, a and θ are parameters controlling the shape of sigmoidal input-output function as a determining the value of the maximum slope while θ giving the position of maximum slope, s_1 and s_2 are the external inputs.

The interesting aspect of this model lies in that, it is different from the rest models illustrated since it is derived from, and normally used for the neuron populations rather than single neuron. So, it deals with the interconnections among neurons instead of the membrane potential analysis. If all the parameters are chosen correctly, there will be a stable limit cycle phenomenon emerging as shown in Figure B.6 and B.7, where it's worth noticing that $E(t) - t$ relation denotes the exciting proportion of excitatory subpopulation at each instant [78] [54] [31].
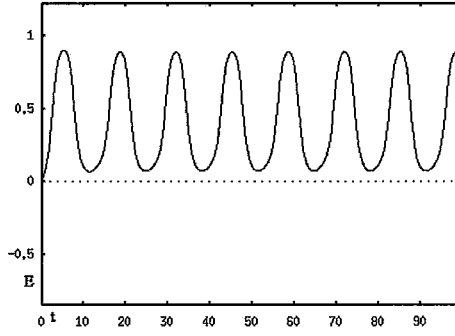
Figura B.6: The E-T relationship - the exciting proportion of excitatory subpopulation at each instant.
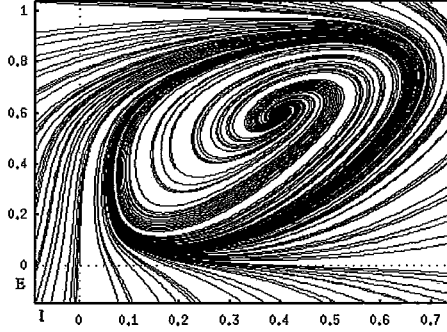
Figura B.7: The E-I phase portrait of a flow of trajectories shows a stable limit cycle phenomemon. In this simulation the parameters are chosen as: $w_{11} = 8, w_{12} = -6, w_{21} = 10, w_{22} = -1, \tau_e = 1, \tau_i = 3, s_1 = -2, s_2 = -6, a_e = a_i = 1, \theta_1 = \theta_2 = 0, r_e = ri = 0$.

B.3 State-of-the-art on Neurolocomotion

Legged animals usually adopt various gait patterns in their terrestrial locomotion for various reasons, e.g., avoiding dangers, adapting terrain, or just obeying the willingness of changing gaits. Although many biological experiments have shown that generation of animal's gait patterns is the result of interactions between CNS and feedback of external stimulations, which induces popular admission of the existence of CPGs, the neural mechanisms underlying CPGs are still not well understood. One of the crucial questions undetermined is that, whether a unique CPG is sufficient for governing switching among various gait patterns or different CPGs are required to correspond to different gaits in the real-life biological systems[24]. Until nowadays many models have been suggested on CPGs mechanism of vertebrate and invertebrate animals, for instance, biped gait model [10] [71] [72], quadruped gait model [67] [21] [20] and hexapod gait model [11] [22], most of them follows these two lines and based on the coupled, nonlinear oscillator method for modeling.

B.3.1 A Neuromodulatory Approach

As a model for legged-locomotion control, Grillner proposed that each limb of an animal is governed by a separate CPG [44] [45], and that interlimb coordination is achieved through the actions of interneurons which couple together these CPGs. With this scheme, gait transitions are produced by switching between different sets of coordinating interneurons, i.e., a locomotor CPG is reconfigured to produce different gaits.

Grillner's strategy has been adopted, in spirit, by several CPGs modeling studies. For instance, Bay and Hemami [10] used a CPG network of four coupled van der Pol oscillators to control the movements of a segmented biped. Each limb of the biped was composed of two links, and each oscillator controlled the movement of a single link. Bipedal walking and hopping were simulated by using the oscillators' output to determine the angular positions of the respective links. Transitions between out-of-phase and in-phase gaits were generated by changing the nature of the interoscillator coupling, e.g., the polarities of the network interconnections were reversed to produce the walk-to-hop transition.

This approach is, in principle, physiologically reasonable. For instance, the notion that supraspinal centers may call on functionally distinct sets of coordinating interneurons to generate different gaits is plausible but not yet experimentally established. In addition, from a different but relevant perspective, it has been shown that rhythmic neuronal networks can be modulated, e.g., reconfigured, through the actions of neuroamines and peptides, and thereby they are enabled to produce several different motor patterns [64].

B.3.2 A Synergetic Approach

Synergetics deals with *cooperative phenomena*. In synergetics, the macroscopic behavior of a complex system is characterized by a small number of collective variables, which in turn govern the qualitative behavior of the system's components [24].

Schoner and colleagues used a synergetic approach in a study of quadrupedal locomotion [67]. They analyzed a network model that was made up of four coupled oscillators, each oscillator represented a limb of a model quadruped. The phase difference among

limbs were used as collective variables to characterize the interlimb coordination patterns of this discrete dynamical system. Gait transitions were simply modeled as phase transition, which could also be interpreted as bifurcations in a dynamical system.

This approach is significant in that it relates system parameter changes and stability issues to gait transitions. Its primary weakness, however, is that the physiological relevance of the relative-phase coupling terms is unclear.

B.3.3   A Group-theoretic Approach

According to the arguments of Collins [24], the traditional approach for modeling a locomotor CPGs has been to set up and analyze, either analytically or numerically, the parameter-dependent dynamics of a hypothesized neural circuit. Motivated by Schoner et al.'s works, Collins et al. deal with the CPGs dynamics from the perspective of group theory [21][22]. They considered various networks of symmetrically coupled nonlinear oscillators and examined how the symmetry of the respective systems leads to a general class of phase-locked oscillation patterns, with this approach the transitions between different patterns can be modeled as symmetry-breaking Hopf bifurcation. It is a common sense that, in the standard Hopf bifurcation, the dynamics of a nonlinear system changes as some parameter is varied, it means that an old limit cycle (corresponding to a periodic solution) may disappear and several new limit cycles may appear, or saying, as the symmetries reach the least level, the chaotic phenomena may arise theoretically.

The theory of symmetric Hopf bifurcation predicts that symmetric oscillator networks with invariant structure can sustain multiple patterns of rhythmic activity. It emphasize that one intact CPG architecture is sufficient for host all possible pattern changes, which is different from the aforementioned neuromodulatory approach. Also different from Schoner et al.'s typical synergetic approach, which only analysized the symmetries and phase-relationship of observed gait patterns, the group-theoretic approach is a method with the capability of prediction, i.e., it will deduce all symmetry types and then relate them to possible gait patterns [21].

This approach is significant in that it provides a novel mechanism for generating gait transitions in locomotor CPGs. Its primary disadvantage, however, is that its model-independent features can not provide information about the internal dynamics of indivi-

dual oscillators.

B.4   A General Gait Pattern Model

In order to avoid the conjugate symmetry groups after bifurcations, a general network with 4n cells was proposed by Golubitsky et al. [43] to denote the locomotion symmetries of $2n$-legged animals, with the capability of generating the appropriate kinds of gaits, where n is the number of pairs of legs. This biologically inspired model is shown to be a potential prototype for almost all observed gaits in quadrupeds, hexapods and multi-legged animals such as the centipedes. In Figure C.1(a) and (b), the network contains 2 cycles of $2n$ cells, labelled with $1, 3, 5, ..., 4n-1$ and $2, 4, 6, ..., 4n$ respectively. Each circle corresponds to the identical cells, the unidirectional lines denote the identical, single couplings running from cell i to cell $i + 2 (\mathrm{mod}\, 4n)$ and the bidirectional lines denote the identical reciprocal couplings between cell $2i - 1$ and $2i (\mathrm{mod}\, 4n)$. Only 2n cells of the top level are connected with the legs, the other $2n$ cells of the bottom level are assumed to be the auxillary or supporting part of the top level CPGs model, it is interesting to see that this architecture is analogous with the animal body if we imagine the top level cells as the animal legs and the whole bottom as the animal back. In the next appendix we will confirm, theoretically and experimentally with PDP algorithms, that Golubitsky et al.'s proposal, i.e., the strategy of $4n$-cells for $2n$-legged animal, is meaningful and implementable for gait research and robot control purpose.

The traditional method for treating the above coupled system is that, suppose each cell can be expressed by its n-dimensional state variables $X_i(t) = (x_i^1(t), x_i^2(t), ..., x_i^n(t))$, where $X_i(t) \in \Re^n$, then a large-scaled ODE group , e.g., $\frac{dx}{dt} = f(x, \lambda), f : \Re^n \times \Re \to \Re^n$, can be formulated according to the reciprocal couplings among the neighboring cells and/or their internal dynamics, depending whether the cells themselves are endogenous or not (for the possible oscillatory formula, see Section B.2 of this appendix). In this approach, although the possibly existed symmetries do influence the solutions of ODE by means of forcing the multiple eigenvalues to occur, we don't need to process the symmetries explicitly by following the classical solution manners. However, since this approach is strongly model-dependent, in the sense that different ODE model must be constructed

on different types of CPG structure, the number of state variables, and coupling types, etc., in some cases, some other approaches can be used as alternatives.

From the standpoint of equivariant Hopf bifurcation theory, the most important aspect of the network is its spatio-temporal symmetry group, in our case, it is

$$\Gamma \cong Z_{2n}(\omega) \times Z_2(\kappa)$$

The cyclic subgroup Z_{2n} cycles corresponding pairs of cells around their respective loops, and the subgroup Z_2 interchanges left and right cells in corresponding positions. More clearly, in group notation, Z_{2n} is generated by

$$\omega = (1\ 3\ 5\ ...\ 4n-1)(2\ 4\ 6\ ...\ 4n)$$

and Z_2 is generated by

$$\kappa = (1\ 2)(3\ 4)...(4n-1\ 4n)$$

After permutation, the cell's characteristics and the coupling type should be preserved. Here we will only exploit the spatial symmetry explicitly since, if any periodic solution arising via Hopf bifurcation is transformed by an element of Γ, then the result is equivalent to a phase shift on that solution. As Golubitsky et al. argued, this general network is model-independent, in the sense that the symmetries of any legged animals can be described by symmetry group Γ, or more precisely, the symmetry subgroup $\Sigma \subset \Gamma$, which is broken from Γ. For different animals with different legs, it's enough to modify the number of cell pairs without changing the architecture of the network itself. Before we could go further, it's indispensable to know how the general gait model can undergo the bifurcation (including equivalent Hopf bifurcation and, possibly the steady-state bifurcation) to generate various gaits, here Golubitsky et al's original contribution will be followed.

Suppose as before that each cell has m-dimensional state space $\Re^m$, then the total state space owned by Golubitsky's coupled network is

$$U = \Re^{4nm} \equiv \underbrace{\Re^m \times ... \times \Re^m}_{4n}$$

and symmetry group Γ acts on this space by permuting the 4n components (each a vector of dimension m). Until now we know that for a behavioral transmuting system with

symmetry group Γ bifurcates to let periodic behavior (with remained symmetry described by symmetry subgroup $\Sigma \subset \Gamma$) to occur, it is crucial for Jacobian matrix to have a pair of simple purely imaginary eigenvalues. In many cases, although not all, we can get multiple imaginary eigenvalues instead of the simple ones in the presence of action of symmetry group, thus a degenerated Hopf bifurcation is formed. According to the spirit of equivariant Hopf bifurcation theorem, the state space U on which symmetry group acts should be divided into the irreducible subspaces in one of the two forms shown in "Equivariant Hopf Bifurcation Theorem" of Subsection $A.2.2$, i.e., the divided subspace should be Γ-simple. Restricted in these subspaces, the standard Hopf bifurcation theorem can be utilized to obtain periodic solutions which are different from subspace to subspace, since "Γ-simple" is somewhat equivalent to "simple eigenvalue"[42].

For the purpose of breaking space U into real irreducible subspaces, as a first step U is complexified to get a complex space

$$V = \Im^{4nm} \equiv \underbrace{\Im^m \times ... \times \Im^m}_{4n} \equiv \underbrace{\Im \oplus ... \oplus \Im}_{m} \times ... \times \underbrace{\Im \oplus ... \oplus \Im}_{m}$$

where V is the sum of one-dimensional irreducible subspace over $\Im$, these subspaces are V_{jk} where $0 \leq j \leq 2n - 1$ and $k = 0, 1$. To define V_{jk}, let $\xi = e^{\frac{2\pi i}{2n}} = e^{\frac{\pi i}{n}}$ be a primitive $2n^{th}$ root of unity. Then V_{jk} is spanned over $\Im$ by

$$v_{jk} = (1, (-1)^k; \xi, (-1)^k \xi; \xi^2, (-1)^k \xi^2; ...; \xi^{2n-1}, (-1)^k \xi^{2n-1})$$

so V_{jk} can be written as

$$V_{jk} = \{v_{jk} \| 0 \leq j \leq 2n - 1, k = 0, 1\} = \{\xi^j, (-1)^k \xi^j \| 0 \leq j \leq 2n - 1, k = 0, 1\}$$

obviously V_{jk} is a full collection of one of the corresponding internal state variables of the $4n$ cells on $\Im$.

Observe that for an internal state variable of a cell on $\Im$, i.e., v_{jk}, the action of the symmetry group Γ is

Ipsilateral symmetry ω: $v_{jk} \mapsto \xi^j v_{jk}$

Bilateral symmetry κ: $v_{jk} \mapsto (-1)^k v_{jk}$

so that the subspaces V_{jk} are Γ-invariant.

For simple discussion, let's only consider one side rotation $Z_{2n}(\omega)$ since double sides subject is the same situation. Suppose $V_j = \{\xi^j \| 0 \le j \le 2n - 1\}$, we'll have the complex portrait in Figure B.8. Clearly there are two points where no imaginary eigenvalues to occur, hence only steady-state bifurcation rather than Hopf bifurcation can happen when the eigenvalues pass imaginary axis with nonzero speed. The Hopf bifurcation will happen for the rest region with imaginary eigenvalues [1] as they cross the imaginary axis with nonzero speed and various periodic oscillation modes will be achieved [42][43].
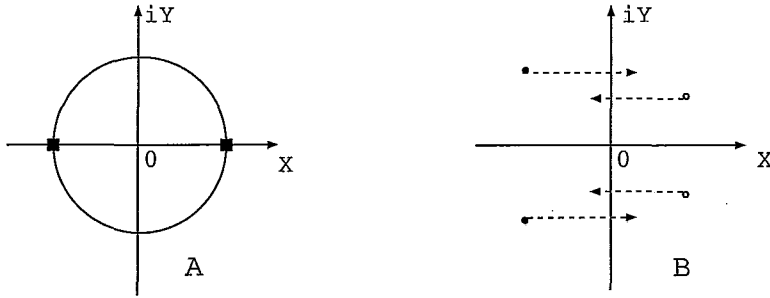
Figura B.8: Demonstration diagram of the eigenspace. (a) the Hopf bifurcation region and steady-state bifurcation region, (b) demonstration of the eigenvalues crossing imaginary axis with local dynamics of Hopf bifurcation, i.e., periodic oscillation occurs and vanishes.

So, we can get:

$$V_{jk} = (1, (-1)^k), \quad \text{when j} = 0,$$
$$V_{jk} = (-1, (-1)^{k+1}), \quad \text{when j} = n.$$

The conjugate eigenvalues, i.e., $v_{jk} \oplus v_{2n-j,k}$, exist when $1 \le j \le n - 1$.

From aforementioned induction, the corresponding decomposition of U into irreducibles is into the representations U_{jk} where

$$U_{jk} = \begin{cases} Re(V_{jk}) & \text{if } j = 0, n \\ Re(V_{jk} \oplus V_{2n-j,k}) & \text{if } 1 \le j \le n - 1 \end{cases}$$

As a summary, we can conclude that, for $m = 1$(each cell has only one internal state variable) condition as induced above, the network equations can undergo steady-state

---

[1]It's worth noticing that, Hopf bifurcation means the phenomena of periodic oscillations arise or vanish after the bifurcation point, under some conditions [58]. We can also see from Figure B.8(*b*), the left half space will undergo the emergence of periodic oscillation while the right half of vanishing procedure, both are Hopf bifurcation. Following Golubitsky's convention of calling emergence of periodic oscillation as symmetry-breaking Hopf bifurcation, in the gait research, we can thus call the vanishing of periodicity as symmetry-collecting Hopf bifurcation.

bifurcations corresponding to the eigenvalue subspaces $U_{00}, U_{n0}, U_{01}, U_{n1}$; and the Hopf bifurcation corresponding to eigenspaces for which $j = 1, ..., n - 1$. For $m \geq 2$, we can have at least,

$$V_{jk} = V_{jk}^1 \oplus V_{jk}^2, \text{when } j = 0, n$$

Hence the condition of Γ-simplicity is satisfied for $v_{jk}, (j = 0, n)$, that is, the network can undergo Hopf bifurcations corresponding to any of the subspaces U_{jk} when $m > 1$. It is fortunate to know that the standard model equations for neurons have $m \geq 2$ [25], so only Hopf bifurcation will be considered in any irreducible subspace later. And, with the stated induction and theoretic background in mind, it is always possible to simplify the complex bifurcation problem with symmetries into the pure group theory calculations in our gait pattern research [21].

B.5 Conclusion

Through the state-of-the-art introduction of this appendix, we can get a contour knowledge of the emergent research results and interests on *rhythmic pattern neuronal networks*, or saying, *oscillatory neuronal networks*, in which oscillations are the major features [12]. Based on this understanding, it is impossible to study the biological pattern formation system without understanding the biological oscillator models. Generally speaking, from the viewpoint of characteristics of solutions, all the four oscillator models (including Wilson-Cowan neuro-population model) are the qualitative descriptions of neuronal models which more focus on the model's physiological explanation except Hodgkin-Huxley model, which is a numerical solution, or more exactly, the quantitative proximation method, in the sense that it emphasizes on the simulated accuracy of stimulated response curves of voltage-dependent channel conductances. From the viewpoint of generalities, van der Pol's oscillator model is a more multi-adaptive one since its foundation is a general oscillation circuit, whereas the other four are all based on the specific neurophysiological model. In some more details, FN oscillator model is constructed, purely from the viewpoint of HH and VDP models instead of some concrete physical model. In order to strenghen the physiological significance of FN model, it can be considered as the

reduction form of HH model [33]. A Fitzhugh-Nagumo/Hodgkin-Huxley hybrid was formulated and studied by Morris and Lecar, and they insisted that the relaxation kinetics is first order for simplicity consideration, besides they also argued that precise kinetics is not essential for the description of all excitation effects [60]. So we can also treat ML model as the reduction of HH equation in the sense that, HH model provides an exhausted numerical approximation of the experimental results of potassium and sodium conductance while ML model achieve the conductances from the channel open levels. It is worth noticing that these oscillator models may share some common features and in some conditions they may be commutable, e.g., a system of mutually coupled van der Pol equations can be derived from the Wilson-Cowan model which is for the dynamics of a number of excitatory and inhibitory neural subsets [54].

It is reasonable to assume that an intact locomotion system consists of three components, i.e., the *central nervous system, central pattern generator* and *motor system*, where the motor system may be constituted by the aforementioned oscillator models. As to the CPGs, which plays as a crucial component, although its physiological and anatomical explanation is quite plausible, many approaches have been proposed for its functionalities, especially from the macroscopic viewpoint without exploring detailed dynamical features. Among various methods introduced, this research will continue on the assumption of that, a unique CPG architecture can host the integral types of organic rhythms, e.g., there is only one CPG architecture corresponding to locomotion, respiration, heartbeating, etc., respectively. With this assumption, this research incorporate a general model introduced by Golubitsky et al. [43] and engages in developing a novel, analogous gait prediction and realization method based on the hybrid of parallel and distributed theory (i.e., SER/SMER), dynamical system and group theory, also it put some emphasis on the digital circuit simulation and implementation of the real life system.

Apêndice C

Constructing a Rhythmic Pattern Generator for Hexapodal Animals

C.1 Introduction

Many research approaches towards modelling mechanisms of coupled neural oscillations are mainly based on the dynamical system theory[10] [67] [85]. Thus most works must be initiated by a specific mathematical dynamic model on the real life systems, i.e., these model-dependent analyses are only efficient for a specific system, and meanwhile they usually leave a gap between research and realization. An alternative method, which is model-independent by employing graph dynamics owned by all graph topologies, has been proposed to model the collective behavior of purely inhibitory neural networks [82]. As we'll describe, *Scheduling by Edge Reversal* and its generalization, *Scheduling by Multiple Edge Reversal* algorithms can be applied to predict or reproduce the interesting behaviours of many biological oscillatory neuronal networks, especially *central pattern generators* (CPGs), just assuming some form of *postinhibitory rebound* (PIR)[77] at the neuron's model level.

It'll be shown how different biological building blocks under SER or SMER can be used to model biological motor systems much more simply and effectively. In order to illustrate the new approach, cockroach's three rhythmic gait patterns are chosen as case study in this thesis. Nevertheless, it is suggested that the technique can be extended to reproduce most invertebrate and vertebrate rhythmic movements provided that they can be described topologically. The whole types of building blocks can be hopefully synthesized into custom hardware (ASICs) with the help of FPGA technologies. So, a general-purpose

61

robot can be easily constructed with this control core if a suitable hardware platform with some degrees of freedom is supplied.

This appendix is organized, mainly, in four sections. Section $C.2$ is a typical collection of the hexapodal animal's gait patterns and some analysis on their SER/SMER building block construction. Section $C.3$ includes some crucial comments on custom hardware design and simulation. A vivid, computer-based hexapodal gait experiment is offered in Section $C.4$, with three typical gaits, i.e., fast, medium and slow speed model realized. At last, a preliminary theoretic research on gait generation and transition, based on the non-linear dynamics of neural oscillator theory, is described and some tentative conclusions are given.

C.2 Hexapodal Gaits and Corresponding Building Blocks

C.2.1 The Architecture of Hexapodal Gaits

Out-of-Phase (Walking and running) and in-phase (hopping) are the major characteristics of observed gaits in bipeds[1], while in quadrupeds, more gait types were observed and enumerated by Alexander [2], as walk, trot, pace, canter, transverse gallop, rotary gallop, bound and pronk. Unlike bipeds and quadrupeds, the locomotion of hexapods can have more complicated combinations of leg movements, however, despite the variety, some general symmetry rules should still be obeyed and remained as the basic criteria for gait prediction and construction, for instance, it is a generally accepted agreement that multi-legged (normally more than six legs) locomotion often shows the traveling wave phenomena sweeping along the chain of oscillators [21] [43]. As descriptively developed by Wilson, two assumptions on predicting the model of insect gaits are [79]:

- Waves of forward leg movement run from posterior to anterior, no leg moves forward until the one behind is placed in a supporting position.

- Contralateral legs of the same segment are half a period out of phase with one another.

---

[1]As we discuss the gait types, we just concern about the more "natural" ones and ignore those which can be achieved through training, e.g., we treat the human hopping with only one leg as a typical example of gait gained through training.

If the detailed phase correlations among the six legs of an insect are ignored, the locomotion of an hexapodal insect, saying a cockroach, can be classified roughly as fast, medium and slow speed type, respectively. However, if those detailed informations are included, then some enumerating types can be found in Golubitsky et al.'s manuscript [43], it's easy to demonstrate that SER/SMER scheme serves well for both cases, just recalling that this general methodology is model- and topology-independent. Here we confirm to follow the aforementioned research line of a unique CPG mechanism for hosting an integral spectrum of organic rhythms, and design an architecture for locomotion purpose.

Golubitsky et al. proposed that in order for a symmetric network of identical cells to reproduce the phase relationships found in gaits of a $2n$-legged animal, the number of cells should be (at least) $4n$ [43], with each leg corresponding to two cells for behavior modelling. This conclusion is found matched with our inhibitorily coupled neurons' representation for each leg, organized under SER/SMER scheme. Followed Golubitsky's schematic modification, we can continue to get the architecture-isomorphic substitution of their CPG networks and utilize this model throughout our macroscopic/microscopic research.

(a)   (b)   (c)
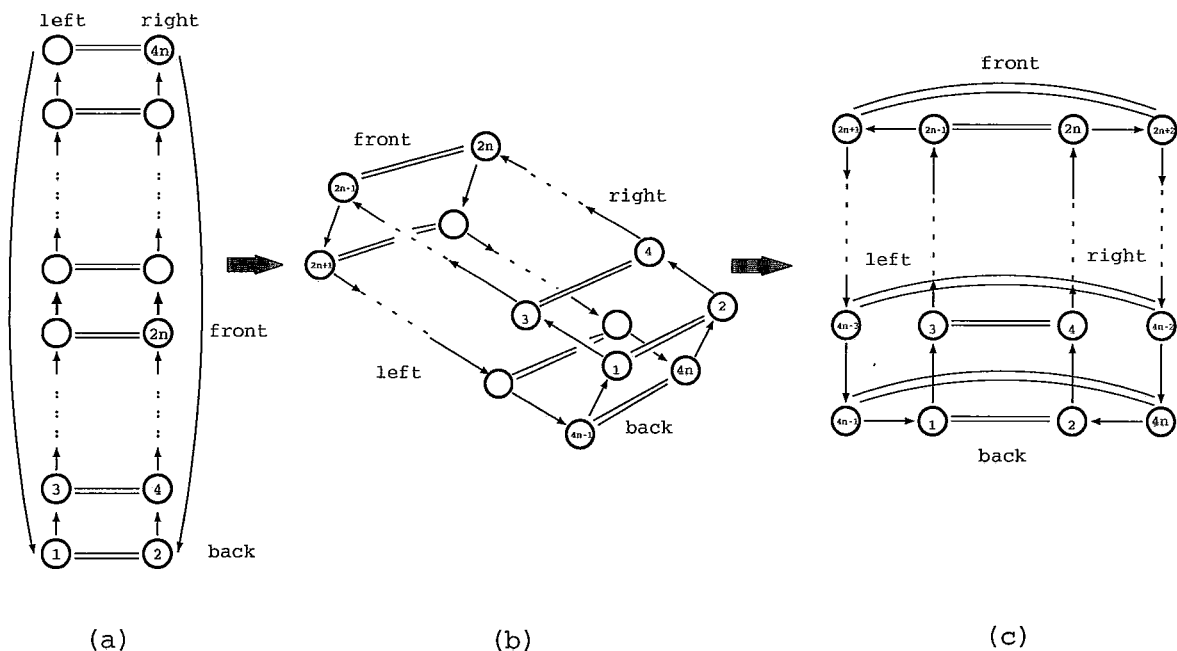
Figura C.1: The isomorphic transition of a general multi-legged locomotive, driving motor architecture, where diagrams (a) to (b) are reproduced from works of Golubitsky et al., i.e., they folded up the (a) network to eliminate long-range connections and created a structure with repeated modules. The diagrams (b) to (c) are obtained based on the same structural idea which extends the left and right parts to get another equivalent network.

It may be a misunderstanding that the coupled limbs in the insects will reciprocally interact directly because of the straight mechanical viewpoint as shown above. However, some further investigation will give evidences[9] that they don't interact, or at least not as much as people may think, they are all controlled by CPGs only, not themselves interactively. For instance, if they depend on each other so much, it's hard to explain the movements of a leg with the other amputated. So it appears clear that through the functionalities of CPGs, the flexor and extensor neurons will construct a relatively independent oscillatory system representing the possible behavior of one leg and the interlimb phase relationship will exist automatically. So next general architecture can be achieved naturally.

The locomotion architecture may generally consist of three parts, i.e., the oscillation system as driving motor, CPGs as pattern source and CNS as command source. This architecture can thus be constructed by the model with reciprocally inhibitory relationship between the so-called flexor and extensor motor neurons in each leg, which is signified by coupled gross lines in Figure C.2. The CPGs, as the core of this mechanical architecture, convert different willingness signals from CNS to the bioelectronical-based rhythmic signals for driving the flexor and extensor respectively. These motor neurons are essentially relaxation oscillators, i.e., a pair of flexor and extensor forms a bistable system in which each neuron switches from one state to another when one of its two internal thresholds is reached and back when another threshold is reached again.

In order to facilitate the circuit implementation of such a complicated biological model, we project down only the oscillator system and utilize SER/SMER distributed control sheme as a partial substitution of the mechanism of CPGs, i.e., only the preprogramming ability for rhythmic generation is simulated while CPGs functionalities of connecting CNS and oscillator systems are not able to be substituted by SER/SMER scheme. Nevertheless, through some suitably predefined, static steady states, an approximate Hopfield net seems to be organized with some characteristics like self-organization [69]. Since it is argued that animal's walking speed is largely determined by the relative firing time between flexor and extensor [63], so the different speed can be achieved by simply adjusting the rate of space occupancy of each relaxation oscillator, or namely, choosing different types of building blocks for different speed patterns. It is worth observing that this he-
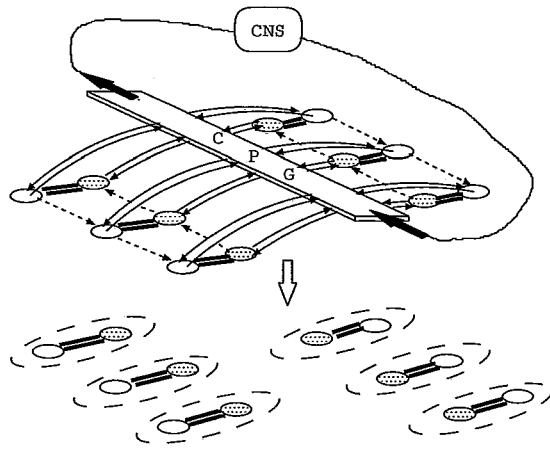
Figura C.2: An general architecture for legged locomotion. Interconnections between CPG and each neuron representing CPG command output and feedback from controlled neuron are denoted by double arrow lines; the dashed arrow lines between ipsilateral neurons imply waves of forward leg movement running from posterior to anterior, no leg moves forward until the one behind is placed in a supporting position; flexor and extensor are denoted by dotted and undotted circles respectively.

xapodal model can be suitably extended to simulate the movement of any legged animals effectively.

C.2.2 Constructing Building Blocks for Desired Patterns

Of long-standing interest are questions about rhythm generation in networks of nonoscillatory neurons, where the driving force is not provided by endogenous pacemaking cells. A simple mechanism for this is based on reciprocal inhibition between neurons, if they exhibit the property of postinhibitory rebound (PIR) [77]. Instead of focusing on low-level neuronal features, e.g., membrane potential functions, the next step is to choose and analyse a representative case study and build a corresponding SER- or SMER-driven artificial CPGs network. The three common gait patterns of cockroach, i.e., slow walk, medium speed walk and fast walk are investigated. Figure C.3 shows the CPG's mutual inhibition structure and corresponding gait phase relationship between six legs. The understanding of the changes in topology and internal parameters between different gaits is inspired by the contribution of P.A. Getting [38], who argued that modulation of building blocks can greatly alter network operation, even generate a totally new network. This modulation is normally induced by command signals from CNS or the intrinsic characteristic of building block itself.

In the case of cockroach's fast walk pattern, SER could be directly applied to initiate
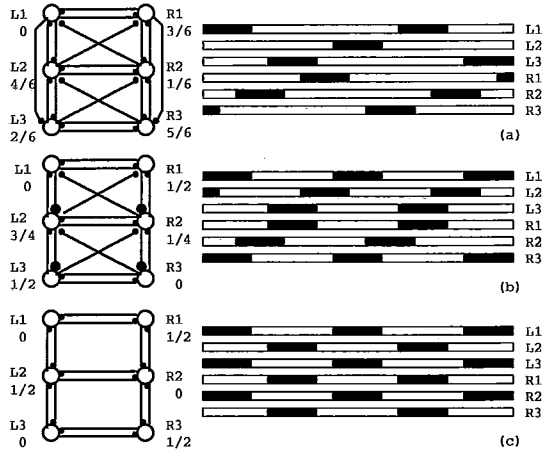
Figura C.3: Mutual inhibition structures and phase relations between six legs, each leg represented by one electrically compact nodes, filled circle and its size denote inhibition and its strength (a) Slow walk (b) Medium speed walk (c) Fast walk.

oscillation and coordinate the movement of the six legs (see Figure A.6 for reference). For the more complicated rhythmic leg movements of slow and medium speed, in which the fire of neighbor nodes is not exactly out of phase and some phase overlapping exist, first one has to construct the corresponding building block under SMER, then organize the artificial CPG network with different building block configurations. A graphic expression of two typical cockroach gait patterns is formulated in Figure C.5.

From the phase relationship presented in Figure C.3(a) and (b), one can choose a suitable configuration from the corresponding firing circulation patterns introduced in Figure C.4, for each of the six nodes in the relative speed model, in order to construct the six-leg rhythmic movement shown in Figure C.5 *left* and *right* respectively. Then, self-organized circulation patterns in cockroach's gait on slow and medium speed can be generated by building blocks under SMER.
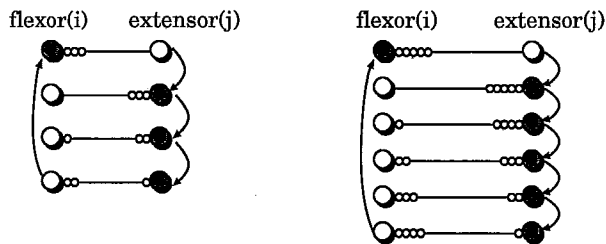
Figura C.4: One possible scheme of firing circulation patterns of building blocks, black for firing and white for idle. **Left** four possible configurations for medium speed gait pattern and; **right** six possible configurations for slow gait pattern.

It is important to understand the concept of a building block, since it is the building

block which should obey SMER, rather than the constructed model of gait patterns. A mutually inhibitory relation between neighboring flexor neurons is assumed so that building blocks are solely reponsible for gait pattern generation and transition. By anatomical view, cockroach's leg movement is driven by flexor and extensor motor neurons, the flexor will lift a leg from the ground while extensor does the opposite. This can be mapped into our building block perfectly, taking neuron i and j in a building block as flexor and extensor respectively (see Figure C.4). Now, a rough insight is apparent, i.e., there is an interesting timing relationship between flexor and extensor during different speed models. As cockroach's walking speed increase, the firing time for extensor (corresponding stance) will decrease dramatically, while firing time for flexor (corresponding swing) keep basically constant, what matches exactly with biological experiments [63]. This insight confirms that cockroach's speed is determined largely by extensor firing, i.e., the time duration of a leg on ground.
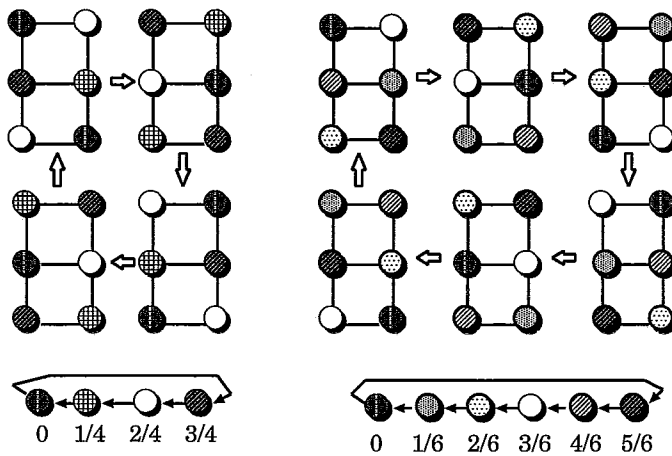
Figura C.5: The coordinated rhythmic patterns among six legs. **Left** medium speed, 0 - exciting, 2/4 - inhibited; **right** slow speed, 0 - exciting, 3/6 - inhibited.

It's a common sense that animal's locomotion behavior is a continuous procedure. Our gait analysis method only samples some typical points from these continuous, high-dimensional waveforms (the number of dimensions is equal to the number of animal legs), which are the snapshots with at least one leg supporting ground substantially and, ignoring all other snapshots which may contribute little for the model retrieval. As we've argued, the building block is constructed by flexor and extensor neurons, so it's clear that there are two sampling points in one leg's locomotive period representing the firing of flexor and extensor respectively. This method is especially useful for facilitating the digital cir-

cuit implementation, as we'll show below. Since a kind of high-pass-filter characteristic is a common property more or less observed in every real neuron [9][59], and this property may be naturally simulated by the hysteretic phenomena of mechanical oscillation, so we believe that these sampled points can lead to smooth, continuous waveforms for behavioral simulation.

Next, four snapshots of a graphic experiment with cockroach's medium speed gait is offered. The rhythmic order exhibited is: $(L1R3)$ $R2$ $(L3R1)$ $L2$ ....
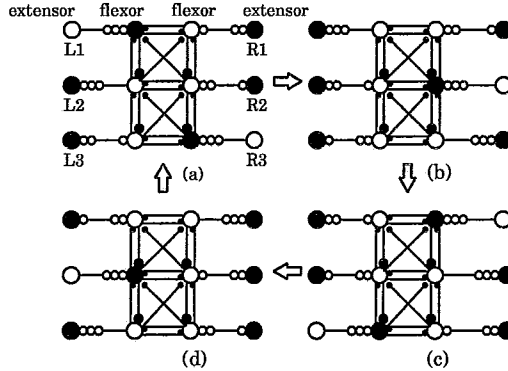
Figura C.6: The cockroach's medium speed gait pattern reconstructed with building block from Figure C.4, the six flexor neurons' firing threshold is 3, six extensor neurons' is 1.

C.3   Model Implementation

C.3.1   Model Optimization

There are various solutions available for the reduction of generalized SMER algorithm to it's deductive SER algorithm, which is more concrete and can be simulated easily by the multiphase circuit synthesis method proposed by França et al. [36].

One of the solutions, namely, node multiplicity method, is introduced briefly, according to the original contribution of Barbosa et al.[8]. A circuit simulation is offered with the high-level, HDL-based design methodology using **Xilinx Foundation Series** software [81], the concurrent nature of VHDL makes it tailor made for our distributed project, the experiment results are compared with the real life biological phenomena at last.

Node Multiplicity Method

This solution is based on the construction of a heavy-load instance of SER algorithm from the instance of SMER algorithm.

Let $G = (N, E)$ be the graph under SMER, and $G' = (N', E')$ as its target graph under SER, denoted by L the least common multiple of $r_1, ..., r_n$ (i.e., r_i in section 2.2) and define $q_i = L/r_i$ for all $n_i \in N$. The following are the steps to obtain G'.

- For each $n_i \in N$, let N' contain q_i nodes, denoted by $n_i^1, ..., n_i^{q_i}$. Let $Q_i = \{n_i^1, ..., n_i^{q_i}\}$.

- For each $(n_i, n_j) \in E$, let E' contain the $q_i + q_j$ edges needed for the nodes in $Q_i \cup Q_j$ to be arranged in a cycle. Assuming that $q_j \geq q_i$, these edges will be deployed in such a way that, beginning at either $n_j^{q_j}$ or $n_i^{q_i}$, a traversal of the cycle in decreasing order alternates either $\lfloor q_j/q_i \rfloor$ or $\lceil q_j/q_i \rceil$ nodes in Q_j with one node in Q_i, until $q_i/gcd(q_i, q_j)$ nodes from Q_i have been traversed. The choice between $\lfloor q_j/q_i \rfloor$ and $\lceil q_j/q_i \rceil$ must be such that $\lceil q_j/q_i \rceil$ is picked exactly $(q_j \bmod q_i)/gcd(q_i, q_j)$ times, while $\lfloor q_j/q_i \rfloor$ is picked in the remaining $(q_i - q_j \bmod q_i)/gcd(q_i, q_j)$ times. At this point, the cycle's first segment is completed. The process continues likewise until the $gcd(q_i, q_j)$ segments needed to use up all $q_i + q_j$ nodes have been built. Segments are linked to one another by taking them in the order they were built and connecting the last node added to a segment to the first node added to the next segment. At the end, the cycle returns to the first node added (either $n_j^{q_j}$ or $n_i^{q_i}$) from the last one added (either n_i^1 or n_j^1 respectively).

Having built G', we next construct an orientation, call it ω_0', of the edges in E'. For every $(n_i, n_j) \in E$ such that $q_j \geq q_i$, the edges constituting the simple cycle described above are oriented by ω_0' in such a way that, in the subgraph induced in G' by $Q_i \cup Q_j$, the first node added to the cycle is the only sink and the last node added is the only source [8].

The above description is a general method for obtaining the heavy-load SER version of biological building blocks from the original SMER version, in the sense that each oscillator in a building block may have pre-specified reversability greater than 1, which is helpful for constructing more complicated gait patterns. However, in our current case of three gait types with the flexor's reversability being always set to 1, the optimization procedure can be greatly simplified.

Model Reduction Method

As an example, the optimization of the medium speed pattern of an hexapodal animal under node multiplicity method is offered. This kind of optimization is in fact a transfer from SMER solution to SER solution for model realization, it is purely for the purpose of implemental facility in the sense that the node and edge circuitries are ready for VLSI implementation (see the following Subsection).

The firing circulation patterns of building blocks for medium speed of an hexapodal animal is like Figure 4.5(a), an optimized firing circulation of building blocks can be obtained based on the following calculation.

$$r_i = 3, r_j = 1 \rightarrow L = 3$$

$$q_i = L/r_i = 1 \rightarrow Q_i = \{n_i^1\}$$

$$q_j = L/r_j = 3 \rightarrow Q_j = \{n_j^1, n_j^2, n_j^3\}$$

Compared with Figure C.6, the next figure is an alternative medium speed gait pattern reconstructed by the optimized building blocks. Since the key point in gait analysis is phase relationship among all legs, as we can see, this relationship can exist automatically if the initial configuration of the optimized building block for each leg is chosen correctly. In Figure C.7, each flexor requires to access all incident edges, i.e., both the set of edges within building blocks represented by plain arrowlines and the set of virtual edges between neighboring flexors represented by line-dotted arrowlines, in order to fire. Fortunately we don't need to consider the virtual edges in the case of suitable choice and configuration of building blocks, the gait model circulates well and any rhythmic patterns can thus be generated for digital circuit design and FPGA implementation smoothly.

C.3.2   Model Implementation with Custom Hardware

Based on the aforementioned analysis of the realization methodology of animal gait generation and transition CPGs mechanism, the simulation and synthesization of legged locomotion is conducted utilizing **Xilinx Foundation Series** $v1.4$ software [81]. In both schematic and HDL design flows, reconfigurable building blocks may be constructed, under the principles of SER/SMER scheme, to perform the gait transition (see Figure C.8),
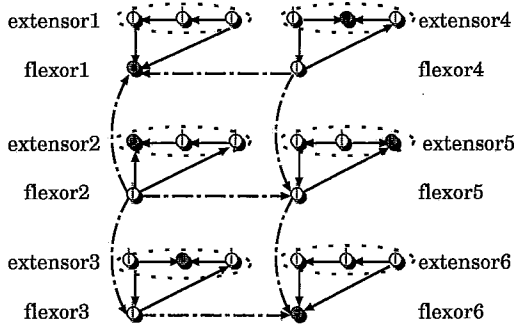
Figura C.7: The cockroach's medium speed gait pattern reconstructed with optimized building blocks, three nodes within the dashed circle represent an extensor while the other one represents its coupled flexor. This figure corresponds to configuration (a) in Figure C.6.

i.e., it can be configured, at any time, from one definite speed pattern to another according to the external signal coming from CNS, hence the reconfigurable building block alone can also represent the combination of oscillation system and CPGs.

The principal potency of SER/SMER scheme stays in the fact that it may deal with the asynchronous problems as efficiently as the synchronous ones, for the signal-driven nature of the building block, which is an operational engine constructed under SER/SMER, makes the whole system time-independent, or namely, no global clock is needed. Unfortunately, since asynchronous circuits are not well served by current FPGA architectures [48], in the sense that various hazards may be unavoidably introduced as the asynchronous circuit is realized, which may lead to the wrong logic and the whole circuit system may oscillate at last. For simple consideration and without loss of the efficiency of gait simulation, we'll adopt the synchronous circuit in our design.
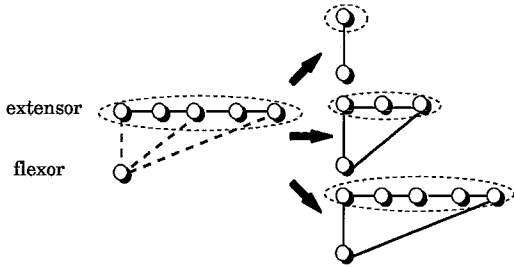
Figura C.8: An undirected graph representation of the reconfigurable building block, here it may lead to three types of configured building blocks corresponding to three different speeds. The directions of edges of a resulting building block should also be configured according to which leg this building block belongs to.

Circuit Design

It may be more clear to introduce the relative circuit corresponding to the former abstract graph digrams. The graph shown in Figure 4.8 was implemented principally by two simple circuit blocks, namely, the node controller and edge controller, each node and edge corresponds to one of these controllers respectively.

- *The Node Controller* - In this model a node starts operation according to an AND gate that samples all the tokens incident to a node. The tokens represented by arrowheads in Figure C.9 are now supposed the true logic levels entering AND gate, which sets the node's FF when that node becomes a sink. If a totally asynchronous environment is assumed, after operating for τ_{op} time units, the processing logic must produce a corresponding *end-of-operation* signal that is used to reset the node's FF through an OR gate. The situation is the same for an alternative synchronous environment. In both environments an external delay circuit may be needed for each node controller, here the difference is whether this delay circuit is governed by a global clock or not. Operation also depends on a Stop/Run signal. During initialization, while tokens are being fed with their proper values, Stop is used. Run is active from then on.
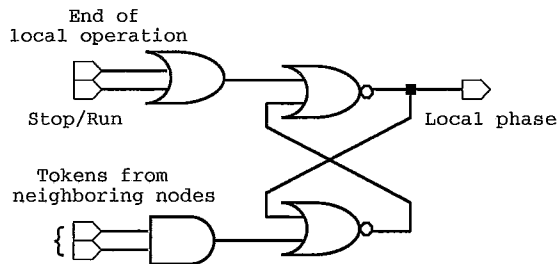
Figura C.9: Schematic for the Node Controller

- *The Edge Controller* - A toggle flip-flop with preset is used as a token generator. The preset input is used for initialization, while the output values represent the tokens themselves. Outputs are routed according to the desired token acyclic pattern, in our gait circuit it's important to configure this edge controller for a desired walking speed and various gait patterns can be achieved depending on this configuration. Whenever a node ceases its operation, it generates an end of operation

72

signal, which is sent to all the edge controllers incident to the node, where it toggles the edge flip-flops.
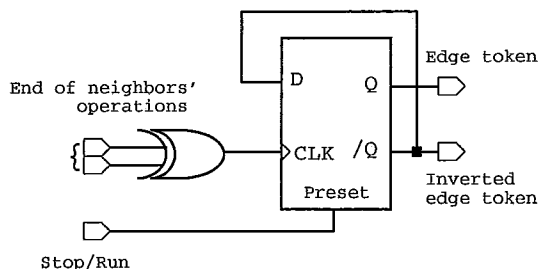
Figura C.10: Schematic for the Edge Controller

HDL Design and Simulation

A complete procedure of high-level design has been conducted in this testing period, with three reconfigurable gait patterns loaded in one Xilinx $XC4010XL$ FPGA chip. The adopted method to implement the gait generation and transition utilizes a pre-defined VHDL listing format to describe the circuit behavior. Below is a template of the behavioral VHDL code required for this operation. There are totally six inner-loop process representing the six legs respectively with each process in the similar structure. In each process the signal assignment statements are pipelined together in sequential mode while all the six processes will execute concurrently. At last the concurrent signal assignment statements are followed for combinatorial outputs of the flexor and extensor motor neurons.

At the last of the intact program the combinatorial ouputs are assigned to the flexors and extensors based on the principles of SER/SMER scheme, i.e., each motor neuron will fire if and only if it has all its edges directed to itself. The following table describes the condition of consumed resources in one $XC4010XL$ chip for synthesizing three aforementioned locomotive patterns. Besides, there are still one global buffer, BUFGLS and STARTUP used respectively.

It is intuitive that phase relationship among six legs in this simulation is the same with the biological-based analysis in Figure C.3. The sole difference is that, there may exist some phase overlap among six legs in the real neuronal motor system because of the mechanical hysteresis while our SER/SMER-based waveforms are the results of relaxation oscillations, which can thus be treated exactly as the CPGs driving outputs. Considering

73

```
entity functional_unit is
    port ( port declarations );
end functional_unit;

architecture behavior of functional_unit is
    type and signal declarations;
begin
    process 1
    begin
        if during initialization then
            pattern initialization;
        elsif clock pulse arriving then
            case state-of-leg is
                when slow-initialization =>
                    ( current-slow-state );
                when medium-initialization =>
                    ( current-medium-state );
                when fast-initialization =>
                    ( current-fast-state );
                when slow-state =>
                    if slow-state-continue then
                        state-of-leg <= next-slow-state;
                    elsif slow-state-changed then
                        decide changed pattern;
                    end if;
                when medium-state =>
                    if medium-state-continue then
                        state-of-leg <= next-medium-state;
                    elsif medium-state-changed then
                        decide changed pattern;
                    end if;
                when fast-state =>
                    if fast-state-continue then
                        state-of-leg <= next-fast-state;
                    elsif fast-state-changed then
                        decide changed pattern;
                    end if;
            end case;
        end if;
    end process 1;
end behavior;
```

Figura C.11: VHDL template for a single process corresponding to one leg movement.

74
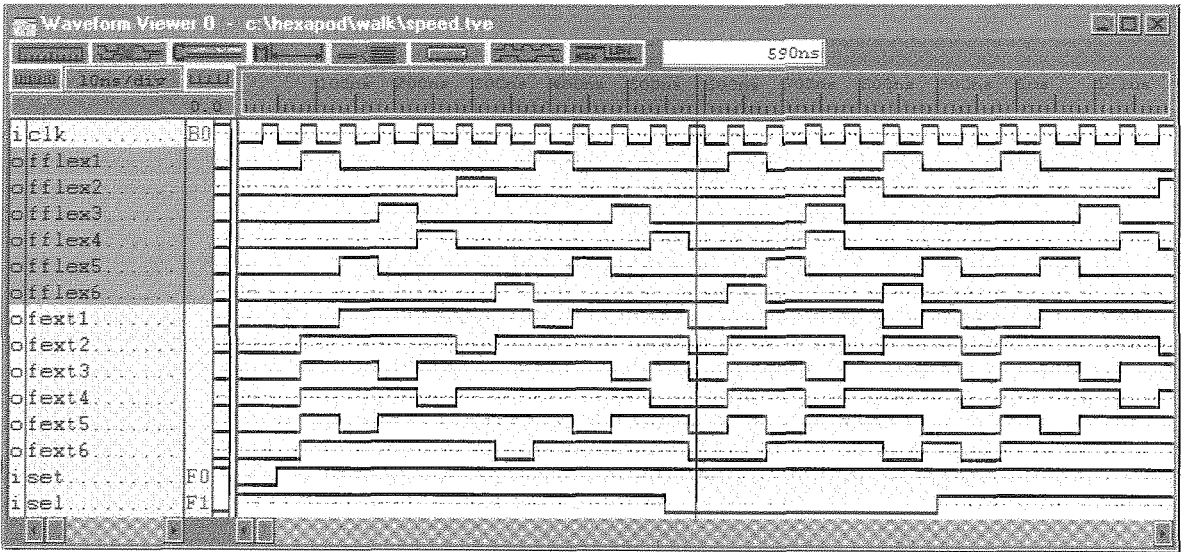
Figura C.12: Simulated waveforms of hexapodal animal's different gaits. The system is started as signal *set* is high, either slow or medium speed is chosen as signal *sel* is high or low respectively.

the operation of the mechanical platform, one period of low level output to all motor neurons (including flexor and extensor) is designed to allow system depolarization during gait transition.

Tabela C.1: The condition of usage of resources for embedding three gait patterns in $X4010$.

No. of CLBs				No. of bonded IOBs	
238 out of 400				17 out of 63	
FF	Latch	4-in LUT	3-in LUT	Flop	Latch
142	0	437	89	0	0

C.4   Computer-based Experiment of Hexapodal Gait

An simple experiment of hexapodal gaits is conducted based on the IBM PC compatible computer, with a robot kit named *STIQUITO* as the controlled platform. Stiquito is a six legged, insect shaped robot, it uses the contraction property of shape memory alloy actuator wire, *Nitinol*, for driving the legs. The controller (here is the PC and driving circuitry) has the facility to drive the legs forward, sychronize the leg movements and control the direction of turning, etc.. The value of this simple simulation lies in that, almost all gait patterns, from the rough classification or classification with detailed phase relationship, can be programed and made visually under a quite reasonable functionality/price rate.

75

C.4.1 The Mechanic Part of Mobile Stick Insect

We made the mechanic part of mobile stick insect, i.e., the *Stiquito*, adopting the assembly components from Mills J.W. et al. of Indiana University [26]. The unique characteristic of this platform lies in that, no traditional motor actuator is used, and as a substitution, *Nitinol*, the shape memory alloy wire is employed to mimick the real life movement system of animals, which is obviously a more natural way. As shown in Figure C.13 the six resilient music lines connecting with *Nitinol* wires represent six legs and they all interconnected by some aluminium tubes without soldering needed. As we've already argued and known, the coupled flexor and extensor are generally indispensable for legged locomotion. However, only *Nitinol* is used in this simple experiment and can be treated as the extensor, with flexor absent, at the first glance. In fact, although it may be better to add the flexors, it is also acceptable to take music line's instinctive resilience as the virtual coupled flexors for rough simulation.
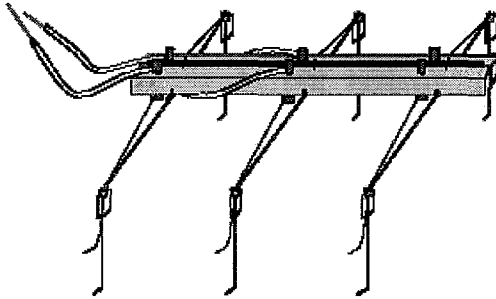
Figura C.13: A schematic diagram of Stiquito – the mechanic part.

This diagram is pretty self-explained in the sense that how this robot can be controlled by our PC and peripheral circuits. Normally, the main controls needed to get different gaits are as follows.

- Some way of activating the legs in different order so that some different gaits can be retrieved.

- Some way of controlling the displacement of the leg. This facility is used to turn the robot in different directions. For instance, less displacement for left legs and more displacement for right legs may make the robot to turn left [65].

76

- Some advanced way of adding more equipments to the robot platform for it to get more ability in adapting the complex terrains and therefore to adjust its gait patterns adaptively, in this case, some sensing and feedback instruments, e.g., the camera and foot sensors, may be needed.

As a simple and preliminary study, the controller designed here will only be required to determine the sequence and phase periods of signals being sent to the individual leg actuator to produce simple walking, i.e., in this experiment only the first control is effectively realized, and the second control won't be difficult provided that a suitable robot platform can be found.

C.4.2   The Controller Part of Mobile Stick Insect

This part consists of two components — PC controlling and Darlinton circuit driving. We use C language to generate six controlling signals outputting from the parallel port. Since the legs are controlled by the Nitinol wires, the more the number of cycles for which the leg is activated, the more the time for which current is passed through the Nitinol wire and the more the leg swings backward. Thus the determination of frequency of the driving signal and its rate of space occupancy are very important for controlling the locomotive rhythm, and because of this timing limitation, some modification is needed if any transplant may be realized. Only six data output pins are employed for six legs respectively in this simple experiment. Disposal is the measure of how many cycles a leg should be activated, it may be used to control the movement direction of *Stiquito*. For instance, if the less number of active cycle disposed to left legs than which is disposed to right ones, then right legs move more than left legs and so the *Stiquito* turns towards left.

The current output of the parallel port pins is not sufficient to drive the legs effectively. So the Darlington high current driver circuit is indispensable, the Nitinol wire and music wire are serially connected between the power supply and collector of the second level transistor, as shown in Figure C.14.

It is just this simple, computer-based experiment by which we are motivated and began the work of synthesize three gait patterns into a single chip of FPGA, whose basic methodology has been illustrated in the previous section. The use of SER/SMER as the
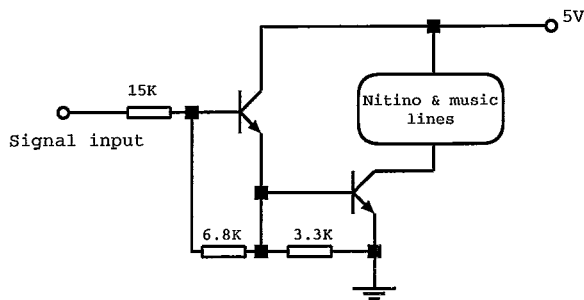
Figura C.14: Control circuit for one leg – the Darlington high current driver circuit. The first level transistor controls the second level transistor which is a switcher, output current is about 550mA as this switcher closes and zero as it opens.

basic dynamics of the locomotive circuits turned out to be a quite general and timing-independent strategy. Theoretically, with this methodology we can find reconstructive solutions to almost all the legged animal's gait pattern collection, which was provided by Collins et al.[21][22][20] using the symmetry-breaking Hopf bifurcation theory.

C.5 A Proposed Mathematical Dynamical Model

In addition to the macroscopic approach which will be introduced as the emphasis in this thesis, a formal method treating the pattern formation and gait transition[2] may be an alternative solution, such as the example given here. Among the typical mathematical oscillator models introduced in appendix B, Wilson-Cowan model is probably the best candidate as a proposed mathematical explanation of the complex biological behavior, especially on explanation of SER/SMER mechanism underlying locomotion, because of its macroscopic standpoint on describing the dynamics of average activities of two neural populations [78]. Let's recall this model encountered before, which is normally represented by two coupled, excitatory and inhibitory neurons showing the population behavior with large scale, internal connections and individual potentials inside this population. This model is based on mean field theory and allows a drastic reduction in the number of variables in large scale models of neural activities. With reference of the statement of Pearson's contribution [63], and the simulated results that the duration of active potential of inhibitory neuron population passing the threshold is less than that of excitatory neuron population, we could assign the inhibitory neuron population as representative of flexor

---

[2]As we know, the gait transition in spatio-temporal structure can correspond to symmetry-breaking or symmetry-collecting Hopf bifurcation, and each corresponding bifurcation diagrams can be computed.

population while excitatory neuron population as representative of extensor population, now it's clear that the WC oscillator model just corresponds to one of our biological building blocks. According to our biological hypothesis of adopting the SER/SMER scheme to simulate locomotive CPGs mechanism, which is initially introduced in the first chapter, the PIR characteristic should be assumed and it stipulates a purely inhibitory network. In this case we'll employ the modified Wilson-Cowan model (Equation $C.1$) of two oscillators with connections between inhibitory populations [12], as shown in Figure C.15(a).

$$\begin{cases} \frac{dE_1}{dt} = -E_1 + (1 - r_e E_1) F_e(w_{11} E_1 - w_{12} I_1 + P) \\ \frac{dI_1}{dt} = -I_1 + (1 - r_i I_1) F_i(w_{21} E_1 - w_{22} I_1 + Q - \alpha I_2) \\ \frac{dE_2}{dt} = -E_2 + (1 - r_e E_2) F_e(w_{11} E_2 - w_{12} I_2 + P) \\ \frac{dI_2}{dt} = -I_2 + (1 - r_i I_2) F_i(w_{21} E_2 - w_{22} I_2 + Q - \alpha I_1) \end{cases} \qquad (C.1)$$

where $w_{11}, w_{12}, w_{21}, w_{22}$ are all scalars denoting connecting strength between neurons, P and Q are the inputs of excitatory and inhibitory neurons, respectively, and α is the control parameter. The rest variables are with the same significances as in Section $B.2.5$.

(a)   (b)   (c)
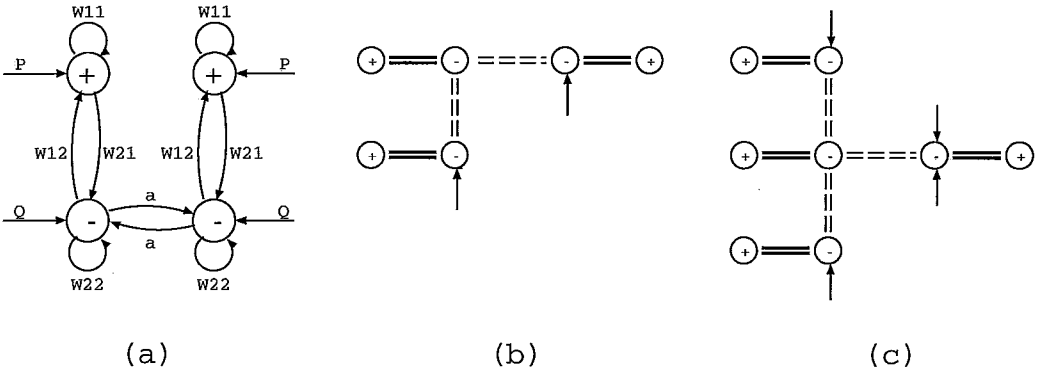
Figura C.15: The coupled neuron structures, (a) An architecture explained by equation $C.1$; (b) An architecture shows the head and tail organization of insect's locomotive structure, which could be represented by a 3-dimensional Wilson-Cowan oscillator model, the arrows are external input; (c) An architecture of organization of the rest part of insect's locomotive structure, which could be represented by a 4-dimensional Wilson-Cowan oscillator model.

It is our understanding that many legged animals with some degree of complexity, i.e., with more than four legs (not including four legged ones because of their simplicity), could be organized by two components shown in the above figure, upon which the high dimensional Wilson-Cowan model could be built and nonlinear, dynamical system theory etc. can be applied to investigate the bifurcation and pattern formation process. It is also worth noticing that a single Wilson-Cowan model which contains only one inhibitory neuron population and one excitatory neuron population should be modelled as a

relaxation oscillator, a formal version of aforementioned building blocks. Some traditional techniques from dynamical system theory, e.g., the Poincaré map, need to be used to investigate numerically the system behavior without solve the ODE groups.

C.6 Discussions

Based on the above introduction of background, state-of-the-art description and some works which are just under development, it is now quite clear that the research of neuronal oscillator underlying CPGs could be divided into two aspects, one is the heavily investigated, formally theoretical approach; the other lies in the application field, which is by far less inquired. We have successfully constructed some applicable instances through the parallel and distributed schemes, and we'll show further by enumeration that, there do exist some regulations to describe the symmetries among the various insect's gait patterns with these schemes. Moreover, the locomotive system itself is a very good example of dynamical system, some numerical analysis can of course be conducted for retrieving and predicting more details of this system.

Apêndice D

ANN Implementation of SMER

On recognition of the aforementioned mathematical description and state-of-the-art research on rhythmic and locomotive activities of vivid creatures, especially the successful (though roughly) application of parallel and distributed algorithm, e.g., *SER* and *SMER*, on modelling *CPGs* mechanisms, we find that it is not only worthy but also necessary and applicable to set up a *neural networks* framework governed by *SER/SMER* for developing its great potential on rhythmic pattern computations. Based on this consideration, a series of *Hopfield*-like neural networks are created as the media loading *SER/SMER* concepts.

D.1 Introduction

SER has the potential to provide the greatest concurrency among scheduling schemes on resource-sharing system, which require neighbors in this system to operate alternately [6]. The mutual exclusion characteristic between any two neighboring nodes coupled under *SMER* makes this scheduling scheme suitably tailored for simulating *post-inhibitory rebound (PIR)*, a widely employed neuronal mechanism underlying locomotion and other rhythmic activities. Besides, the dynamical behaviors of *SMER* scheme depends heavily on the initial allocation of shared resources, different configurations may lead to different cycling behaviors and even deadlock or starvation. This feature leaves us a research space on how to mimic *CPGs* with *SMER* to simulate numerous rhythmic patterns while avoiding possible wrong design. Despite undeterminated details of *CPGs*, many works have been proposed focusing on the coordination of creature system's components and their phase relationship on dealing with rhythmic patterns. Following this paradigm,

we've shown the potency of *SMER* by mimicking various hexapodal gaits in Appendix *C*. However, this kind of strategy is somewhat intuitive, and due to the discrete nature of *SMER*. It is obviously more efficient in digital simulations instead of analogous application.

On the other hand, the analogous behaviors are ubiquitous in the real world. They are continuous rather than discrete in time domain, better described by analogous circuitry rather than digital one. Although as a research technique, we can grasp some snapshots from a continuous procedure and treat them with discrete methodologies, it is undoubtedly a better style to adopt an analogous or continuously evolving system directly, for modeling the real counterpart. In this appendix, a series of novel *ANN* structures, namely *Oscillatory Building Blocks (OBBs)*, are proposed. These *OBB* nets are similar to *Hopfield* networks and governed by *SMER* algorithm, they can be classified into two major categories, i.e., simple *OBB* and composite *OBB*, depending on the network complexity.

One of the primary disadvantages of *SER/SMER* is the need to preprogram the system by a centralized entity [6]. However, as we adopt this scheduling scheme as a virtual *CPG* to retrieve animal's gaits, preprogramming is a natural process in the sense that, any animals' *CPGs* can be treated as a self-adaptive learning system inherited from its maternal body, some unchanged, simple rhythmic patterns such as respiration and mascuration are embedded in *CPG* as it is created, some others such as locomotions may need some training, a procedure similar to preprogramming. In these cases, some theoretically potential disadvantages of *SER/SMER* may be eliminated by a functional organ's manipulation while the theory is employed in application field.

We'll argue that any networks, no matter how complicated their topology may be, could always be composed by simple and/or composite, analogous *OBBs*, among which the design of simple *OBBs* is crucial, for it is the foundation of making composite *OBBs* and the whole net. A simple *OBB* only contains two coupled, mutually exclusive nodes. If we choose different internal parameters for the simple *OBB* system, we can get different duty factors and phase relationships between the two nodes. Even more complicated phase relations could be obtained by combining simple *OBBs* together, in some order. Theoretically we can retrieve any rhythms with our design.

The organization of this appendix is as following. First the famous Hopfield neural

networks is introduced in Section D.2, to inspire the idea on *OBBs* model construction. A design framework of simple and composite *OBBs* is proposed by the strict manner, including their architectures, properties and organization methods, etc., in Section D.3. Section D.4 introduces some topology problems and the adaptivity of the mechanism of *SMER*-like asymmetric Hopfield model, where we confirm that no matter what topology a network may have (e.g., trees, rings, mixture), its activities are tractable with *OBB* networks. A brief discussion is followed as the end in Section D.5.

D.2   Hopfield neural network model

In 1982 J.J.Hopfield published a most influential paper on the prominent emergent properties of one kind of neural model which rekindled great interest of scientists in neural network analysis. Different from McCulloch-Pitts (MCP) neural model in which neurons are intrinsically boolean comparators with limited inputs, Hopfield studied the biological structure of the large-scale interconnected neural systems and proposed his model with the emphasis on the neural system's whole behavior and properties. In his model a single neuron is simplified to be represented by a simple electronic device containing resistor, capacitor and a nonlinear component stipulating the input-output relationship. The dynamics of an interacting system of N coupled neurons in Hopfield model can be described by a set of coupled nonlinear differential equations governed by Kirchhoff's current law.

$$C_i \frac{dV_i}{dt} = \sum_{j=1}^{N} W_{ji} f_j(V_j) - \frac{V_i}{R_i} + I_i$$

where $i = 1, ..., N$. This equation expresses the net input current charging the input capacitance C_i of neuron i to potential V_i as the sum of three sources: (i) postsynaptic currents induced in neuron i by presynaptic activity in neuron j, (ii) leakage current due to the limit input resistance R_i of neuron i, and (iii) input currents I_i from other neurons external to the circuit. The model retains two important aspects for computation: dynamics and nonlinearity [51][53].

Hopfield classified his models into two categories, namely symmetric and asymmetric models. Between any two coupled neurons i and j in a Hopfield net, if the synaptic weight from neuron i to neuron j is equal to synaptic weight from neuron j to neuron i, then this is a symmetric Hopfield neural network, or Hopfield neural network by default since it's

so widely used; otherwise it's called asymmetric Hopfield neural network. The most prominent property of symmetric model is its autoassociation, i.e., the network energy keeps diminishing and finally reaches the local minima as the system states evolve. Unlike symmetric model, there are less research works on asymmetric models because they correspond to complicated oscillatory behaviors and the mathematical tools to manipulate and understand them at a computational level are limited. However, asymmetric Hopfield model may exhibit oscillation and chaos. In some neuron systems like CPGs, coordinated oscillation is the desired computation of the circuit, so proper combinations of asymmetric synapses can enforce chosen phase relationships between different oscillators [53]. In recognition of Hopfield model's properties, we proposed a novel methodology to embed the SMER algorithm into asymmetric Hopfield neural networks, we'll show this methodology is successful in simulating all CPGs patterns induced by Golubitsky's symmetric Hopf bifurcation theory.

D.3   Dynamic Features of OBBs

The SMER algorithm can be implemented schematically using a network like asymmetric Hopfield model with some modifications on the peripherical feedback control circuitry according to the interconnecting topology of given interactive system. Similarly to the dynamics of Cellular Neural Networks [16] [17], the coupled input and output voltages of each cell in these networks are normalized to digital low or high level while the internal potential is continuous within the normalized interval $[0, 1]$. The SMER based OBBs can be classified into two types by complexity, namely simple and composite. The simple OBBs only consist of two interconnected cells with pre-specified reversabilities. The composite ones may contain the arbitrary number of simple OBBs with any topology, the purpose of introducing composite OBBs is to facilitate a high density network construction in which a definite combination of some simple OBBs are employed frequently. The prototypes of both types of OBBs should follow Lemma $A.2$ for initial shared resources arrangement and configuration to avoid possible abnormal operation, e.g., deadlock or starvation during oscillation.

Definition D.1 *The simple oscillating building block (OBB) is defined to be an asymme-*

tric Hopfield network composed by two coupled nonlinear neurons where each neuron has one output to its coupled countpart and three inputs from its former internal state, the output of its countpart and a negative feedback from the output of itself respectively. ■

D.3.1 Dynamics of Simple OBB Networks

Now consider a sub-multigraph of $M(N, E)$, call it M^{ij}, only induced by a pair of neighbors n_i and n_j, with r_i and r_j as their reservabilities, respectively, and e_{ij} as the shared resources between them, where the number and configuration of e_{ij} shared resources should obey Lemma $A.2$ strictly. In this paper we always adopt $e_{ij} = r_i + r_j - \gcd(r_i, r_j)$ for description concordance. A basic asymmetric Hopfield network named simple OBB will be worked out based on these parameters in this subsection.

System Architecture

In this nonlinearly coupled system, we decide that postsynaptic potential (PSP) of each cell depends on three factors, i.e., its former PSP state, the impact of coupled neighboring cells and the negative feedback of this cell itself, without considering the external impulse. Each cell's nonlinear characteristic between PSP input and cell output is a specifically sigmoid function (see Figure D.1), or namely the heaviside type.

The system architecture may be treated as two coupled MCP neurons. Each cell has an input from its coupled counterpart and an input from the output of itself. A cell's PSP is the sum of its former PSP state, the weighted output of its coupled neighboring cell and the negative weighted feedback output of this cell itself. After nonlinearization, the input PSP will become biological output membrane voltage, to stimulate the other cells (see Figure D.2). Each cell's output has a RC circuit, which is somewhat like a simple low-pass filter. This circuit can also simulate the membrane electro-activities of real neurons. However, their parameters should be chosen in such a way that, taking neuron i as the example, $R_i >> R_{iout}$ [1], and C_i in a suitable value, otherwise the output waveform would be less than the normalized standard level (here assumed 1), possibly lead to the whole system halt; meanwhile charging features exist obviously instead of the pure pulses.

---

[1] Here R_{iout} is the output resistance of cell i.
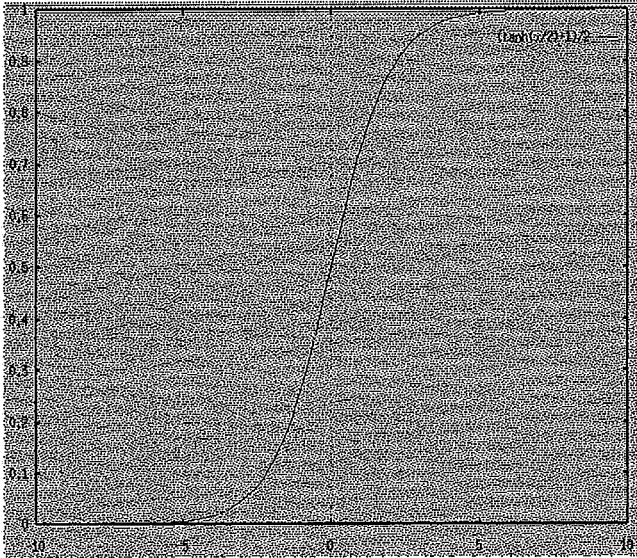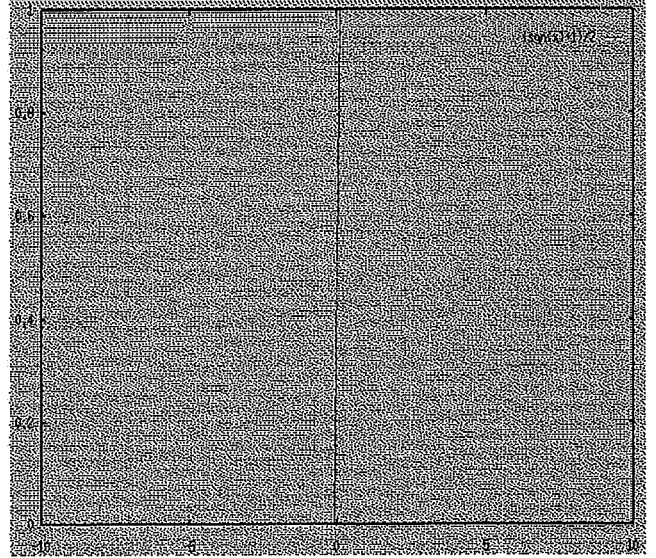
Figura D.1: The sigmoidal function and its specific heaviside type. (a) sigmoid function $tanh(ax) = \frac{e^{ax}-e^{-ax}}{e^{ax}+e^{-ax}}$, (b) its heaviside type with $a \to \infty$.
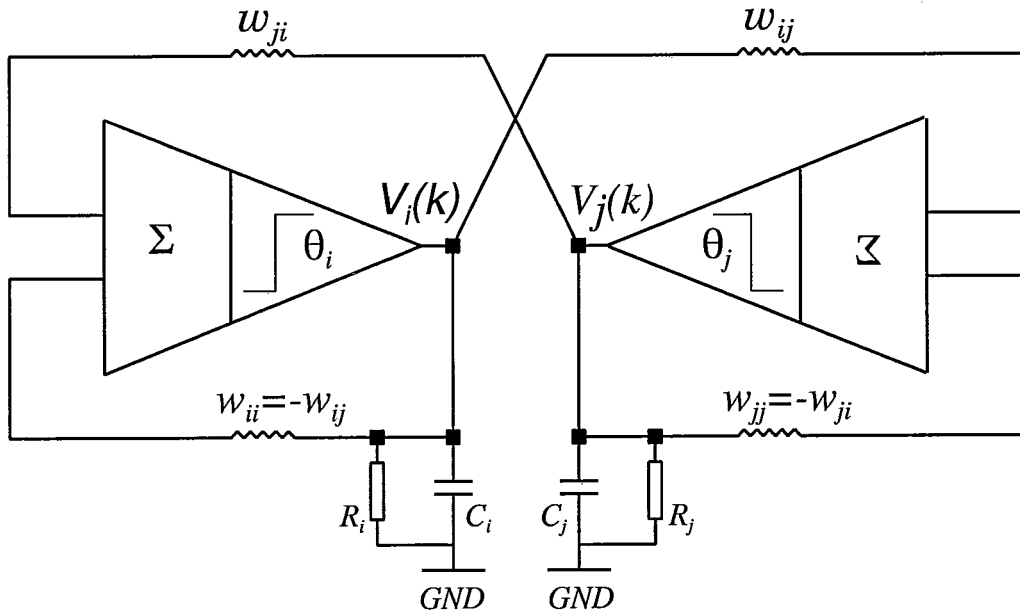
Figura D.2: A schematic representation of the simple OBBs architecture.

86

Calculation and Arrangement of System Parameters

The choices of system parameters, such as the cell thresholds and synapse weights, and the scheduling criteria of chosen system parameters are crucial to model a two-node SMER-based OBB as a pair of artificial neurons i and j. In our model, let $r = max(r_i, r_j)$ and $r' = h(r)$, where h is a function of getting highest integer level and multiplying it with 10, e.g., $h(r) = 10$, if $0 < r < 10$ and $h(r) = 10^{n+1}$, if $10^n \leq r < 10^{n+1}$, (notice that n is a natural number). Hence we can further design cell i and j's threshold θ_i, θ_j and their synapse weights w_{ij}, w_{ji} as the following.

$$\theta_i = \frac{max(r_i, r_j)}{r_i + r_j - \gcd(r_i, r_j)} \tag{D.1}$$

$$w_{ij} = \frac{max(r_i, r_j)}{r'} \tag{D.2}$$

$$\theta_j = \frac{min(r_i, r_j) - \gcd(r_i, r_j)}{r_i + r_j - \gcd(r_i, r_j)} \tag{D.3}$$

$$w_{ji} = \frac{min(r_i, r_j)}{r'} \tag{D.4}$$

We schedule the system parameters by comparing two nodes' reversabilities, if $r_i > r_j$, then we have two equivalent parameter arrangement schemes.

Scheme I $\theta_i > \theta_j$ and $w_{ij} > w_{ji}$

Scheme II $\theta_j > \theta_i$ and $w_{ij} > w_{ji}$

These scheduling schemes ensure that the behaviour of SMER-based Hopfield netwoks match its original SMER explanation naturally, i.e., node with smaller reversability (correponding to smaller threshold in Hopfield net) will oscillate with a higher frequency than its companion does. The difference equation of this system can be formulated as following, each cell's self-feedback strength is $w_{ii} = -w_{ij}$, $w_{jj} = -w_{ji}$ respectively and firing rate function is the heaviside type. It's worth noticing that k is the local clock pulse of each cell, a global clock is not necessary.

$$\begin{cases} M_i(k+1) = M_i(k) + w_{ji}v_j(k) + w_{ii}v_i(k) \\ M_j(k+1) = M_j(k) + w_{ij}v_i(k) + w_{jj}v_j(k) \end{cases} \tag{D.5}$$

where,

$$\begin{cases} v_i(k) = max(0, sgn(M_i(k) - \theta_i)) \\ v_j(k) = max(0, sgn(M_j(k) - \theta_j)) \end{cases} \tag{D.6}$$

We consider the designed circuit as a conservative dynamical system in the ideal case, i.e., the total energy is constant, no loss or complement is allowed, the sum of two cell's PSP at any time is normalized to 1. It's not difficult to see that this system has the ability of self-organized oscillation with firing rate of each cell arbitrarily adjustable. We'll prove later that there doesn't exist starvation or deadlock in this system no matter what initial state it may have. However, like most dynamical systems, our model also has a limit in the dynamical range, i.e., there exist some singular points as each cell's PSP equals to its threshold, in this way the system may evolve into another different oscillation behavior or even halt. Within dynamical range, some attracting properties show that this design is a suitable one for implementation of SMER algorithm.

System Properties

By transferring discrete SMER algorithm into its analogous, asymmetric Hopfield net host, we find that this self-organized oscillating network has some properties, which constitute the fundamentals for further complicated rhythmic network design. The criteria for choice of system parameters in the aforementioned way are important and consistent with those for the initial choice of SMER circulation, in order to avoid the possible system deadlock and unfairness.

Theorem D.1 *The coupled, two-node OBB system governed by SMER is a starvation- and deadlock-free oscillation system.*

Proof: Let's assume this circuit is a conservative system without damping and noise, and we also ignore the delay of synapse. Since the energy of this two-node, ideal system is invariant, we set the normalized system potential is 1 and the normalized potential of cell i is $a \in [0, 1]$, so the potential of cell j should be $b = 1 - a \in [0, 1]$. From equation (5.5) we get $M_i(k+1) + M_j(k+1) = M_i(k) + M_j(k)$, it also means the system energy is invariant. Hence, if $a > \theta_i$ then $b = 1 - a < 1 - \theta_i = \theta_j$. Similarly, if $a < \theta_i$ we can get $b > \theta_j$.

So it's impossible for two coupled cells to fire simultaneously. It's intuitive to understand the circuit mechanism that, if any cell fires, its PSP will keep decreasing by the value of coupling strength with regard to its neighbor per local pulse, until its PSP passes down through its threshold and the cell becomes idle. Meanwhile, the PSP of idle cell keeps increasing by the same value per local pulse until it becomes firing. This process will keep repeating and it guarantees the starvation- and deadlock-free oscillating mechanism of this circuit for two-node SMER system, the PSP of each cell is continuously changeable within $[-1, 2]$. ■

This kind of circuit has another prominent property which is essential for designing a CPG system, i.e., the oscillation system's convergence or periodicity consideration. The theorem can be described as that, no matter what the initial PSP value will be, a definite circuit with the coupled cells' reversabilities designated will converge to a definite oscillating period. However, since the converge procedure depends strongly on the cells' reversabilities and initial conditions, which is randomized and impossible to be determinated, the proof of this theorem needs some more description. First, let's imagine there is one line with length of l (l is real), and arrange a part of line l with the length of l_1, $l > l_1$, at the left side of l (see Figure D.3). Now we make a repeating operation on this line: everytime cut the left l_1 part of line l and put it to the right side, meanwhile shift the rest of line l to the left until the original left point is met, every point on line l follows FIFO rule. In this situation, after some operations can all points on line l match their original ones before operation, so that a cycle is obtained? Let's transfer this physical problem into mathematical form, with the sequence description, hence we have a preliminary lemma.

Lemma D.1 *The limit of sequence $\{a_N\}$ is zero if $\{a_N\}$ is monotonically decreasing sequence and satisfying $a_{N+1} = a_{N-1} - \lfloor \frac{a_{(N-1)}}{a_N} \rfloor a_N$, with the initial conditions of $a_0 = l$ and $a_1 = l_1$.*

Proof: Since $\{a_N\}$ is a monotonically decreasing sequence, i.e., $0 \leq a_{N+1} < a_N$, we have

$$\lim_{n \to \infty} a_N = b \geq 0$$

89

If $b > 0$, there always exists a sufficiently big integer N such that: $a_N - a_{N+1} < b$. However, from

$$a_{N+2} = a_N - \lfloor \frac{a_N}{a_{N+1}} \rfloor a_{N+1}$$

we have :

$$a_N = \lfloor \frac{a_N}{a_{N+1}} \rfloor a_{N+1} + a_{N+2} \geq a_{N+1} + b$$

so the result is $a_N - a_{N+1} \geq b$, which is contrary to $a_N - a_{N+1} < b$. So we can only have $b = 0$. ∎
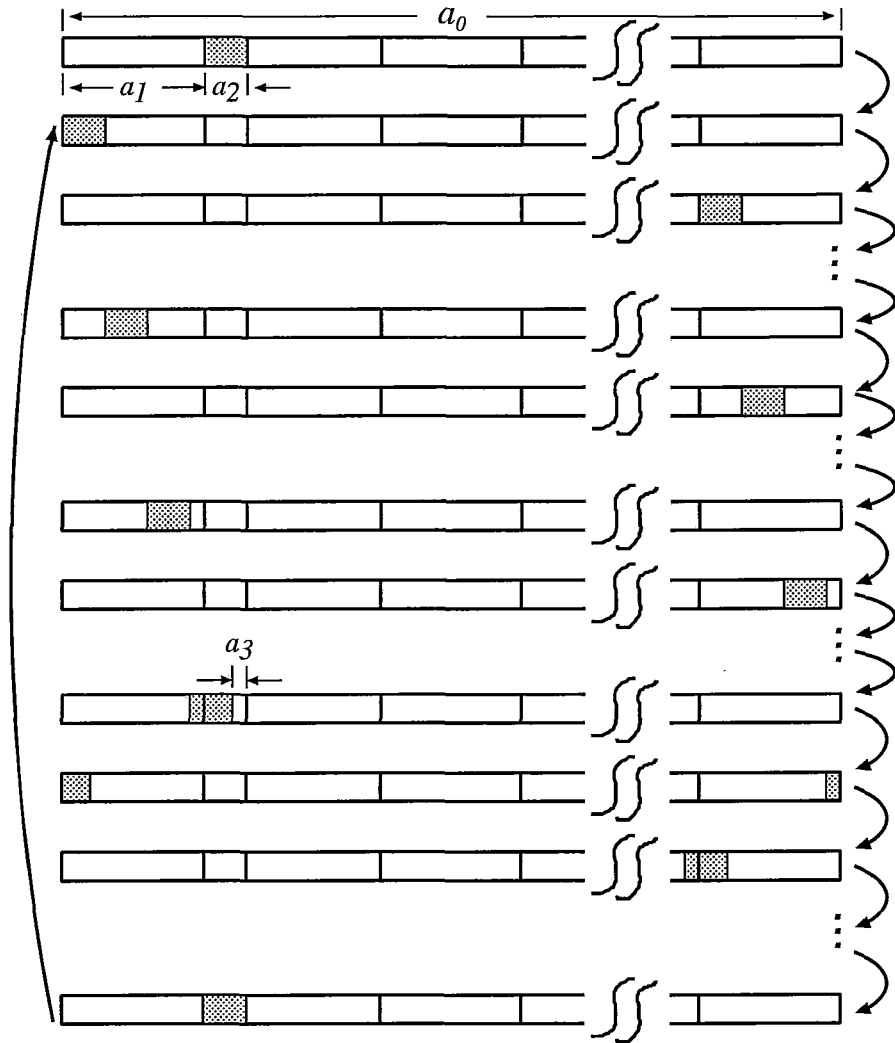

Figura D.3: An example for understanding Lemma $D.1$.

As a prerequisite lemma, it provides a simple while practical rule which will surely lead to a periodical oscillation. For a two-node, discrete SMER case, its periodical oscillation is apparent and has been proven [8][35]. However, an asymmetric Hopfield neural net

90

with embedded SMER mechanism is a continuous behavior system, at least in its internal state, moreover, the initial PSP of each net cell is randomly chosen within a normalized scope $[-1, 2]$, should this net has a periodical oscillation like its SMER prototype? The following theorem guarantees the net's behavior.

Theorem D.2 *The asymmetric Hopfield neural network governed by SMER always has an oscillating cycle, no matter what initial potentials may be.*

Proof: Without loss of generality, we suppose in the coupled two nodes system, $r_i > r_j$, and initially node j is firing, i.e., $M_j(0) > \theta_j$, $M_i(0) < \theta_i$. No matter what initial PSP node j may have, after a convergence procedure, node i and j will arrive at a pulse when they are at their final firing stage: $M_j(0) \in (\theta_j, \theta_j + w_{ji})$, $M_i(0) \in (\theta_i - w_{ji}, \theta_i)$. After that, node i will fire and, since $w_{ij} > w_{ji}$, $\frac{w_{ij}}{w_{ji}} = a$, node i fires for only one pulse and becomes idle again, from now on node j will fire from an interval from which it will always begin its firing. A four-step interval cycle is shown below.

I $M_j(0) \in (\theta_j, \theta_j + w_{ji})$, $M_i(0) \in (\theta_i - w_{ji}, \theta_i)$

II $M_j(1) \in (\theta_j - w_{ji}, \theta_j)$, $M_i(1) \in (\theta_i, \theta_i + w_{ji})$

III $M_j(2) \in (\theta_j + (a-1) * w_{ji}, \theta_j + a * w_{ji})$, $M_i(2) \in (\theta_i - a * w_{ji}, \theta_i - (a-1) * w_{ji})$

IV Some convergence procedure is followed, and system state return to state I.

Apparently it is the case of prerequisite Lemma, so every point within the interval of length w_{ji} will match its original position after certain pulses and the theorem is immediately proved. ∎

Numerical Experiment

A computer simulated example of this simple OBBs type net is conducted on the predefined cell reversabilities $r_i = 3$ and $r_j = 2$ with the arbitrarily chosen initial PSP. The numerical integration is conducted by the 5th-order Runge-Kutta method and the bioelectronical activities in the membrane channels are simulated by adopting membrane conductances and capacitors for each cell (see Figure D.2). According to the above

analytic steps, we can obtain the following results, here both threshold and weight are calculated except the initial PSP, which is randomly chosen.

Node i: $\theta_i^j = 0.75$, $w_{ij} = 0.3$, $M_i(0) = 0.02$

Node j: $\theta_j^i = 0.25$, $w_{ji} = 0.2$, $M_j(0) = 0.98$

Tabela D.1: State and internal potential circulation of two-node system, step 3 - 7 is a cycle.

Step	Node i		Node j	
	State	Potential	State	Potential
0	0	0.02	1	0.98
1	0	0.22	1	0.78
2	0	0.42	1	0.58
3	0	0.62	1	0.38
4	1	0.82	0	0.18
5	0	0.52	1	0.48
6	0	0.72	1	0.28
7	1	0.92	0	0.08

The system will experience a convergence process at beginning, upon chosen initial PSP, then it reaches a cycle of periodical oscillation (see Figure D.4). Table D.1 shows two-node system's evolving states and corresponding internal PSP of each cell.

D.3.2 Dynamics of Composite OBB Networks

The composite OBBs net is a generalized version of the aforementioned simple OBBs networks. It may have more nodes and therefore, more complicatedly organized topologies. The definition of Macroneuron should be given first before the definition of a composite OBB can be provided.

Definition D.2 *A macroneuron is defined to be a node i which satisfies $\forall i \in N$ where N is the set of nodes in multigraph $M(N, E)$.* ∎

Definition D.3 *The clone, which may have individually distinct reversability and represent coupling characteristics of its host macroneuron with one of neighboring macroneurons, is the unique type of component of its maternal cell - the macroneuron whose number of clones is equal to the number of its coupled macroneurons.* ∎
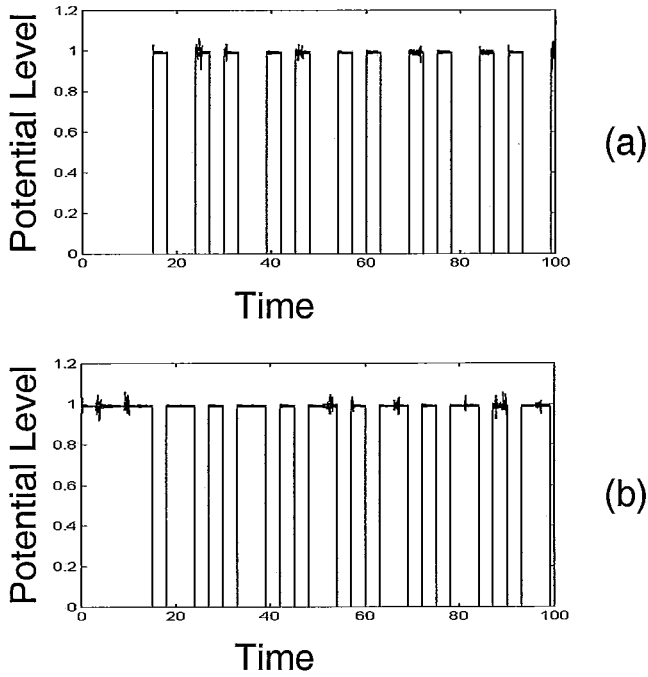
Figura D.4: Oscillating waveforms of two-node SMER system. (a) node i waveform, (b) node j waveform.

Definition D.4 *The composite oscillating building block (OBB) is defined to be a combined network of a set of simple OBBs in the way that each neuron of a simple OBB is a unique clone of a unique macroneuron.* ◗

Figure D.5 provides an example of two manners of describing network topology, one follows the custom of França's contribution [35] while another use the macroneuron expression for network implementation. Now consider an intact multigraph $M(N, E)$, consisting of a set of, say m, nodes (or macroneurons) $N =< n_1, n_2, ...n_m >$ and a set of edges $E =< ..., x_{ij}, ... >$, where $i \neq j$, $i, j \in [1, m]$, $x_{ij} = 1$ denotes macroneurons n_i and n_j connected, $x_{ij} = 0$ for n_i and n_j disconnected. Since we only consider the combination of any two macroneurons, 1_{ij} is equivalent with 1_{ji}, so we just ignore one in the edge set to make the network an undirected one. Each clone of a macroneuron n_i has its own reversability r_i^k, where k is the sequence number of a clone within the macroneuron n_i and $k \in [1, m]$. There are e_{ij} shared resources on the corresponding edge 1_{ij} between any two interconnected macroneuron n_i and n_j, with their number and configuration obey Lemma $A.2$ too.

Figura D.5: Two equivalent ways to illustrate the SMER algorithm, $r_i = r_m = r_n = 1, r_j = 2, r_k = 3$. **left**. original SMER description, **right**. an alternative description facilitates network implementation.

The Architecture and Computation

The composite OBBs networks, with the mathematical description similar to that of the simple OBBs networks, is equivalent to a system consisting of a number of subsystems which are actually the simple OBBs networks, i.e., an edge with shared resources in the num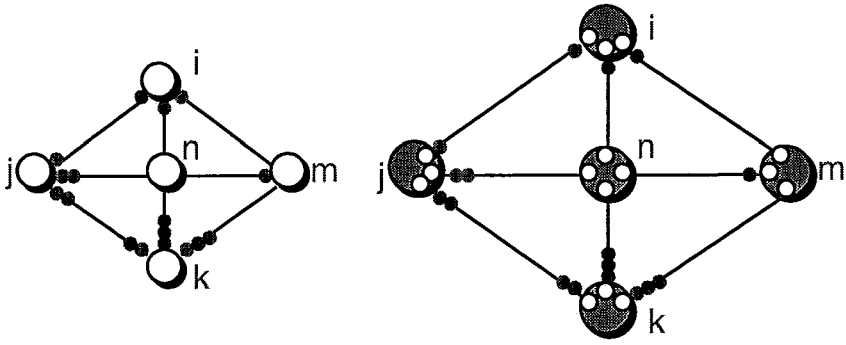ber of e_{ij} and two clones of two respective macroneurons connected by this edge. The number of edges in the composite net significates the number of subsystems, obviously the subsystem is just the simple OBB and its construction rules are the same as before. The main structural feature of the composite net is that, by dissecting the composite system into various simple ones, each macroneuron of the composite net is splitted into its corresponding clones (the set of clones share the same local clock as their maternal cell). According to the definition of clones, each clone is a component of both the corresponding simple OBB net and macroneuron, the number of clones of a macroneuron depends on the number of edges with which the macroneuron in the composite net is connecting. According to the principles of SMER, a macroneuron of a composite net will fire if and only if all its clones fire, thus the outputs of its clones are multiplied logically to denote its state in the composite net, and this state value is combined with the state value of its coupled cell to determinate the next state of their coupled, simple OBB net. A schematic diagram of the dissected composite OBBs networks is shown in Figure D.6, which is a modified version of Hopfield net in the sense that additional feedbacks from the logical sum combination of two outputs of coupled nodes in the composite net are provided to control the transition of the shared resources on each corresponding edge, i.e., only as a cell is firing, the shared resources on all edges pertaining to this cell will fully or partially

94

transit to another cell coupled by the corresponding edge.

The calculation of the amount of shared resources transitted between two coupled nodes depends on the choice of treatments. In the theoretical SMER algorithm, a firing cell n_i should have no less than r_i discrete, shared resources pertained to it from each of its neighboring nodes, where r_i is a digit, so n_i will release exactly r_i shared resources to all its neighbors at the end of its local clock during its firing period. However, in our neural network implementation version of SMER algorithm, the amount of shared resources on an edge is always taken as 1, which is regarded analogically as the sum of the PSP values of two nodes n_i, n_j interconnected by this edge, or equivalently, the total energy of the conservative subsystem of the composite OBBs net. When a cell, say n_i, is at the end of its local clock during its firing period, it'll release the shared resources owned in its weight-equivalent amount, w_{ij} which is the function of system parameters r_i and r_j, to its neighbor n_j, thus the amount of shared resources pertained to n_i is now a fraction within the scope of $[0, 1]$.

As the generalized version, the composite OBBs nets can represent much more complicated oscillating neuronal nets than the simple ones, they can also reproduce much more rhythmic patterns than the simple ones. Since it's impossible to assign a unified threshold to a cell which may have more than one connecting direction, the usual way to analyse this kind of nets is, as we've mentioned, to dissect them into the subsystems of simple nets, where formulae $(D.1)$ - $(D.6)$ for determining the weights, thresholds and dynamical behaviors of nodes in simple OBBs nets are still valid for subsystems of composite nets. However, some significant modifications should be made to organize these subsystems into composite OBBs nets according to the general output formula of a cell n_i.

$$V_i(k) = V_i^1(k) * V_i^2(k) * ... * V_i^n(k) \qquad (D.7)$$

or in a more compact form:

$$V_i(k) = \prod_{j=1}^{n} V_i^j(k) \qquad (D.8)$$

where the superscript sequence $1, 2, ..., n$ means the clone number of a macroneuron

n_i of the composite net. The specificity of the composite OBB network lies in that a macroneuron has n clones if it has n coupling macroneurons, each clone of a macroneuron is directly in charge of the coupling with another clone of another macroneuron to form a simple OBB. The firing activity of a macroneuron can be absolutely influenced [2] by its coupled macroneuron's connecting clone, which is a different phenomenon from those usually treated in many neural models where a cell's neighbors play the accumulative effects on the cell and sometimes if the effect of only one neighbor is neglected, the cell's dynamics may keep unchanged. This new characteristic, namely *all-or-none*, embodies that a network upon OBB is a typical asynchronous distributed system which is message-driven, the state of any anonymous macroneuron is determined by a set of atomic clones. It's worth noticing that, an alternative *Node Multiplicity Method* (NMM) was proposed by Barbosa et al. [8] to transfer the SMER cases into SER ones, which provides an optimal method for understanding and application of SMER schemes. In the studies of our OBBs net, the simple one consisting of two neurons with different reversabilities may also be transferred into the specific, composite OBBs net of SER cases by employing NMM, i.e., this SER-driven net only consists of a closed loop with every clone of a macroneuron having the same reversability whose value is 1.

Numerical Experiment

A computer simulated example of this composite OBBs type net is conducted with a four-node SMER-like asymmetric Hopfield net, on the pre-defined cell reversabilities $r_i = 4$, $r_j = 3$, $r_k = 2$ and $r_p = 1$ with the arbitrarily chosen initial PSP. The net topology is described by its node set $< n_i, n_j, n_k, n_p >$ and edge set $< 1_{ij}, 0_{ik}, 1_{ip}, 1_{jk}, 0_{jp}, 1_{kp} >$. The crucial point to achieve the desired rhythmic patterns from this composite network is to choose the initial PSP values properly for every subsystems. The proper initial PSP of each clone should be determined by considering the firing sequence of each macroneuron in the discrete SMER case, otherwise, random choice of initial PSP may lead to system halt, for example, no clone cells should be idle if its macroneuron is firing initially. In this

---

[2]Being absolutely influenced means that a macroneuron, saying n_i, shouldn't fire even if all its clones except only one are firing, this unique idle clone connects macroneuron n_i's coupled macroneuron n_j which is also not necessarily firing although at least one of macroneuron n_j's clone connecting macroneuron n_i is firing.

experimental case, each macroneuron has two clones for it has two neighbors. The output voltage of a macroneuron is the multiplication of outputs of its two clones. Each clone of the macroneuron couples with another clone of coupled macroneuron, which composing a simple OBB. The simple OBB's behavior is controlled by the feedback of its two coupled macroneurons' firing activity [3], i.e., two clones' PSP potentials in the simple OBB will be re-arranged only if one of their coupled macroneurons fires.

Node i to j: $\theta_i^j = 0.667$, $w_{ij} = 0.400$, $M_i^j(0) = 0.700$

Node j to i: $\theta_j^i = 0.333$, $w_{ji} = 0.300$, $M_j^i(0) = 0.300$

Node i to p: $\theta_i^p = 1.000$, $w_{ip} = 0.400$, $M_i^p(0) = 1.050$

Node p to i: $\theta_p^i = 0.000$, $w_{pi} = 0.100$, $M_p^i(0) = -0.050$

Node j to k: $\theta_j^k = 0.750$, $w_{jk} = 0.300$, $M_j^k(0) = 0.800$

Node k to j: $\theta_k^j = 0.250$, $w_{kj} = 0.200$, $M_k^j(0) = 0.200$

Node k to p: $\theta_k^p = 1.000$, $w_{kp} = 0.200$, $M_k^p(0) = 1.070$

Node p to k: $\theta_p^k = 0.000$, $w_{pk} = 0.100$, $M_p^k(0) = -0.070$

D.4 Network Topologies

Generally speaking, the oscillating mechanism of asymmetric Hopfield model under SMER can be employed in a network with any topology to generate oscillation. However, some distinct characteristics may exist among different nets. In this section, the novel mechanism is adopted in two different network topologies, we may compare the possible difference. Suppose an undirected, finite graph $M(N, E)$, any node within M has at least one edge connecting it with another node, and all nodes can be reached if starting from this node. If there is no route existing from any node to itself, then this network is called tree net, otherwise, nontree net. For both kinds of nets, each node may have more than one neighbor, hence it should be splitted into corresponding clones, a pair of coupled clones

---

[3]Simple OBB's behaviors don't depend on the activity of their directly coupled clones.

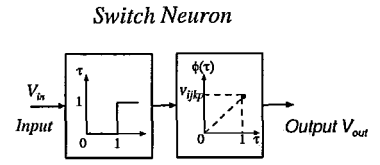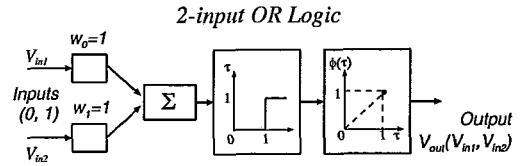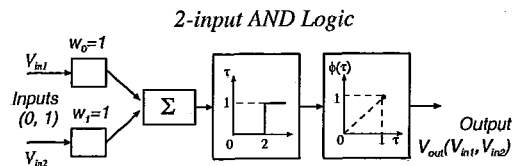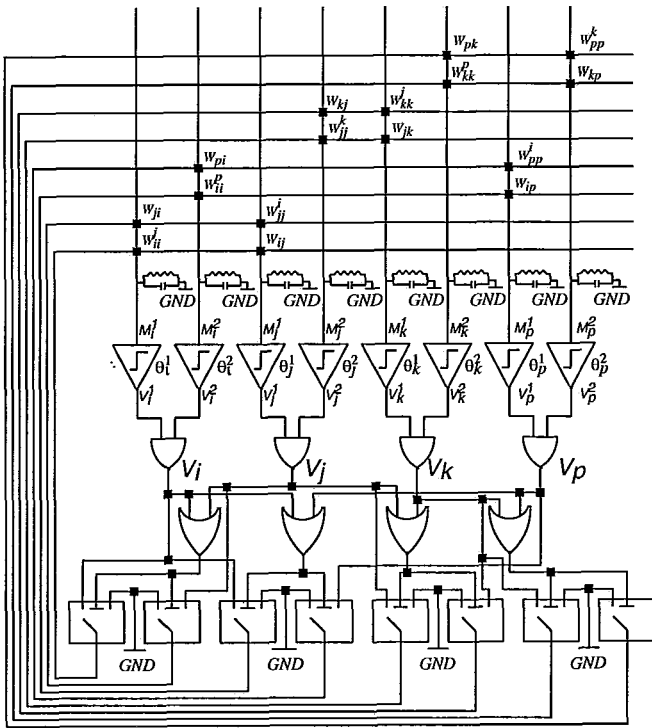Figura D.6: Network schematic structure (**left**), and MCP expression of AND, OR and Switch Neurons (**right**).
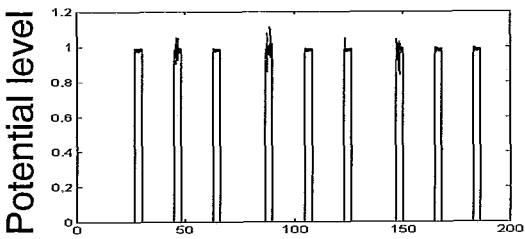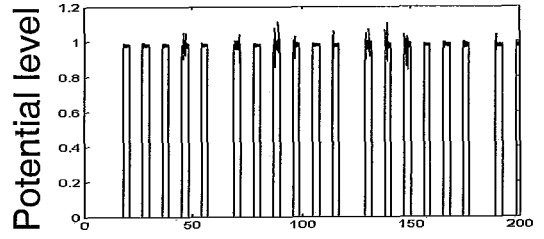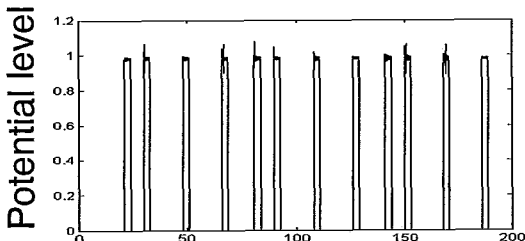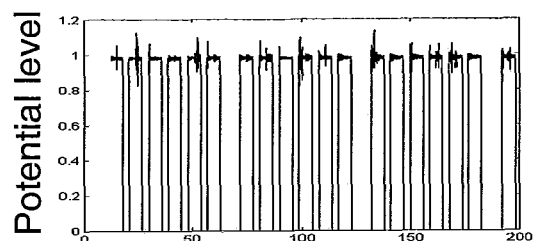
Figura D.7: Oscillating waveforms of four-node SMER system. (a) node i waveform, (b) node j waveform, (c) node k waveform, (d) node p waveform.

and their edge compose a simple OBB. The following is the pseudo-code operation of a macroneuron in an asymmetric Hopfield network under SMER.

Tabela D.2: Pseudo-code operation of a macroneuron

```
/*Program: Macroneuron_firing_function*/
CONST:
r[i : 1...m]:integer;
threshold[i, j : 1...m], weight[i, j : 1...m]:real;


VAR:
membrane[i, j : 1...m]:real;
firing[i]:boolean;


Initial state:
membrane[i, j] := random;
firing[i] := false;


Action at i local pulse:
if (∃j∈(1, m)|(j! == i) ∧ (weight[i, j]! == 0) ∧ (membrane[i, j] <threshold[i, j]))
            begin
                    firing[i] := false;
                    await not(membrane[i, j] <threshold[i, j]);
                    continue;
            end
else
    begin
            firing[i] := true;
            if (∀j ∈ (1, m)|(j! == i) ∧ (weight[i, j]! == 0))
            begin
                    membrane[i, j] :=membrane[i, j]−weight[i, j];
                    membrane[j, i] :=membrane[j, i]+weight[i, j];
                    continue;
            end
    end
```

D.4.1   Tree Net

A tree net normally has a root and many successors, one node can connect with many successors while only one parent node in a tree, at terminals each node has only one connection with its parent (see Figure D.8). By adopting the oscillation mechanism of

asymmetric Hopfield model under SMER, it is obvious to see that, no matter how to arrange the initial PSP for each clone around every simple OBB, the tree net won't stop oscillation, the same property as employing the mechanism of SMER directly on this net.

(a)   (b)
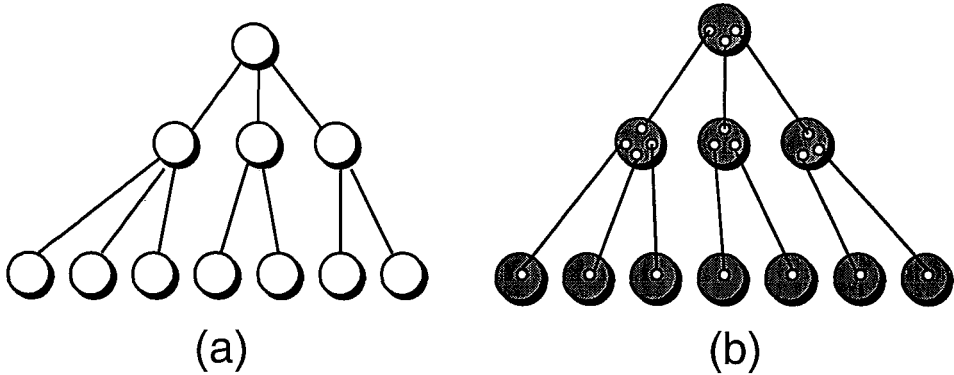
Figura D.8: Tree network and its conversion. (a) a tree, (b) a tree's clone conversion.

Proposition D.1 *The tree net governed by mechanism of asymmetric Hopfield model under SMER won't halt.*

Proof: We mark the terminal node level as the first level, the neighboring node of the terminal nodes as the second level, and so on, the root node could be k level ($k \geq 2$). Suppose a system halt would occur, when all first level nodes will also stop activities. Since the first level nodes have only one neighbor each, so the second level nodes have all their shared resources, which are shared with the third level nodes, less than their active threshold respectively. This assertion will keep true for every level until the root node, so the root should be firing, which conflicts with the assumption, the proposition is proved immediately. ∎

D.4.2 Nontree Net

In a nontree graph $M(N, E)$, there exist at least one route cycle. A node in this route means that, if starting from this node, there is a route returning back to itself. This kind of graph is always active, i.e., at least one node is firing at each clock pulse, under our mechanism except a cyclic route exsits.

Proposition D.2 *The nontree net won't halt except a cyclic route occurs.*

Proof: If a cyclic route occurs in a nontree graph, then no node on this cyclic route will fire. In this case any firing node coupled to one node on cyclic route will release its potential and keep idle forever, and so on until this procedure expands to all net, hence all net halts. If no cyclic route occurs in the nontree graph, let's suppose the net will halt. In this case the node on the route cycle with enough potential from both neighbors won't fire, which means at least one coupled neighbor out of the route cycle is keeping their shared potential but idle forever, and so on. Finally it leads to two possibilities, one is that a closed route cycle is followed to return back to this idle node, a case conflicts with the condition. Another is that, at last a terminal node which has sole connection is reached, and the terminal node will fire, a case proved in Proposition $D.1$. Hence the proposition is proved. ∎

D.5 Discussions

A methodology on how to combine SMER discrete algorithm with analogous ANN mechanism to generate stable dynamical behaviors is proposed. Some fundamental properties of this novel architecture, namely the asymmetric Hopfield net under SMER, are also proved. Different from previous works on implementations of Hopfield neural networks in parallel computers [35], which were mainly based on symmetric Hopfield net and hence employing its descending-energy-gradient property, the new implementation of asymmetric Hopfield nets have the necessary capabilities to represent every aspect of SMER dynamics without any additional constraints. This mechanism can reflect an ideal oscillating system under ideal environments, i.e., the system global energy is kept unchangeable.

The most interesting aspect of this approach is that it provides a reliable and complete conversion for SMER algorithm from discrete to analogous domain, and it is applicable for any topology system under SMER updating dynamics. Since the organization of any node's output is determined by the outputs of its clones, no limit is imposed on a node for its external connections. The system maintains the auto-organization feature as its state evolves, which greatly facilitate to organize the large-scale networks and evaluate the net activities, provided that the network is applicable under SMER mechanism. Notice however, that under this SMER-based ANN solution, some topics on its dynamical scope

deserve further research. For instance, the state of a simple OBB will be undetermined if two nodes' PSPs are equal to their thresholds respectively. It seems that the initial PSP of each node shouldn't have the last efficient bit in common, otherwise a halt will be inevitable after the system evolves to PSP-equal-threshold state.

Biological oscillation is one of the potential applications in which the asymmetric Hopfield model under SMER can be employed. We have tried to apply SMER directly on modelling animal CPGs, a way shown efficiently due to both algorithm and object need some topological descriptions. An even more graceful simulation can be conducted with this methodology embedding SMER.

Apêndice E

Legged Locomotion Controlled by Artificial CPGs

The exciting thing about a modular oscillatory building block is that, just like what its name describes, it does not only specifies a class of neural circuits, but presents the building blocks from which many different types of rhythmic patterns can be formed. Furthermore, dynamic reconfigurability adds another attractive aspect to the capabilities of constructed CPGs. Indeed, one can organize a network with numerous simple or composite OBBs which is big enough to mimick all rhythmic patterns a living creature may have, just adjusting the coupled weights and/or thresholds between each simple OBBs. Now that the possible methodology for building artificial CPGs is clear, the consequent task is to explore the possible CPGs architecture of different legged animals.

E.1   Introduction

Some enumerative studies on the general model proposed by Golubitsky and his colleagues [43] are presented giving insight into the fact that all gait patterns generated by this model is reasonable and applicable with OBB networks. After that, some other gaits, e.g., the turning gait, are also explored even though they are not discussed in Golubitsky's group model.

   The definition of locomotion is the action of moving from place to place. Our interest lies in sustainable locomotion, in which some rhythmic oscillations should involve, not those instantaneous action such as a dog jumping once and immediately stopping at the same point. It is fundamental for an animal's sustainable locomotion to be featured with the following characteristics:

1. Moving in straight line and by incremental distance.

2. Having the capability of turning around if necessary.

3. Having the capability of planning path and avoiding risk.

In this appendix we'll introduce that the CPGs model made from our neural network mechanism possesses the first two properties. As to the third one, it is not difficult for our model if some decision-making strategies are added, however, it is not within the thesis scope.

A full classification scheme on locomotion is given by Figure E.1. The first level of locomotion is divided into air, land and water, classified by the type of propulsion media that is used. Air locomotion pushes air to achieve movement while land and water locomotion push earth and water in some specific organized manners respectively. The legged locomotion to which we concentrate is an important part of all types of locomotion in the natural world. The near neighbor of legged locomotion is body locomotion, adopted by, e.g., the snake and lamprey. Some investigators argued that body locomotion can be simulated with the same method as used in analysis of centipedal types [62]. Some other industrially well-known locomotion such as wheeled or tracked types are also not discussed here because of their man-made nature.
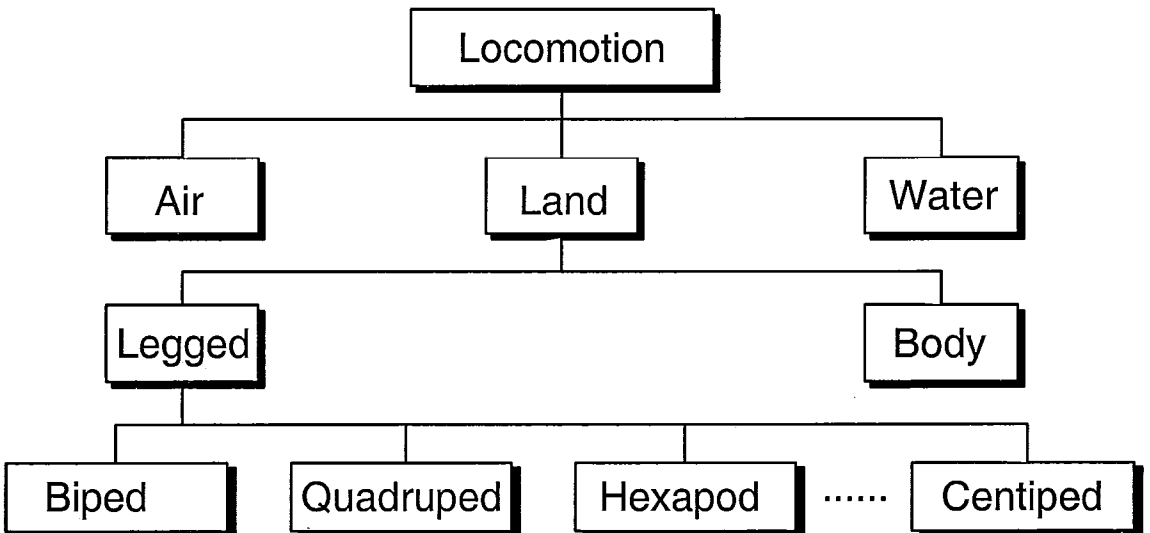
Figura E.1: The creature's locomotion organization graph existing in the natural world.

To achieve stable in general, a land animal has to repeatedly do four things in any order:

1. Remove ground contact points from the rear of the body,

2. Place ground contact points in front of the body,

3. Shift weight forward,

4. Maintain equilibrium throughout all motions.

Thus a stable gait defines a cyclical pattern that achieves these steps.

Definition E.1 *A gait can be defined to be a series of periodic rhythmic patterns genera-ted by CPGs to drive muscular system for achieving locomotion.* ∎

E.1.1 Gait Generated by Symmetry

Group theory, as a tool of modern mathematics, takes the charge of representing a physi-cal problem in a formal while simpler way. Golubitsky et al. proposed that, if a dynamic system possesses some kind of symmetry describe by a finite abelian group, generically the nonreal eigenvalues of the linearization of the system of ordinary differential equa-tions (ODE) of the physical object are simple. Then, periodic solutions modelling system behavior can be produced by simple Hopf bifurcation from equilibria. After bifurcation, various branches will correspond to various cyclical patterns which can be expressed with symmetric groups. This methodology provides a substantial theoretic basis for explaining the pattern formation, and hence the gait morphology.

E.1.2 Gait Implemented with OBB Nets

As one can perceive so far, the leg movement of an animal is a coordinated procedure instead of isolated behavior, which is conducted by CPGs. However, by what method may a CPG adopt to adjust this kind of coordination? Since the animal locomotion can be treated as the movement of an abstract, rigid body on which the legs attach, and the body has weight, every snapshot of gait cycle is also a snapshot of weight re-scheduling. Although the biologists have to decide the immediate order of weight re-scheduling and related leg movement, i.e., whether weight re-scheduling leads to leg movement or the contrary, the consequence is unique that the body weight is keeping re-scheduling among

all legs during the locomotive cycle. So we can surely view weight re-scheduling as the method which a CPG employs to coordinate legs. In this sense, the asymmetric Hopfield nets under SMER will be an optimal tool in gait research.

E.2   Gait Represented by Group

Recall those statements in Section B.4. Golubitsky et al.'s gait model suggests that in the trivial state, the state space of the coupled network of a 2n-legged animal can be divided into $2(n + 1)$ irreducible real subspaces, U_{m0}, U_{m1} where $0 \leq m \leq n$, located on the left side of complex plane which correspond to $2(n + 1)$ primary gaits respectively.

Another way of explaining gaits from bifurcation with symmetry is to construct a lattice of subgroup from general symmetry group. Suppose $X(t)$ is the solution of ODE system $dX/dt = f(X, \lambda)$ which possesses symmetry Γ, this elegant method involves three steps [43] [14]:

1. Classifying all subgroup $J \subset \Gamma$ consisting of symmetries that preserve the trajectory $X(t)$, i.e., $\gamma \in J$ if $\gamma\{X(t)\} = \{X(t)\}$.

2. For each J classify all subgroups L which are the purely spatial symmetry group of $X(t)$, i.e., $\gamma \in L$ if $\gamma X(t) = X(t)$, such that J/L is cyclical.

3. Spatio-temporal subgroups of $\Gamma \times S^1$ can be identified with pairs of subgroups $L \subset J$, each J/L pair specifies a class of associated gait pattern.

Theoretically, a dynamic system with symmetry can undergo symmetry-breaking bifurcation to get more other rhythmic patterns (here the gaits), until finally the sytem will possess no symmetry in structure, a state described by the unit element 1 in group. Then no gait is achieved at that time, according to the gait definition.

Theorem E.1 *Every gait pattern generated by Golubitsky's symmetry-breaking Hopf bifurcation has its solution scheme of SMER.*

Proof: Now that a gait is defined to be a cycle of a motion pattern, it has a corresponding purely spatial symmetry group, $H \cong L \subset J$, to describe its topology structure and operation specifications. Clearly this structure is nontree type. As it's implied in nontree

theorem, any nontree type architecture can be solved with SMER. The theorem immediately follows. ∎

Since there are so many gait patterns, recognized or unrecognized, in the natural world, we choose to treat four typical kinds of animals (biped, quadruped, hexapod and centiped) for a detailed SMER solution scheme.

E.3   Studio of Gait Rhythms

Recall that Golubitsky's general gait model with symmetry $Z_{2n}(\omega) \times Z_2(\kappa)$ [1], where ω is a generator of cycle and κ a generator of contralateral permutation, $2n$ is the leg number and n is leg pair. This model has been proven to be able to generate almost all gait patterns with some kind of symmetry for legged animals. We confirm further, from the macroscopic and distributed points of view, that the $Z_{2n}(\omega) \times Z_2(\kappa)$ general model is optimal on the generation of gait patterns. Also we show the remarkable potential of asymmetric SMER Hopfield neural networks on rhythmic pattern formation. By building artificial CPG from this general gait pattern model, some basic criteria on macroneuron interconnection should be followed.

1. Any two macroneurons in a CPG network should be coupled directly if their activities are exactly out of phase.

2. The ipsilateral macroneurons should be connected to form a cyclic undirected ring.

3. If the phase difference between one macroneuron and anyone of its contralateral macroneurons (in the same surface) is less than that between this macroneuron and its ipsilateral neighbors then two contralateral macroneurons have additional connection.

4. Based on the above connection different arrangement of initial membrane potential may lead to different patterns or system halt.

We'll concerntrate on the primary gaits in this studio. The corresponding relation between flexor neurons and animal legs are arranged as following, with flexor 1 to rear

---

[1]This expression itself denotes a statically standing animal

left, 2 to rear right, 3 to second rear left, 4 to second rear right, ..., $2n - 1$ to front left and $2n$ to front right. The rest neurons, from $2n + 1$ to $4n$, are used to form a general model for symmetry consideration and facilitating wave propagation [43]. In some cases, e.g., a model where the cyclic rings may exist such as walk of quadruped, it is not very accurate to specify the $2n + 1$ to $4n$ neurons as extensors like Buono and Golubitsky argued [14], due to the phase relation in a cyclic ring.

In order to show how to implement all possible gait patterns employing OBB methodology, we adopt aforementioned general model by modifying it into a completely connected network. We remain the general model shape (shown in Figure 4.1b) and let each neuron connect with all the other ones. Obviously one can find biological support for this connection in that the coupling strength becomes weaker with the increment of distance between sections.

E.3.1   Bipedal Locomotion

Bipedal locomotion is relatively simple compared with multi-legged locomotion, in the sense that two legs are either in-phase or half a period out-of-phase. Different from the popular methods employed on bipedal gait research which are mainly based on the kinematic and mechanic point-of-view [72][28], we can greatly simplify bipedal gait research by adopting the newly method introduced in Appendix D and put the emphasis on the retrieval of biological rhythms.

The CPG network for bipedal locomotion consists of a set of four macroneurons $< 1, 2, 3, 4 >$, we relate $1, 2$ to the left and right flexors of two legs, and $3, 4$ to their corresponding extensors, respectively. The network architecture arrangement for in-phase locomotion to occur is that, each flexor connects with both extensors and vice-versa without connections between bilateral flexors and extensors. There are totally four connections in in-phase network architecture, the system parameters are designed to let the flexor or extensor pair fires at first and a firing circulation will be followed. For out-of-phase locomotion to occur, the four macroneurons are linked like a ring, i.e., a flexor links with its extensor and bilateral flexor, and an extensor links with its flexor and bilateral extensor. The system parameters are designed for out-of-phase locomotion so that one flexor and its non-coupled, diagonal extensor fire first, then the other pair fire to form a circulation.

Although Golubitsky et al. asserted that only two neurons are needed in case of bipedal locomotion due to its simplicity, 4 macroneurons are adopted in our architecture for the clarity purpose of network architecture as well as model consistency.

E.3.2 Quadrupedal Locomotion

There are six primary gait patterns bifurcated from the general symmetry model "stand": pronk, pace, bound, trot, jump, walk. Each one breaks the general symmetry of $Z_4(\omega) \times Z_2(\kappa)$ while remains some kind of symmetry. Among the totally eight macroneurons $\{1, ..., 8\}$ in this system we always take its subgroup $\{1, ..., 4\}$ as the set of flexors corresponding to rear left, rear right, front left, front right respectively, and the upper layer macroneurons represent flexors and the lower layer ones for extensors. There are totally sixteen coupling connections in all six gait pattern structures. The primary gaits are all SER case.

Pronk ($Z_4(\omega) \times Z_2(\kappa)$)

Pronk is a gait pattern during which four legs lift and contact the ground together, so one can immagine that it has the same symmetry group with original stand, i.e., the symmetry is not broken. There are some difficulties in explaining this gait by Golubitsky's theory, they argued that by varying only coupling strengths between cells the network of general model can produce all gaits, except pronk, by Hopf bifurcation [14]. However, it's very easy to retrieve pronk behavior using OBB network by only adjusting the coupling strengths (see Figure E.2).

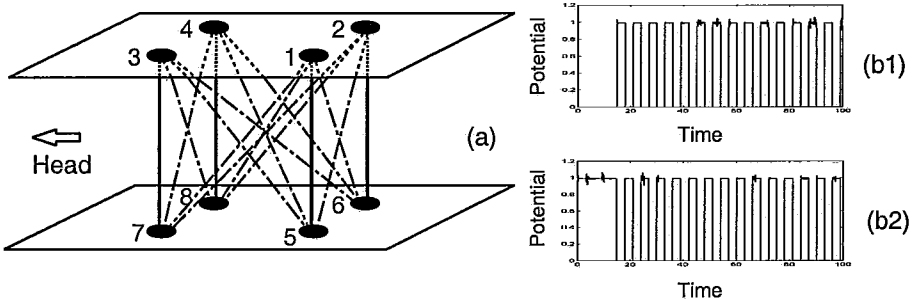Figura E.2: The pronk gait, (a) coupled architecture, (b) numerical results of each leg, b1, b2 correspond to macroneurons 1, 5 respectively, the other coupled pair has the same result. Reversability of each macroneuron is set to 1, macroneuron thresholds and initial membrane potentials in the upper layer are 1 and 0.66 while in the lower layer are 0 and 0.34 respectively, each coupling connection has the same strength 0.1.

This net is indeed equivalent to the simple OBB only, however we employ its original graph derived from the complete graph, the weights of not connected macroneurons are 0. In this case each flexor has four clones connecting with four extensors which are exactly out of phase. The criterion for initial membrane potential arrangement is to let the macroneurons in the same layer have the same potentials.

Trot ($Z_4(\kappa\omega)$)

Trot is a gait pattern that one pair of diagonal legs are in phase and the two pairs of diagonal legs are half a period out of phase. According to the interconnection regulations we can get the coupled architecture as shown in Figure E.3(a). Each flexor has four clones with two connecting extensors and two for other flexors respectively; each extensor also has four clones with two connecting flexors and two for other extensors respectively. The arrangement of initial membrane potential is to let macroneuron pair 1, 4 and 6, 7 fire simultaneously, and with a half period of phase difference macroneuron pairs 2, 3 and 5, 8 fire simultaneously.
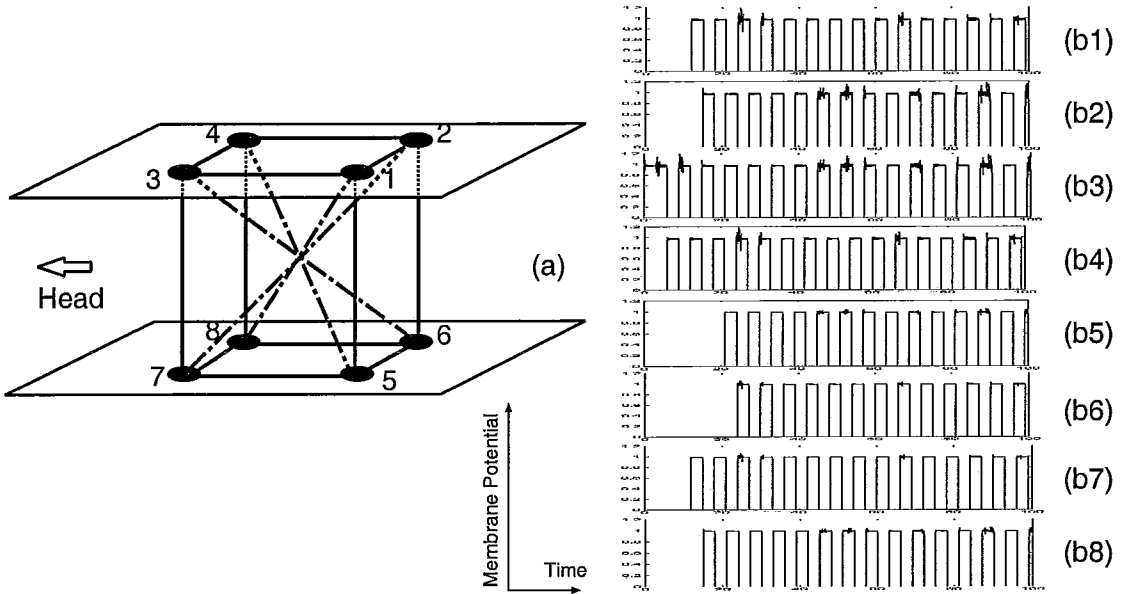
Figura E.3: The trot gait, (a) coupled architecture, (b) numerical results of each leg, $b1, b2, b3, b4$ correspond to macroneurons $1, 2, 3, 4$, and $b5, b6, b7, b8$ to $5, 6, 7, 8$ respectively.

All the macroneuron reversabilities are 1, The arrangement of system parameter matrices of θ_{ij}, $M_{ij}(0)$ and W_{ij} are as following. In W_{ij} matrix, the diagonal values are negative feedbacks of each clones themself; in θ matrix, a value of 0 may have different meanings, if the diagonal symmetry position of 0 is 1, then this 0 means there is

a connection between these two macroneurons while corresponding clone's threshold is 0, otherwise 0 means there is no connection between these two macroneurons. Any parameter with subscript ij means that this parameter belongs to macroneuron i which is connecting with macroneuron j.

$$
\theta_{ij} = \begin{pmatrix}
0 & 0 & 1 & 0 & 1 & 0 & 0 & 0 \\
1 & 0 & 0 & 1 & 0 & 0 & 0 & 0 \\
0 & 0 & 0 & 0 & 0 & 0 & 1 & 0 \\
0 & 0 & 1 & 0 & 0 & 0 & 0 & 0 \\
0 & 0 & 0 & 1 & 0 & 0 & 0 & 0 \\
0 & 1 & 1 & 0 & 1 & 0 & 0 & 0 \\
0 & 1 & 0 & 0 & 1 & 0 & 0 & 0 \\
1 & 0 & 0 & 1 & 0 & 1 & 1 & 0
\end{pmatrix}
$$

$$
W_{ij} = \begin{pmatrix}
-0.1 & 0.1 & 0.1 & 0 & 0.1 & 0 & 0 & 0.1 \\
0.1 & -0.1 & 0 & 0.1 & 0 & 0.1 & 0.1 & 0 \\
0.1 & 0 & -0.1 & 0.1 & 0 & 0.1 & 0.1 & 0 \\
0 & 0.1 & 0.1 & -0.1 & 0.1 & 0 & 0 & 0.1 \\
0.1 & 0 & 0 & 0.1 & -0.1 & 0.1 & 0.1 & 0 \\
0 & 0.1 & 0.1 & 0 & 0.1 & -0.1 & 0 & 0.1 \\
0 & 0.1 & 0.1 & 0 & 0.1 & 0 & -0.1 & 0.1 \\
0.1 & 0 & 0 & 0.1 & 0 & 0.1 & 0.1 & -0.1
\end{pmatrix}
$$

$$
M(0)_{ij} = \begin{pmatrix}
0 & -0.07 & 1.16 & 0 & 0.82 & 0 & 0 & -0.02 \\
1.07 & 0 & 0 & 1.16 & 0 & -0.16 & 0.04 & 0 \\
-0.16 & 0 & 0 & -0.03 & 0 & -0.08 & 0.82 & 0 \\
0 & -0.16 & 1.03 & 0 & -0.14 & 0 & 0 & -0.16 \\
0.18 & 0 & 0 & 1.14 & 0 & -0.04 & 0.09 & 0 \\
0 & 1.16 & 1.08 & 0 & 1.04 & 0 & 0 & 0.08 \\
0 & 0.96 & 0.18 & 0 & 0.91 & 0 & 0 & -0.09 \\
1.02 & 0 & 0 & 1.16 & 0 & 0.92 & 1.09 & 0
\end{pmatrix}
$$

There are some limits on initial membrane potential configuration scope of a gait. If the clone of a macroneuron is firing initially, then it should have initial value as:

$$
M_{ij}(0) \in \begin{cases} (0, 0.1) & \text{if } W_{ij} = 0.1 \text{ and } \theta_{ij} = 0 \\ (1.0, 1.1) & \text{if } \theta_{ij} = 1 \end{cases}
$$

If it is idle initially, then it is assigned with the following initial value:

$$
M_{ij}(0) \in \begin{cases} (\text{-}0.1, 0) & \text{if } W_{ij} = 0.1 \text{ and } \theta_{ij} = 0 \\ (0.9, 1.0) & \text{if } \theta_{ij} = 1 \end{cases}
$$

In other words, the initial membrane value of a clone should have a scope of $2w_{ij}$ with the center point of its threshold. This configuration garantees that system oscillation will start from the very beginning without possible deadlock occuring due to unsuitable choice

111

of initial potentials. If the initial potential value of a clone is not set within the specified scope, two possibilities may occur: a self-organizing procedure if excursion is not very large or deadlock if excursion is large. In the initial configuration of this trot gait there exists a self-organizing procedure. As we already know, a normal trot gait should be in an order as $(23)(58) \rightleftharpoons (14)(67)$, however, according to the simulated wave in Figure E.3(b) there is an initial self-organizing procedure as $3 \rightarrow 4 \rightarrow 3 \rightarrow (14)7 \rightarrow (23)8 \rightarrow (14)7 \rightarrow (23)(58) \rightleftharpoons (14)(67)$. Although a self-organizing procedure is not harmful and it is even a charming point of neural networks, we'd like to employ a regulated general method which adopts the initial potential scope in pace, bound and jump gait pattern simulations to avoid possible deadlock and facilitate network organization.

Walk $(Z_2(\kappa\omega^2)$

Walk is a gait pattern that the contralateral legs move with half a period phase difference while ipsilateral legs move with a quarter period phase difference. According to the interconnection regulations we can get the coupled architecture as shown in Figure E.4(a). Each flexor has four clones with two connecting extensors and two for flexors; each extensor also has four clones with two connecting flexors and two for extensors. The arrangement of initial membrane potential is to let the pairs of flexors and extensors fire in the turn of $(18)(36)(72)(54)$ with a quarter period phase difference.
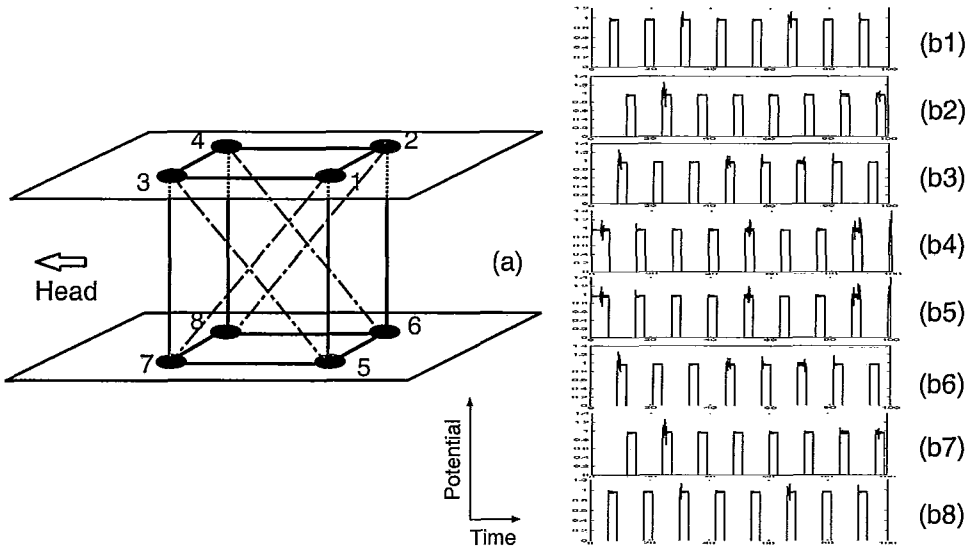

Figura E.4: The walk gait, (a) coupled architecture, (b) numerical results of each leg, $b1, b2, b3, b4$ correspond to macroneurons $1, 2, 3, 4$ and $b5, b6, b7, b8$ to $5, 6, 7, 8$ respectively.

112

All the cell reversabilities are 1. By matrix calculation, we can get the following parameters corresponding to the results, in this case the gait pattern will repeat this sequence: $(4,5) \to (1,8) \to (3,6) \to (2,7)$, here macroneuron sets $< 1,2,3,4 >$ and $< 5,6,7,8 >$ are flexor and extensor collections respectively.

$$\theta_{ij} = \begin{pmatrix} 0 & 0 & 0 & 0 & 0 & 0 & 0 & 0 \\ 1 & 0 & 0 & 0 & 0 & 0 & 0 & 0 \\ 1 & 0 & 0 & 0 & 0 & 0 & 0 & 0 \\ 0 & 1 & 1 & 0 & 0 & 0 & 0 & 0 \\ 1 & 0 & 1 & 0 & 0 & 0 & 0 & 0 \\ 0 & 1 & 0 & 1 & 1 & 0 & 0 & 0 \\ 1 & 0 & 1 & 0 & 1 & 0 & 0 & 0 \\ 0 & 1 & 0 & 1 & 0 & 1 & 1 & 0 \end{pmatrix}$$

$$W_{ij} = \begin{pmatrix} -0.1 & 0.1 & 0.1 & 0 & 0.1 & 0 & 0.1 & 0 \\ 0.1 & -0.1 & 0 & 0.1 & 0 & 0.1 & 0 & 0.1 \\ 0.1 & 0 & -0.1 & 0.1 & 0.1 & 0 & 0.1 & 0 \\ 0 & 0.1 & 0.1 & -0.1 & 0 & 0.1 & 0 & 0.1 \\ 0.1 & 0 & 0.1 & 0 & -0.1 & 0.1 & 0.1 & 0 \\ 0 & 0.1 & 0 & 0.1 & 0.1 & -0.1 & 0 & 0.1 \\ 0.1 & 0 & 0.1 & 0 & 0.1 & 0 & -0.1 & 0.1 \\ 0 & 0.1 & 0 & 0.1 & 0 & 0.1 & 0.1 & -0.1 \end{pmatrix}$$

$$M_{ij}(0) = \begin{pmatrix} 0 & -0.05 & -0.03 & 0 & 0.07 & 0 & -0.02 & 0 \\ 1.05 & 0 & 0 & 0.04 & 0 & 0.02 & 0 & 0.03 \\ 1.03 & 0 & 0 & 0.05 & 0.04 & 0 & -0.06 & 0 \\ 0 & 0.96 & 0.95 & 0 & 0 & -0.02 & 0 & -0.07 \\ 0.93 & 0 & 0.96 & 0 & 0 & -0.02 & -0.05 & 0 \\ 0 & 0.98 & 0 & 1.02 & 1.02 & 0 & 0 & 0.05 \\ 1.02 & 0 & 1.06 & 0 & 1.05 & 0 & 0 & 0.05 \\ 0 & 0.97 & 0 & 1.07 & 0 & 0.95 & 0.95 & 0 \end{pmatrix}$$

Pace $(Z_4(\omega))$

Pace is a gait pattern that the ipsilateral legs are in phase while contralateral legs are half a period out of phase. According to the interconnection regulations we can get the coupled architecture as shown in Figure E.5(a). Each flexor has four clones with two connecting extensors and two for contralateral flexors; each extensor also has four clones with two connecting flexors and two for contralateral extensors. The arrangement of initial membrane potential is to let, for example, the ipsilateral flexors 1, 3 and contralateral extensors 6, 8 fire simultaneously first, and then the others.

Since all the macroneuron reversabilities are 1. By matrix calculation, we can get the following parameters corresponding to the results, the symmetry existing in θ matrix is

Figura E.5: The pace gait, (a) coupled architecture, (b) numerical results of each leg, $b1, b2, b3, b4$ correspond to macroneurons $1, 2, 3, 4$ and $b5, b6, b7, b8$ to $5, 6, 7, 8$ respectively.

due to arrangement of coupled clone pair and choice of threshold, a detailed relation can be found in Section $E.4$ on hexapod gait.

$$
\theta_{ij} = \begin{pmatrix}
0 & 0 & 0 & 0 & 0 & 0 & 0 & 0 \\
1 & 0 & 0 & 0 & 0 & 0 & 0 & 0 \\
0 & 1 & 0 & 0 & 0 & 0 & 0 & 0 \\
1 & 0 & 1 & 0 & 0 & 0 & 0 & 0 \\
1 & 0 & 1 & 0 & 0 & 0 & 0 & 0 \\
0 & 1 & 0 & 1 & 1 & 0 & 0 & 0 \\
1 & 0 & 1 & 0 & 0 & 1 & 0 & 0 \\
0 & 1 & 0 & 1 & 1 & 0 & 1 & 0
\end{pmatrix}
$$

$$
W_{ij} = \begin{pmatrix}
-0.1 & 0.1 & 0 & 0.1 & 0.1 & 0 & 0.1 & 0 \\
0.1 & -0.1 & 0.1 & 0 & 0 & 0.1 & 0 & 0.1 \\
0 & 0.1 & -0.1 & 0.1 & 0.1 & 0 & 0.1 & 0 \\
0.1 & 0 & 0.1 & -0.1 & 0 & 0.1 & 0 & 0.1 \\
0.1 & 0 & 0.1 & 0 & -0.1 & 0.1 & 0 & 0.1 \\
0 & 0.1 & 0 & 0.1 & 0.1 & -0.1 & 0.1 & 0 \\
0.1 & 0 & 0.1 & 0 & 0 & 0.1 & -0.1 & 0.1 \\
0 & 0.1 & 0 & 0.1 & 0.1 & 0 & 0.1 & -0.1
\end{pmatrix}
$$

$$
M_{ij}(0) = \begin{pmatrix}
0 & -0.02 & 0 & -0.07 & -0.01 & 0 & -0.09 & 0 \\
1.02 & 0 & 0.05 & 0 & 0 & 0.09 & 0 & 0.02 \\
0 & 0.95 & 0 & -0.02 & -0.03 & 0 & -0.08 & 0 \\
1.07 & 0 & 1.02 & 0 & 0 & 0.03 & 0 & 0.09 \\
1.01 & 0 & 1.03 & 0 & 0 & 0.07 & 0 & 0.03 \\
0 & 0.91 & 0 & 0.97 & 0.93 & 0 & -0.06 & 0 \\
1.09 & 0 & 1.08 & 0 & 0 & 1.06 & 0 & 0.02 \\
0 & 0.98 & 0 & 0.91 & 0.97 & 0 & 0.98 & 0
\end{pmatrix}
$$

114

Jump $(Z_2(\kappa))$

Jump is a gait pattern that the contralateral legs move in phase while ipsilateral legs move with a quarter period phase difference. According to the interconnection regulations we can get the coupled architecture as shown in Figure E.6(a). Each flexor has four clones with three connecting extensors and only one for ipsilateral flexor; each extensor also has four clones with three connecting flexors and one for ipsilateral extensors. The arrangement of initial membrane potential is to let the pairs of flexors and extensors fire in the turn of $(12)(34)(78)(56)$ with a quarter period phase difference.
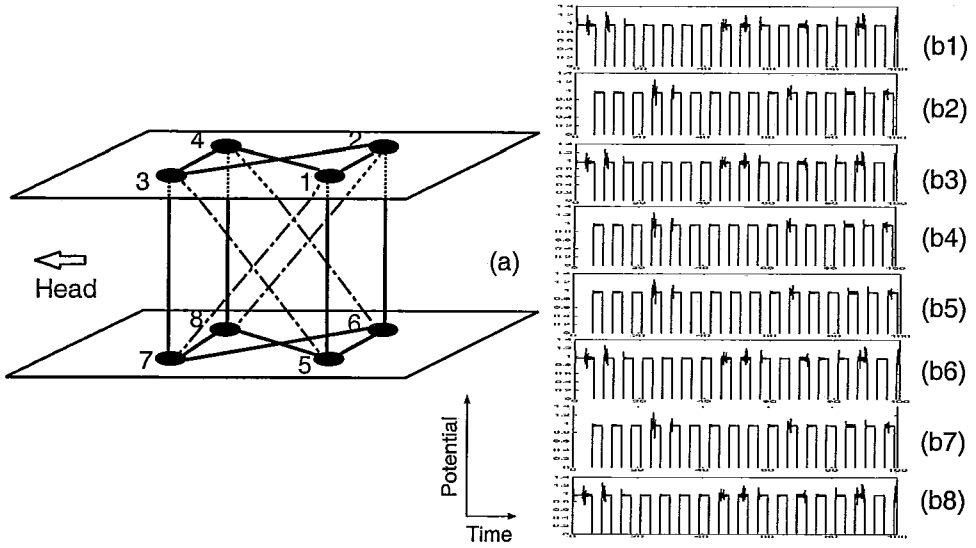

Figura E.6: The jump gait, (a) coupled architecture, (b) numerical results of each leg, $b1, b2, b3, b4$ correspond to macroneurons $1, 2, 3, 4$ and $b5, b6, b7, b8$ to $5, 6, 7, 8$ respectively.

All the macroneuron reversabilities are 1. By matrix calculation, we can get the following parameters corresponding to the results,

$$\theta_{ij} = \begin{pmatrix} 0 & 0 & 0 & 0 & 0 & 0 & 0 & 0 \\ 0 & 0 & 0 & 0 & 0 & 0 & 0 & 0 \\ 1 & 0 & 0 & 0 & 0 & 0 & 0 & 0 \\ 0 & 1 & 0 & 0 & 0 & 0 & 0 & 0 \\ 1 & 0 & 1 & 1 & 0 & 0 & 0 & 0 \\ 0 & 1 & 1 & 1 & 0 & 0 & 0 & 0 \\ 1 & 1 & 1 & 0 & 1 & 0 & 0 & 0 \\ 1 & 1 & 0 & 1 & 0 & 1 & 0 & 0 \end{pmatrix}$$

$$W_{ij} = \begin{pmatrix} -0.1 & 0 & 0.1 & 0 & 0.1 & 0 & 0.1 & 0.1 \\ 0 & -0.1 & 0 & 0.1 & 0 & 0.1 & 0.1 & 0.1 \\ 0.1 & 0 & -0.1 & 0 & 0.1 & 0.1 & 0.1 & 0 \\ 0 & 0.1 & 0 & -0.1 & 0.1 & 0.1 & 0 & 0.1 \\ 0.1 & 0 & 0.1 & 0.1 & -0.1 & 0 & 0.1 & 0 \\ 0 & 0.1 & 0.1 & 0.1 & 0 & -0.1 & 0 & 0.1 \\ 0.1 & 0.1 & 0.1 & 0 & 0.1 & 0 & -0.1 & 0 \\ 0.1 & 0.1 & 0 & 0.1 & 0 & 0.1 & 0 & -0.1 \end{pmatrix}$$

$$M_{ij}(0) = \begin{pmatrix} 0 & 0 & -0.07 & 0 & -0.02 & 0 & -0.05 & -0.09 \\ 0 & 0 & 0 & -0.07 & 0 & -0.02 & -0.01 & -0.04 \\ 1.07 & 0 & 0 & 0 & -0.03 & -0.06 & -0.02 & 0 \\ 0 & 1.07 & 0 & 0 & -0.01 & -0.08 & 0 & -0.02 \\ 1.02 & 0 & 1.03 & 1.01 & 0 & 0 & 0.08 & 0 \\ 0 & 1.02 & 1.06 & 1.08 & 0 & 0 & 0 & 0.05 \\ 1.05 & 1.01 & 1.02 & 0 & 0.92 & 0 & 0 & 0 \\ 1.09 & 1.04 & 0 & 1.02 & 0 & 0.95 & 0 & 0 \end{pmatrix}$$

Bound $(D_2(\kappa, \omega^2))$

Bound is a gait pattern that the contralateral legs move in phase while ipsilateral legs move with a half period phase difference. According to the interconnection regulations we can get the coupled architecture as shown in Figure E.7(a). Each flexor has four clones with two connecting extensors and two for flexors; each extensor also has four clones with two connecting flexors and two for extensors. The arrangement of initial membrane potential is to let the pairs of flexors and extensors fire in the turn of $(12)(34)(78)(56)$ with half period phase difference.
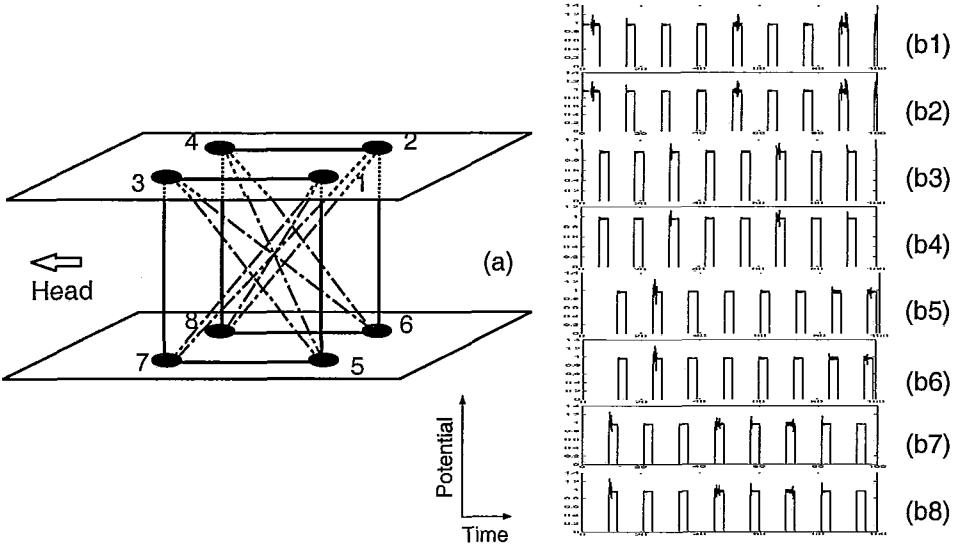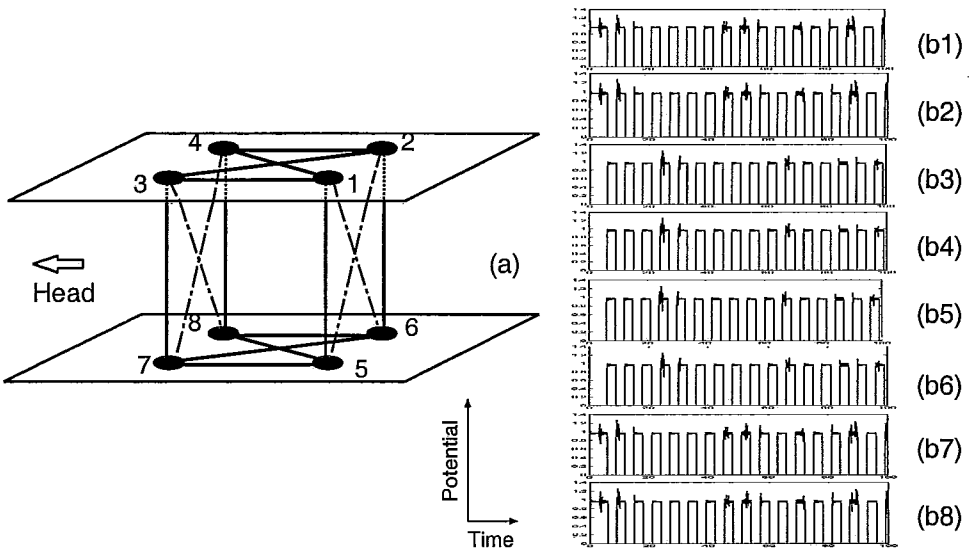

Figura E.7: The bound gait, (a) coupled architecture, (b) numerical results of each leg, $b1, b2, b3, b4$ correspond to macroneuron 1, 2, 3, 4 and $b5, b6, b7, b8$ to 5, 6, 7, 8 respectively.

All the macroneuron reversabilities are 1. By matrix calculation, we can get the following parameters corresponding to the results,

$$
\theta_{ij} = \begin{pmatrix}
0 & 0 & 0 & 0 & 0 & 0 & 0 & 0 \\
0 & 0 & 0 & 0 & 0 & 0 & 0 & 0 \\
1 & 1 & 0 & 0 & 0 & 0 & 0 & 0 \\
1 & 1 & 0 & 0 & 0 & 0 & 0 & 0 \\
1 & 1 & 0 & 0 & 0 & 0 & 0 & 0 \\
1 & 1 & 0 & 0 & 0 & 0 & 0 & 0 \\
0 & 0 & 1 & 1 & 1 & 1 & 0 & 0 \\
0 & 0 & 1 & 1 & 1 & 1 & 0 & 0
\end{pmatrix}
$$

$$
W_{ij} = \begin{pmatrix}
-0.1 & 0 & 0.1 & 0.1 & 0.1 & 0.1 & 0 & 0 \\
0 & -0.1 & 0.1 & 0.1 & 0.1 & 0.1 & 0 & 0 \\
0.1 & 0.1 & -0.1 & 0 & 0.1 & 0.1 & 0.1 & 0.1 \\
0.1 & 0.1 & 0 & -0.1 & 0.1 & 0.1 & 0.1 & 0.1 \\
0.1 & 0.1 & 0 & 0 & -0.1 & 0 & 0.1 & 0.1 \\
0.1 & 0.1 & 0 & 0 & 0 & -0.1 & 0.1 & 0.1 \\
0 & 0 & 0.1 & 0.1 & 0.1 & 0.1 & -0.1 & 0 \\
0 & 0 & 0.1 & 0.1 & 0.1 & 0.1 & 0 & -0.1
\end{pmatrix}
$$

$$
M_{ij}(0) = \begin{pmatrix}
0 & 0 & -0.02 & -0.07 & -0.05 & -0.09 & 0 & 0 \\
0 & 0 & -0.09 & -0.05 & -0.04 & -0.07 & 0 & 0 \\
1.02 & 1.09 & 0 & 0 & 0 & 0 & 0.08 & 0.03 \\
1.07 & 1.05 & 0 & 0 & 0 & 0 & 0.05 & 0.06 \\
1.05 & 1.04 & 0 & 0 & 0 & 0 & 0.03 & 0.09 \\
1.09 & 1.07 & 0 & 0 & 0 & 0 & 0.06 & 0.08 \\
0 & 0 & 0.92 & 0.95 & 0.97 & 0.94 & 0 & 0 \\
0 & 0 & 0.97 & 0.94 & 0.91 & 0.92 & 0 & 0
\end{pmatrix}
$$

E.3.3   Hexapodal Locomotion

From the original "stand" posture of stick hexapodal insects (see Figure E.8) which keeps all structural symmetry with all macroneurons in the 12-cell network permutable, 8 symmetry-breaking branches are bifurcated corresponding to 8 primary gait patterns as shown in Table E.1. Each pattern has a symmetry group which is a subgroup of $Z_6(\omega) \times Z_2(\kappa)$. Among the total twelve macroneurons $\{1, ..., 12\}$ in this system we always take its subgroup $\{1, ..., 6\}$ as the set of flexors corresponding to rear left (RL), rear right (RR), middle left (ML), middle right (MR), front left (FL) and front right (FR) respectively, and the upper layer macroneurons represent flexors and the lower layer ones for extensors. The complexity of numerical simulation of multi-legged animals increases arithmetically as the number of legs increases, e.g., the calculation of hexapodal locomotion needs three 12 $*$ 12 matrices in our analysis. In order to avoid enumerative operations

only one hexapodal gait – rolling tripod is treated and a description of all primary gaits are given in Table E.1. All hexapodal gaits may be simulated under SER algorithm, like quadrupedal cases.
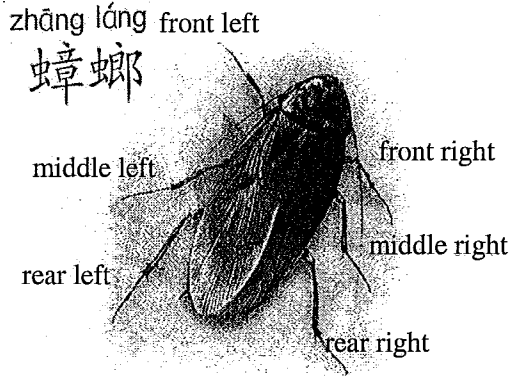

Figura E.8: Cockroach, an hexapodal insect.

Tabela E.1: Hexapodal primary gaits and description.

Gait pattern	Symmetry subgroup	Pattern description	
		ipsilateral legs	contralateral legs
Pronk	$Z_6(\omega) \times Z_2(\kappa)$	in phase	in phase
Pace	$Z_6(\omega)$	in phase	half cycle out
Lurch	$D_3(\kappa, \omega^2)$	half cycle out	in phase
Tripod	$Z_6(\kappa\omega)$	half cycle out	half cycle out
Inchworm	$Z_2(\kappa)$	one-sixth cycle out	in phase
Metachronal	$Z_2(\kappa\omega^3)$	one-sixth cycle out	half cycle out
Caterpillar	$D_2(\kappa, \omega^3)$	one-third cycle out	in phase
Rolling tripod	$Z_2(\omega^3)$	one-third cycle out	half cycle out

The rolling tripod is a gait pattern that ipsilateral legs are one-third period out of phase while contralateral legs are half period out of phase. An algorithm to arrange order of coupled clones of connected macroneurons is required to acquire the symmetric threshold matrix similar to quadruped cases, which may hold additional stability characteristics on gait patterns. A coupled structure with 32 connections is achieved according to the criteria for macroneuron interconnection (see Figure E.9a).

The flexors of different legs of hexapodal rolling tripod gait fire in the order of RL, FR, ML, RR, FL, MR, corresponding extensors fire in the order of FL, RR, MR, FR, RL, ML. A snapshot phase of each macroneuron in the principal flexor layer is: $RL - 0, ML - \frac{1}{3}, FL - \frac{2}{3}, RR - \frac{1}{2}, MR - \frac{5}{6}, FR - \frac{1}{6}$. Based on given locomotive topo-

/*Program: Threshold_determination*/
CONST:
$G(N, E)$;

VAR:
threshold$[i, j : 1...4n]$:*real*;

Action:
for $(i := 1; i \leq 4n; i + +)$
 for $(j := 1; j \leq 4n; j + +)$
  if $(((i, j) \in E) \wedge (i < j))$
   begin
     threshold$[i, j] := 1.0$;
     threshold$[j, i] := 0.0$;
   end
  else
    begin
      threshold$[i, j] := 0.0$;
      threshold$[j, i] := 0.0$;
    end

logy, the threshold, weight and initial potential matrices can be created as in quadrupeds for numerical simulation with the model developped in Appendix D. A flavor of discrete, parallel computation can be tasted by writing down matrices of threshold and initial membrane potential (weight matrix can be determinated according to threshold matrix with all elements being 0 or 0.1) respectively.

$$
\begin{pmatrix}
0 & 0 & 0 & 0 & 0 & 0 & 0 & 0 & 0 & 0 & 0 & 0 \\
1 & 0 & 0 & 0 & 0 & 0 & 0 & 0 & 0 & 0 & 0 & 0 \\
1 & 1 & 0 & 0 & 0 & 0 & 0 & 0 & 0 & 0 & 0 & 0 \\
1 & 1 & 1 & 0 & 0 & 0 & 0 & 0 & 0 & 0 & 0 & 0 \\
0 & 1 & 1 & 1 & 0 & 0 & 0 & 0 & 0 & 0 & 0 & 0 \\
1 & 0 & 1 & 1 & 1 & 0 & 0 & 0 & 0 & 0 & 0 & 0 \\
1 & 0 & 0 & 0 & 0 & 0 & 0 & 0 & 0 & 0 & 0 & 0 \\
0 & 1 & 0 & 0 & 0 & 0 & 1 & 0 & 0 & 0 & 0 & 0 \\
0 & 0 & 0 & 0 & 0 & 0 & 1 & 1 & 0 & 0 & 0 & 0 \\
0 & 0 & 0 & 0 & 0 & 0 & 1 & 1 & 1 & 0 & 0 & 0 \\
0 & 0 & 0 & 0 & 1 & 0 & 0 & 1 & 1 & 1 & 0 & 0 \\
0 & 0 & 0 & 0 & 0 & 1 & 1 & 0 & 1 & 1 & 1 & 0
\end{pmatrix}
$$

$$
\begin{pmatrix}
0 & -0.02 & -0.05 & -0.03 & 0 & -0.08 & -0.05 & 0 & 0 & 0 & 0 & 0 \\
1.02 & 0 & 0.08 & -0.07 & -0.01 & 0 & 0 & 0.03 & 0 & 0 & 0 & 0 \\
1.05 & 0.92 & 0 & -0.03 & -0.07 & 0.02 & 0 & 0 & 0 & 0 & 0 & 0 \\
1.03 & 1.07 & 1.03 & 0 & 0.09 & 0.05 & 0 & 0 & 0 & 0 & 0 & 0 \\
0 & 1.01 & 1.07 & 0.91 & 0 & 0.03 & 0 & 0 & 0 & 0 & 0.08 & 0 \\
1.08 & 0 & 0.98 & 0.95 & 0.97 & 0 & 0 & 0 & 0 & 0 & 0 & -0.03 \\
1.05 & 0 & 0 & 0 & 0 & 0 & 0 & 0.05 & 0.07 & -0.02 & 0 & 0.03 \\
0 & 0.97 & 0 & 0 & 0 & 0 & 0.95 & 0 & -0.02 & -0.07 & 0.03 & 0 \\
0 & 0 & 0 & 0 & 0 & 0 & 0.93 & 1.02 & 0 & -0.02 & 0.06 & -0.07 \\
0 & 0 & 0 & 0 & 0 & 0 & 1.02 & 1.07 & 1.02 & 0 & 0.06 & 0.02 \\
0 & 0 & 0 & 0 & 0.92 & 0 & 0 & 0.97 & 0.94 & 0.94 & 0 & -0.07 \\
0 & 0 & 0 & 0 & 0 & 1.03 & 0.97 & 0 & 1.07 & 0.98 & 1.07 & 0
\end{pmatrix}
$$

E.3.4 Multi-legged Animals

The behavior of multi-legged insect , most typically a centipede with 20 legs on each side, may show many significant features of large-scaled, asynchronous parallel computation. As one has viewed, a multi-legged insect proceeds as if there is a wave propagating along its body sides. The ipsilateral legs in one section, or saying wave period (the spatial period between synchronously moving legs, measured along the length of animal), have a coordinated phase relation ranging from $[0, 2\pi)$, with different legs in corresponding position of different waves having the same phase. From the viewpoint of symmetry-breaking
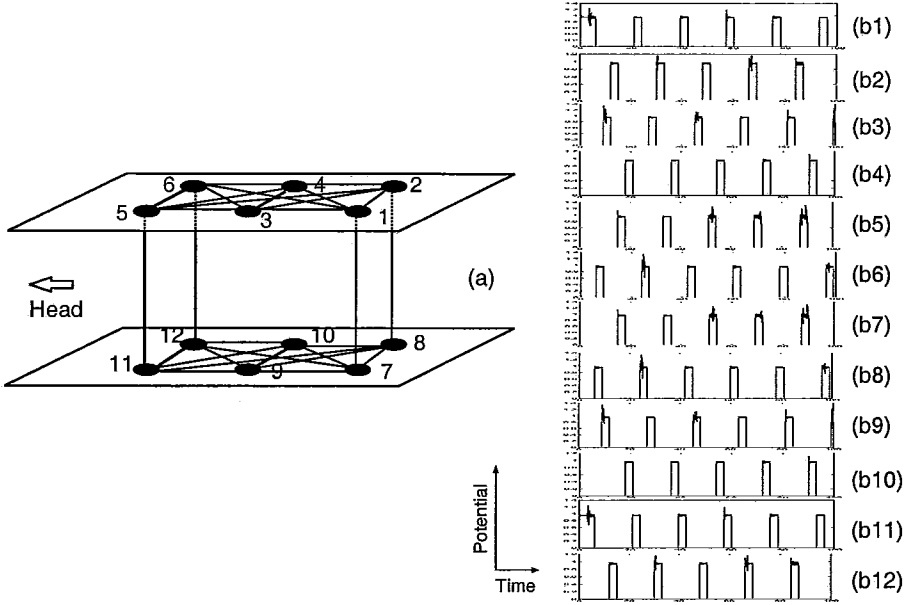
Figura E.9: The hexapodal rolling tripod gait, (a) coupled architecture, (b) numerical results of each leg, $b1, b2, b3, b4, b5, b6$ correspond to macroneurons $1, 2, 3, 4, 5, 6$ and $b7, b8, b9, b10, b11, b12$ to $7, 8, 9, 10, 11, 12$ respectively.

Hopf bifurcation, a centipede should have much more gait patterns than quadrupedal or hexapodal insects due to the significant increment of elements in its symmetry group $Z_{2n}(\omega) \times Z_2(\kappa)$. However, the visible gaits are limited to those related with wave-like sections, normally, various centipede gaits can be classified by two insights: (a). The wave number along an insect body is either an integer or half-an-odd integer (the divided number is an odd integer with denominator of 2). (b). The neighboring contralateral legs are exactly half a period out of phase [43]. If wave number is an integer, the possible choices should always divide the single side number of legs, for instance, in the centipede with totally 40 legs, the possible integer wave number along each side are divisor of 20, i.e., $1, 2, 4, 5, 10$ (except 20 itself since a single leg cannot compose a period). The wave numbers of all visible gaits are either integer or half-an-odd integer type, e.g., a gait observed in 40-legged centipede having only 3 legs striking ground is half-an-odd integer type with 1.5 wave periods on each body side. Figure E.10 *left* presents a centipede insect which has 4 waves along its body side. Since it is in a turning posture, the frequency of its right legs is doubled from that of left side legs, so left side waves are more discernable than right side. Figure E.10 *middle* and *right* represent the phase and coupled relationship of left and right body side of a $2n$-legged insect which has b waves along each body side. The dot macroneurons in the middle and right graphs are the hidden part of its body. We

mark the left body side legs of insect in odd order and right body side legs in even order, both from back to front. We further take leg 1 on the left side as the reference point with a snapshot of phase 0, i.e., at that time flexor of leg 1 is firing so that this leg is completely out of ground.
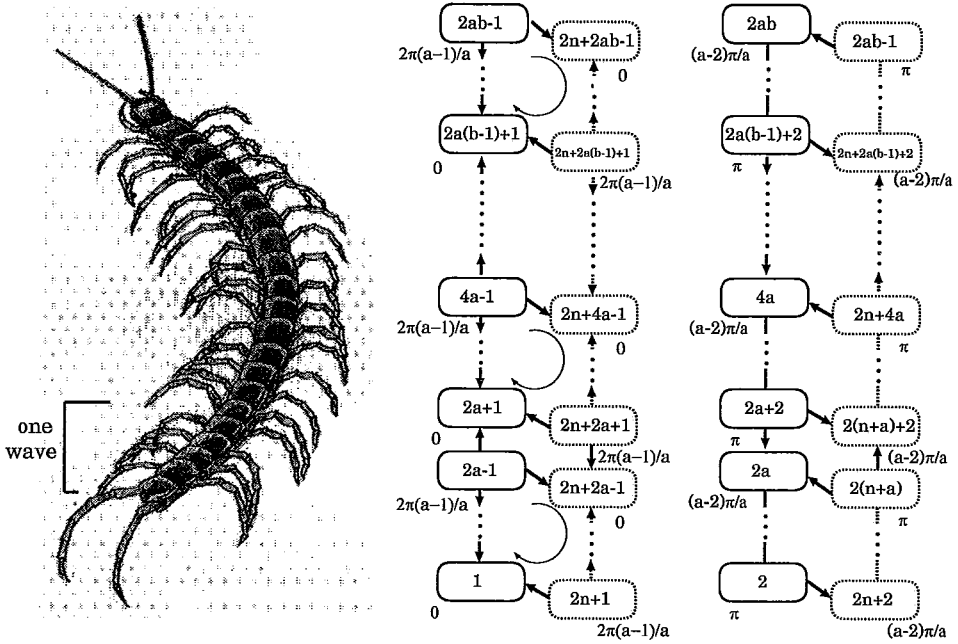
Middle (left body side wave packages):

- 2ab-1 ← 2n+2ab-1 ; $2\pi(a-1)/a$; 0
- 2a(b-1)+1 ← 2n+2a(b-1)+1 ; 0 ; $2\pi(a-1)/a$
- 4a-1 ← 2n+4a-1 ; $2\pi(a-1)/a$; 0
- 2a+1 ← 2n+2a+1 ; 0 ; $2\pi(a-1)/a$
- 2a-1 ← 2n+2a-1 ; $2\pi(a-1)/a$; 0
- 1 ← 2n+1 ; 0 ; $2\pi(a-1)/a$

Right (right body side wave packages):

- 2ab ← 2ab-1 ; $(a-2)\pi/a$; π
- 2a(b-1)+2 ← 2n+2a(b-1)+2 ; π ; $(a-2)\pi/a$
- 4a ← 2n+4a ; $(a-2)\pi/a$; π
- 2a+2 ← 2(n+a)+2 ; π ; $(a-2)\pi/a$
- 2a ← 2(n+a) ; $(a-2)\pi/a$; π
- 2 ← 2n+2 ; π ; $(a-2)\pi/a$

Figura E.10: The centipede's wave-like gaits. **Left**. A 40-legged centipede is proceeding with a gait of 4 waves propogating on each side; **middle**. a $2n$-legged insect's possible left body side wave packages with a and b representing the leg number in a single wave and the wave number along body side, respectively; **right**. a $2n$-legged insect's right body side wave packages.

Since a 40-legged insect will have its three parameter matrices of threshold, weight and initial potential in the size of 80×80, we may represent the behavior of multi-legged insects in a pseudo-code operation instead of the huge numerical description. Note that there is no internal directions within the wave periods of right part of Figure E.10 because of the indetermination of phase 0 position in each wave which depends on the wave number and period of different gait and insect type, or in other words, the concrete circulating direction can only be decided by implementing a specific insect's gait. Also it is interesting to see that no interconnections between macroneurons are given in the figure because of the same reason. It is now imaginable that in a pseudo-code operation, the configuration of initial connecting topology of a specific insect's gait will remain a nontrivial first step. Table E.3 is a pseudo-flow of centipede locomotion. The locomotive topology should be determined in initial state according to the insect's wave numbers and

```
/*Program: Centipede_gait*/
CONST:
N := < 1...4n >;
a := legs_in_wave : integer;
b := n/a, phase[i : 1...4n] : real;


VAR:
threshold[i, j : 1...4n], weight[i, j : 1...4n], membrane[i, j : 1...4n]:real;
firing[i]:boolean;


Initial state: /*determing topological structure*/
E := ∅;
for (x := 0; x≤b − 1; x + +)
    begin
        if (x == 0) continue;
        else
            E := E+(2ax − 1, 2n + 2ax − 1) + (2ax, 2n + 2ax);
        E := E+(2ax + 1, 2n + 2ax + 1) + (2ax + 2, 2n + 2ax + 2);
        for (i := 2ax + 1; i≤2a(x + 1) − 1; i+ = 2)
            begin
                if (i == 1) continue;
                else
                    begin
                        E := E +(i, i − 2) + (2n + i, 2n + i − 2);
                        E := E +(i + 1, i − 1) + (2n + i + 1, 2n + i − 1);
                        E := E +(i, i + 1) + (2n + i, 2n + i + 1);
                        for (j := 2ax + 2; j≤2a(x + 1); j+ = 2)
                            begin
                                diff := ‖phase[j] − phase[i]‖;
                                if ((diff< 2π/a )∧ (diff != 0))
                                    E := E +(i, j);
                                else continue;
                            end
                    end
            end
    end
    Call Threshold_determination;
    Call Weight_determination;
    Call Membrane_determination;


Action:
Call Macroneuron_firing_function;
```

macroneuron interconnection criteria introduced at the beginning of this section.

E.4   Turning Gaits

The retrieval method of straight line gaits of legged animals is indeed a special case of asymmetric Hopfield neural networks under SMER, where the networks have equal coupled weights between any two interconnected macroneurons, and the scheduling scheme is SER instead of SMER. In animal's turning gait the case is a little more general in the sense that the contralateral macroneurons may oscillate with different frequencies, hence they may have different reversabilities. Normally if an animal turns to the left, its left side legs will strike ground with a lower frequency than its right side ones for moving its body load inclined from the straight line along its body length, meanwhile its legs on a body side of the direction to which it turns hold more load and the contralateral legs determine the degree of turning angle.

We may take quadrupedal walking gait as the case study (see Figure E.4 *a*). If a quadrupedal insect turns mildly to the left while walking, its left body side legs will move with, saying, half the frequency of its right body side legs do; if it turns more wildly with large angle in a same time interval of last case, then its left body side legs should move with, saying one-third the frequency of its right body side legs. The choices of these behaviors are completely determined by the advanced *CNS* which is out of our focus, however, these behaviors show that there are some regularities which may be simulated by artificial *CPGs* mechanisms.

Turning gait is easily achieved by adjusting the reversabilities of macroneurons of quadruped insect's walking gait model, and hence we get a different weight matrix as following, it is a mild turning with 2 : 1 frequency-lock between contralateral leg sets. The other two matrices are the same as they are in normal walk gait. By matrices calculation and simulation turning gait waves of each macroneuron are retrieved as shown in Figure E.11.
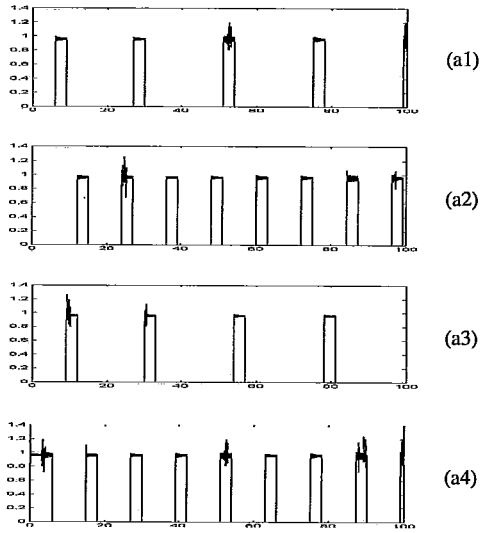
Figura E.11: The quadrupedal turning gait, (a1), (a2), (a3), (a4) correspond to LR, LF, RR, RF legs respectively.

$$W_{ij} = \begin{pmatrix} -0.1 & 0.1 & 0.2 & 0 & 0.2 & 0 & 0.2 & 0 \\ 0.2 & -0.1 & 0 & 0.1 & 0 & 0.1 & 0 & 0.1 \\ 0.2 & 0 & -0.1 & 0.1 & 0.2 & 0 & 0.2 & 0 \\ 0 & 0.1 & 0.2 & -0.1 & 0 & 0.1 & 0 & 0.1 \\ 0.2 & 0 & 0.2 & 0 & -0.1 & 0.1 & 0.2 & 0 \\ 0 & 0.1 & 0 & 0.1 & 0.2 & -0.1 & 0 & 0.1 \\ 0.2 & 0 & 0.2 & 0 & 0.2 & 0 & -0.1 & 0.1 \\ 0 & 0.1 & 0 & 0.1 & 0 & 0.1 & 0.2 & -0.1 \end{pmatrix}$$

E.5 Discussion

The symmetric/asymmetric Hopfield-like neural networks under SMER have the potential to simulate many gait patterns, normal or specific, due to its capabilities of calculation on large-scaled networks in real time. Because of the digital and discrete nature of this new methodology, it might be not so optimal to recover the whole procedure of those behaviors characterized with strong analogous dynamics, however, it does reproduce at least the consecutive snapshot scenes and thus retrieve the dynamic behavior in the macroscopic point-of-view.

Bibliografia

[1] ALEXANDER, I., MORTON, H., *An introduction to neural computing*. 1 ed. New York, Chapman and Hall Press, 1991.

[2] ALEXANDER, R.McN. "The Gaits of Bipedal and Quadrupedal Animals", *Int. J. Robot. Res.* v.3, n.2, pp. 49 - 59, 1984.

[3] ARBAS, E.A., CALABRESE, R.L. "Slow Oscillations of Membrane Potential in Interneurons that Control Heartbeat in the Medicinal Leech", *J. Neurosci.* v.7, pp. 3953-3960, 1987.

[4] ARISTOTLE, *De Partibus Animalium, de Incessu Animalium, de Motu Animalium. In Parts of Animals, Movement of Animals, Progression of Animals*, PEEK, A.S., FORSTER, E.S., (translators), Cambridge, MA, Harvard University Press, 1936.

[5] PEREZ-MUNUZURI, A., PEREZ-MUNUZURI, V., PEREZ-VILLAR, V., et al. "Spiral Waves on a 2-D Array of Nonlinear Circuits", *IEEE Trans. Cir. and Sys. I : Fundamental theory and applications* v. 42, n.10, Oct. 1995.

[6] BARBOSA, V.C., GAFNI, E. "Concurrency in Heavily Loaded Neighborhood-constrained Systems", *ACM Trans. on Programming Languages and Systems*, v.11, n.4, Oct. 1989.

[7] BARBOSA, V.C., *An Introduction to Distributed Algorithms*. 1 ed. Cambridge, MIT Press, 1996.

[8] BARBOSA, V.C., BENEVIDES, M.R.F., FRANÇA, F.M.G., *Sharing Resources at Nonuniform Access Rates*. In:Report ES-412/96, COPPE/UFRJ, Rio de Janeiro, Nov. 1996.

[9] BASSLER, U. "On the Definition of Central Pattern Generator and its Sensory Control", *Biol. Cybern.* v.54, pp. 65-69, 1986.

[10] BAY, J.S., HEMAMI, H. "Modeling of a Neural Pattern Generator with Coupled Nonlinear Oscillators", *IEEE Trans. Biomed. Engr.* v.34, pp. 297-306, 1987.

[11] BEER, R.D., *Intelligence as Adaptive Behavior: An Experiment in Computational Neuroethology.* 1 ed. San Diego, Academic Press, 1990.

[12] BORISYUK, G.N., BORISYUK, R.M., KHIBINIK, A.I., et al. "Dynamics and Bifurcations of Two Coupled Neural Oscillators with Different Connection Types", *Bul. Math. Biol.* v.57, n.6, pp. 809-840, 1995.

[13] BRADLEY, G.W., VON EULER, E., MARTTILA, I., et al. "A Model of the Central and Reflex Inhibition of Inspiration in the Cat", *Biol. Cybern.* v.19, pp. 105-116, 1975.

[14] BUONO, P.L., GOLUBITSKY, M., *Models of Central Pattern Generators for Quadrupedal Locomotion: I. Primary Gaits.*, Preprint, Dept. of Mathematics, Univ. of Houston, June 21, 1999.

[15] CALABRESE, A., FRANÇA, F.M.G. "A Randomised Distributed Primer for the Updating Control of Anonymous ANNs". In: *Proceedings of the International Conference on Artificial Neural Networks*, pp. 585-588, Sorrento, Italy, 1994.

[16] CHUA, L.O., YANG, L. "Cellular Neural Networks: Theory", *IEEE Trans. Cir. and Sys.* v.35, n.10, Oct. 1988.

[17] CHUA, L.O., YANG, L. "Cellular Neural Networks: Application", *IEEE Trans. Cir. and Sys.* v.35, n.10, Oct. 1988.

[18] CHUA, L.O., ROSKA, T. "The CNN Paradigm", *IEEE Trans. Cir. and Sys. I : Fundamental theory and applications* v.40, pp. 147-156, 1993.

[19] CHUA, L.O., HASLER, M., MOSCHYTZ, G.S., NEIRYNCK, J. "Autonomous Cellular Neural Networks: A Unified Paradigm For Pattern Formation and Active Wave Propagation", *IEEE Trans. Cir. and Sys. I : Fundamental theory and applications* v.42, n.10, Oct. 1995.

[20] COLLINS, J.J., RICHMOND, S.A. "Hard-wired Central Pattern Generators for Quadrupedal Locomotion", *Biol. Cybern.* v.71, pp. 375-385, 1994.

[21] COLLINS, J.J., STEWART, I.N. "Coupled Nonlinear Oscillators and the Symmetries of Animal Gaits", *J. Nonlinear Sci.* v.3, pp. 349-392, 1993.

[22] COLLINS, J.J., STEWART, I. "Hexapodal Gaits and Coupled Nonlinear Oscillator Models", *Biol. Cybern.* v.68, pp. 287-298, 1993.

[23] COLLINS, J.J., STEWART, I. "A Group-theoretic Approach to Rings of Coupled Biological Oscillators", *Biol. Cybern.* v.71, pp. 95-103, 1994.

[24] COLLINS, J.J., "Gait transitions". In: Arbib, M.A. (eds), *The Handbook of Brain Theory and Neural Networks*, 1 ed., pp. 420-423, New York, the MIT press, 1995.

[25] COLLINS, J.J., CHOW, C.C., CAPELA, A.C., et al. "Aperiodic Stochastic Resonance", *Phys. Rev.* v.E54, pp. 5575-5584, 1996.

[26] CONRAD, J.M., MILLS, J.W., *STIQUITO – Advanced Experiments with a Simple And Inexpensive Robot*. 1 ed. Piscataway, IEEE Computer Society Press, 1996.

[27] DIJKSTRA, E.W., "Cooperating Sequential Processes". In: Genuys, F. (eds), *Programming Languages*, 1 ed., pp. 43-112, New York, Academic Press, 1968.

[28] DUTRA, M.S. "Modeling of a bipedal locomotor using nonlinear oscillators", *Intl. J. Intel. Mechatronics - Design and Production* v.2, n.2, pp. 88-97, Ankara (Turkey), 1997.

[29] EAMES M.H.A., COSGROVE A., BAKER R. "Comparing methods of estimating the total body centre of mass in three-dimensions in normal and pathological gaits", *Human Movement Science* v.18, n.5, pp. 637-646, 1999.

[30] EKEBERG, O., WALLEN, P., LANSER, A., et al. "A Computer Based Model for Realistic Simulations of Neural Networks", *Biol. Cybern.* v.65, pp. 81-90, 1991.

[31] ERMENTROUT, B. "Neural Nets as Npatio-temporal Pattern Forming Systems", Preprint, Dept. of Mathematics, Univ. of Pittsburgh, Oct. 2, 1997.

[32] ERMENTROUT, B. "XPPAUT3.0 - the Differential Equations Tool", Preprint, Dept. of Mathematics, Univ. of Pittsburgh, March. 3, 1997.

[33] ERMENTROUT, B., RINZEL, J. "Analysis of Neural Excitability and Oscillations", Preprint, Dept. of Mathematics, Univ. of Pittsburgh, 1996.

[34] FITZHUGH, R. "Impulses and Physiological States in Theoretical Models of Nerve Membrane", *Biophys. J.* v.1, pp. 445-465, 1961.

[35] FRANÇA, F.M.G., *Neural Networks as Neighborhood-constrained Systems.* Ph.D. thesis, Imperial College, London, England, 1994.

[36] FRANÇA, F.M.G., ALVES, V.C., GRANJA, E.P. "A Multi-phase Asynchronous Timing Scheme". In: *Proceedings of Brazilian Symposium on Integrated Circuits*, pp. 283-292, Gramado, Brazil, Aug. 1997.

[37] GETTING, P.A. "Mechanisms of Pattern Generation Underlying Swimming in Tritonia I. Neuronal Network Formed by Monosynaptic Connections", *J. Neurophysiol.* v.46, pp. 65-79, 1981.

[38] GETTING, P.A. "Emerging Principles Governing the Operation of Neural Networks", *Ann. Rev. Neurosci.* v.12, pp. 185-204, 1989.

[39] GOLUBITSKY, M., STEWART, I. "Hopf Bifurcation in the Presence of Symmetry", *Arch. Rational Mech. Anal.* v.87, pp. 107-165, 1985.

[40] GOLUBITSKY, M., STEWART, I. "Hopf Bifurcation with Dihedral Group Symmetry: Coupled Nonlinear Oscillators.", *Comtemporary Mathematics* v.56, pp. 131-173, American Mathematical Society, 1986.

[41] GOLUBITSKY, M., SCHAEFFER, D.G., *Singularities and Groups in Bifurcation Theory*. Volume I, Springer-Verlag, 1988.

[42] GOLUBITSKY, M., STEWART, I., SCHAEFFER, D.G., *Singularities and Groups in Bifurcation Theory*. Volume II, Springer-Verlag, 1988.

[43] GOLUBITSKY, M., STEWART, I., BUONO, P.L., et al. "A Modular Network for Legged Locomotion", *Physica D* v.115, pp. 56-72, 1998.

[44] GRILLNER, S. "Locomotion in Vertebrates: Central Mechanisms and Reflex Interaction", *Physiol. Rev.* v.55, pp. 247-304, 1975.

[45] GRILLNER, S. "Neurobiological Bases of Rhythmic Motor Acts in Vertebrates", *Science* v.228, pp. 143-149, 1985.

[46] HALL, G.G., "Applied Group Theory". In: Stephenson, G. (eds), *Mathematical Physics Series*, the Whitefriars Press Ltd., London, 1967.

[47] HARRIS-WARICK, R.M., MARDER, E. "Modulation of Neural Networks for Behavior", *Annu. Rev. Neurosci.* v.14, pp. 39-57, 1991.

[48] HAUCK, S., BURNS, S., BORRIELLO, G., et al. "An FPGA for Implementing Asynchronous Circuits", *IEEE Design and Test of Computers* v.11, n.3, pp. 60-69, 1994.

[49] HAZEWINKEL, M., "Bifurcation Phenomena: a Short Introductory Tutorial with Examples". In: Hazewinkel, M., Jurkovich R., Paelinck, J.H.P. (eds), *Bifurcation Analysis: Principles, Applications and Synthesis*, New York, D.Reidel Publishing Company, 1984.

[50] HODGKIN, A.L., HUXLEY. A.F. "A Quantitative Description of Membrane Current and its Application to Conduction and Excitation in Nerve", *J. Physiol.* v.117, pp. 500-544, 1952.

[51] HOPFIELD, J.J. "Neural Networks and Physical Systems with Emergent Collective Properties", *Proc. Nat. Acad. Sci.* v.79, pp. 2554-2558, USA, 1982.

[52] HOPFIELD, J.J., TANK, D.W. "Neural Computation of Decisions in Optimization Problems", *Biol. Cybern.* v.52, pp. 141-152, 1985.

[53] HOPFIELD, J.J., TANK, D.W. "Computing with Neural Circuits: A Model", *Science* v.233, pp. 625-632, 1986.

[54] KAWAHARA, T. "Coupled Van der Pol Oscillators - A Model for Excitatory and Inhibitory Neural Interactions", *Biol. Cybern.*, v.39, pp. 37-43, 1980.

[55] KHALIL, H.K., *Nonlinear Systems*. 1 ed. New York, Macmillan Publishing Company, 1992.

[56] LINKENS, D.A., TAYLOR, Y., DUTHIE, H.L. "Mathematical Modeling of the Colorectal Myoelectrical Activity in Humans", *IEEE Trans. Biomed. Engr.* v.23, pp. 101-110, 1976.

[57] MAEDA, Y., PAKDAMAN, K., NOMURA, T., et al. "Reduction of a Model for an Onchidium Pacemaker Neuron", *Biol. Cybern.* v.78, pp. 265-276, 1998.

[58] MARSDEN, J.E., McCRACKEN, M., *The Hopf Bifurcation and its Applications: Applied mathematics in science 19*. 1 ed. Berlin, Springer-Verlag, 1976.

[59] MATSUOKA, K. "Mechanisms of Frequency and Pattern Control in the Neural Rhythm Generators", *Biol. Cybern.* v.56, pp. 345-353, 1987.

[60] MORRIS, C., LECAR, H. "Voltage Oscillations in the Barnacle Giant Muscle Fiber", *Biophysical J.* v.35, pp. 193-213, 1981.

[61] NAGUMO, J., ARIMOTO, J., YOSHIZAWA, S. "An Active Pulse Transmission Line Stimulating Nerve Axon", *Proc. IRE* v.50, pp. 2061-2070, 1962.

[62] CHURCHLAND, P.S., SEJNOWSKI, T.J., *The Computational Brain*. 1 ed. Cambridge, MIT press, 1992.

[63] PEARSON, K.G. "The Control of Walking", *Sci. Am.* v.235, pp. 72-86, 1976.

[64] PEARSON, K.G. "Common Principles of Motor Control in Vertebrates and Invertebrates", *Annu. Rev. Neurosci.* v.16, pp. 265-297, 1993.

[65] PULLELA, S. "A General Purpose Controller for Stiquito", Preprint, Dept. of Computer Sci., Univ. of Indiana, May, 1998.

[66] RINZEL, J., ERMENTROUT, B., "Analysis of Neural Excitability and Oscillations". In: Koch, C., Segen, I. (eds), *Methods in neuronal modelling from synapses to networks*, pp. 135-171, Cambridge, MIT press, 1989.

[67] SCHONER, G., JIANG, W.Y., KELSO, J.A.S. "A Synergetic Theory of Quadrupedal Gaits and Gait Transitions", *J. Theoret. Biol.* v.142, pp. 359-391, 1990.

[68] SHEPHERD, G.M., *Neurobiology.* 3 ed. Oxford, Oxford University Press, 1994.

[69] SOMERS, D., KOPELL, N. "Waves and Synchrony in Networks of Oscillators of Relaxationand Non-relaxation Type.", *Physica D* v.89, pp. 169-183, 1995.

[70] STEIN, P.S.G. "Motor Systems with Specific Reference to the Control of Locomotion", *Annu. Rev. Neurosci.* v.1, pp. 61-81, 1978.

[71] TAGA, G., YAMAGUCHI, Y., SHIMIZU, H. "Self-organized Control of Bipedal Locomotion by Neural Oscillators in Unpredictable Environment", *Biol. Cybern.* v.65, pp. 147-159, 1991.

[72] TAGA, G. "A Model of the Neuro-musculo-skeletal System for Human Locomotion - I. Emergence of Basic Gait", *Biol. Cybern.* v.73, pp. 97-111, 1995.

[73] TAFT, R., "An Introduction: Eadweard Muybridge and His Work". In: Muybridge, E. (eds), *The Human Figure in Motion*, pp. 7-14, New York, Dover Publications, 1955.

[74] TSUTSUMI, K., MATSUMOTO, H. "A Synaptic Modification Algorithm in Consideration of the Generation of Rhythmic Oscillation in a Ring Neural Network", *Biol. Cybern.* v.50, pp. 419-430, 1984.

[75] TURING, A.M. "The Chemical Basis of Morphogenesis", *Philos. Trans. R. Soc., London, Ser. B* v.237, pp. 37-72, 1952.

[76] ULLSTROM, M., KOTALESKI, J.H., TEGNER, J., et al. "Activity-dependent Modulation of Adaptation Produces a Constant Burst Proportion in a Model of the Lamprey Spinal Locomotion Generator", *Biol. Cybern.* v.79, pp. 1-14, 1998.

[77] WANG, X.J., RINZEL, J. "Alternating and Synchronous Rhythms in Reciprocally Inhibitory Model Neurons", *Neural Computation* v.4, pp. 84-97, 1992.

[78] WILSON, H.R., COWAN, J.D. "Excitatory and Inhibitory Interactions in Localized Populations of Model Neurons", *Biophys. J.* v.12, pp. 1-24, 1972.

[79] WILSON, D.M. "Insect Walking", *Annu. Rev. Entomol.* v.11, pp. 103-122, 1966.

[80] WINTER, D.A., PRINCE, F., PATLA, A.E. "Stiffness Control of Balance During Quiet Standing", *J. Neurophysiol.* v.80, pp. 1211-1221, 1998.

[81] XILINX Programmable Logic Company, "Foundation Series Quick Start Guide 1.4", Xlinx Press, 1997.

[82] YANG, Z.J., FRANÇA, F.M.G., "Generating Arbitrary Rhythmic Patterns with Purely Inhibitory Neural Networks". In: *Proceedings of European Symposium on Artificial Neural Networks*, pp. 53-58, Brugge, Belgium, Apr. 1998.

[83] YANG, Z.J., FRANÇA, F.M.G., "Implementing Artificial CPGs using Fine-grain FPGAs". In: *Proceedings of ACM International Symposium on Field-Programmable Gate Arrays*, 250, Monterey, CA, USA, Feb. 1999.

[84] YANG, Z.J., FRANÇA, F.M.G. "A Discrete Artificial Locomotion CPGs Architecture and its Analog Hopfield-like Conversion", Preprint, COPPE/UFRJ, 1999.

[85] YUASA, H., ITO, M. "Coordination of Many Oscillators and Generation of Locomotory Patterns", *Biol. Cybern.* v.63, pp. 177-184, 1990.